Development of a Versatile, Endothelialized Microfluidic Platform to Investigate Vaso-Occlusion in Sickle Cell Disease

A DISSERTATION
SUBMITTED TO THE FACULTY OF THE
UNIVERSITY OF MINNESOTA
BY

Samantha Rose Schad

IN PARTIAL FULFILLMENT OF THE REQUIREMENTS
FOR THE DEGREE OF
DOCTOR OF PHILOSOPHY

Advised by David K. Wood, PhD

January 2025

© 2025

Samantha R. Schad

Acknowledgments

First and foremost, I would like to thank my advisor, Dr. David Wood. Thank you for welcoming me into your lab and supporting my research endeavors for the past six years. You have challenged me to be a more independent, thoughtful scientist and for that I am extremely grateful. Thank you for encouraging me to share my science with others and for allowing me the opportunity to grow as an engineer both inside and outside of the lab. This work could not exist without your support, and also without the help of the lab you built.

To the Living Devices Lab past and present, thank you for shaping my time here as a graduate student. First to the alumni, who welcomed me and made this lab such a wonderful, friendly place to work. Specifically, to Drs. Katherine Cummins, Heather Bomberger, Geneva Hargis, and José Valdez who were especially generous with their time, knowledge, and mentorship when I was just an eager graduate student lacking any microfluidics experience. I'd also like to thank Abagael Payne, Elizabeth Rono, and Luna Zhang for their support and kindness in the toughest times of my PhD. Thanks for the help that has been provided to both lift my spirits (tamales, cookies, other sweet treats) and advance my science.

A special thank you to funding provided by the National Institutes of Health/National Heart, Lung, and Blood Institute (NIH/NHLBI), and also to all the collaborators who have made this work possible. Specifically, to Yumiko Sakurai and Dr. Wilbur Lam who invited me to Georgia Institute of Technology and taught me the fundamentals of culturing cells in microfluidic devices. Also, to our clinical collaborators both in Boston and Minneapolis who have helped to facilitate access to sickle cell patients.

I would also like to acknowledge the support of my committee members. Dr. Odde, thank you for your impactful mentorship and guidance throughout the years. From recruitment weekend, to learning about microtubules in Cell Engineering, to two rounds as your TA in Transport Processes, I have been grateful to have had you as a

mentor. Dr. Beckman, you have volunteered your time and shared your clinical knowledge and expertise on countless occasions. Your guidance has been tremendously valuable in the execution of this work. Dr. Yoshida, thank you for jumping right in to join the team. I have always respected your contributions to this department and am proud to have you serve on my committee.

Additionally, I would like to recognize the wonderful opportunity I had to participate in industry work during my PhD. Thank you to Dr. Elizabeth Crist, Dr. Sarah Gruba, Tucker Nelson, Brian Schmidt, and Jacob Ludwig for inviting me into your team at Boston Scientific for over a year.

Finally, I would like to express my deepest gratitude to my family and friends. To my family, thank you for supporting me through this entire journey. Most importantly to my parents, Greg and Kathy, I simply would not have made it to graduate school without your unwavering support. To my siblings Erik and Aimee, thank you for setting such a high standard for me to follow. You've all shown me what is possible to achieve with ambition, hard work, and perseverance. To my nephews Leopold and Augustine, niece Cordelia, and sister-in-law Ally, thank you for always putting a smile on my face and offering some much-needed perspective.

To all my friends back home in Illinois around the country, thank you for years of encouragement to make it to this point and for your help maintaining balance throughout this academic pursuit. Also, to those have helped make Minneapolis my home for the last six and a half years, I truly could not have survived the cold winters without you. Especially to Riley and Bryant Hall, I am extremely thankful for your friendship and the weekly reprieve of Tuesday trivia nights.

And lastly, to Dr. Matthew MacEwen. Thank you for being my rock through it all. I could not have made here without your encouragement and support. I am so proud of all that we have achieved together. Moreso, I'm incredibly grateful for the adventures had and memories created along the way. Thank you for helping to make it all possible.

Abstract

Sickle cell disease (SCD) is an inherited autosomal recessive disorder caused by a mutation in the hemoglobin β gene, leading to hemoglobin polymerization, red blood cell sickling, and a cascade of pathophysiological events that culminate in a painful vaso-occlusive crisis (VOC). Despite its discovery over a century ago, treatment options for the millions of SCD patients worldwide remain remarkably limited, thus highlighting the need for a better understanding of its underlying mechanisms. Recently, increased attention has been directed to hypoxia/ischemia reperfusion injury as a driving mechanism of VOC in SCD pathology. While hypoxia and reperfusion are classically thought to induce harmful inflammatory responses associated with apoptosis and symptom onset, a remarkable trait of reperfusion injury is that certain mild or cyclic periods of low oxygen may instead provoke a conditioning effect that ameliorates subsequent severe reperfusion injury. A better understanding of the conditioning effect exerted by hypoxia reperfusion on the endothelium may inform our overall understanding of SCD pathophysiology and offer insight towards therapeutic intervention. Existing in vivo and in vitro models do not reliably inform clinical trials, consequently more physiologically relevant models are needed to explore these fundamental questions about SCD pathophysiology. Therefore, we developed a microfluidic platform that includes three-dimensional endothelial-lined microchannels with physiologically relevant shear stresses in an oxygen-tunable environment. These features enable simulation of hypoxia reperfusion and vaso-occlusion on-chip. We utilized fluorescence microscopy to validate the biological relevance of the endothelial vascular network on-chip, demonstrating appropriate lumen formation, alignment under flow, and cellular function. This microfluidic platform is unique in its ability to recapitulate many of the physiologic components of SCD. Its applications are two-fold: (1) its use as an occlusion assay that quantifies the occlusion incidence of patient blood samples through microvasculature, and (2) its potential to leverage next generation sequencing to explore genomic changes to the endothelium. Using the platform, we demonstrated that endothelial hypoxic preconditioning initiates

a protective effect that reduces incidence of sickle red blood cell occlusion on-chip. We observed average vaso-occlusion rates of 8.89% and 11.78% after cyclic and sustained hypoxia preconditioning compared to 57.93% and 55.05% for atmospheric and physiologic controls, respectively. Moreover, we investigated endothelial gene regulation via RNA sequencing to identify pathways of interest and specific genes that may directly contribute to this protective result. These results offer a better understanding of the mechanistic changes affecting the endothelium during hypoxia reperfusion injury and also support the hypothesis that hypoxia preconditioning may offer a protective effect against VOC in SCD.

Table of Contents

Acknowledgements i

Abstract iii

List of Tables ix

List of Figures x

List of Abbreviations xii

Chapter 1: Comprehensive Review of Sickle Cell Disease and Its Impact 1

1.1 An Introduction to Sickle Cell Disease: Inheritance and Incidence 1

1.2 Clinical Presentation and Complications 3

1.3 A Complex Pathophysiology 7

1.3.1 Hemoglobin polymerization 8

1.3.2 Red blood cell membrane damage and hemolysis 9

1.3.3 Endothelial activation, inflammation, and adhesion 10

1.3.4 Hypoxia reperfusion injury 11

1.3.5 Vaso-occlusion 13

1.4 Therapeutic Challenges Underscore Need for Further Research 14

1.4.1 Pharmaceutical agents 15

1.4.2 Pain management 18

1.4.3 Transfusion therapy 18

1.4.4 Emerging technologies 21

Chapter 2: Overview of Existing Models and Methodologies 23

2.1 Microfluidic Models to Study Hematologic Disease 23

2.2 Oxygen-Tunable Microfluidics 24

2.3 Occlusion Microfluidics 26

2.4 Endothelialized Microfluidics 28

2.5 Leveraging Next Generation Sequencing with Microfluidic Technology 29

2.6 Gaps in Knowledge..... 31
2.7 Goals and Hypotheses..... 33

Chapter 3: A Novel Microfluidic Platform to Study Sickle Cell Disease..... 35
3.1 Introduction..... 35
3.2 Materials and Methods..... 38
3.2.1 Microfluidic device design 38
3.2.2 Microfabrication..... 39
3.2.3 Cell culture..... 40
3.2.4 Microfluidic device endothelialization..... 41
3.2.5 Immunofluorescence staining of the endothelium..... 42
3.2.6 Microscopy and image processing..... 45
3.2.7 Hypoxia treatment..... 45
3.2.8 Blood sample collection..... 46
3.2.9 Blood sample preparation and perfusion..... 47
3.3 Results and Discussion..... 48
3.3.1 Development of an endothelialized, oxygen-tunable microfluidic model.... 49
3.3.2 Microfluidic platform recapitulates SCD microvasculature 51
3.3.3 Endothelium on-chip tolerates hypoxia preconditioning..... 54
3.3.4 Blood perfusion and occlusion modeling on-chip..... 56
3.4 Conclusion..... 58
3.5 Acknowledgments..... 60
3.6 Supplemental Materials..... 61

Chapter 4: Implementation of an Occlusion Assay on-Chip to Explore Effects of Hypoxia Preconditioning and Contributors to VOC..... 64
4.1 Introduction..... 64
4.2 Materials and Methods..... 66
4.2.1 Microfluidic device design, fabrication, and endothelialization 67
4.2.2 Hypoxia preconditioning..... 69
4.2.3 Blood sample collection and preparation..... 70
4.2.4 Occlusion assay..... 71

4.2.5 Microscopy and image processing..... 72
4.2.6 Statistical analyses..... 73
4.3 Results and Discussion..... 74
4.3.1 Measurement of vaso-occlusive incidence on-chip..... 74
4.3.2 Hypoxia preconditioning reduces probability of vaso-occlusion..... 77
4.3.3 Samples from male patients exhibit higher occlusion incidence..... 79
4.3.4 Investigation of clinical predictor variables' contributions to occlusive outcomes..... 81
4.4 Conclusion..... 91
4.5 Acknowledgements..... 93
4.6 Supplemental Materials..... 93

Chapter 5: Leveraging Next Generation Sequencing to Investigate Effects of Hypoxia Preconditioning..... 105
5.1 Introduction..... 105
5.2 Materials and Methods..... 107
5.2.1 Microfluidic device design, fabrication, and endothelialization..... 107
5.2.2 Hypoxia preconditioning..... 109
5.2.3 Microfluidic device de-cellularization and RNA extraction..... 110
5.2.4 RNA quality testing, sequencing, and post-processing..... 113
5.3 Results and Discussion..... 114
5.3.1 Endothelial cells cultured on-chip can be extracted for NGS..... 114
5.3.2 Cyclic hypoxia preconditioning results in more abundant differential gene regulation than sustained hypoxia preconditioning..... 117
5.3.3 Hypoxia preconditioning modulates a number of pathways in SCD..... 118
5.3.4 Differential regulation of gene expression by hypoxia preconditioning may contribute to vaso-occlusive risk..... 122
5.3.5 Temporal response to hypoxia differentially regulates gene expression... 126
5.4 Conclusion..... 128
5.5 Acknowledgements..... 129
5.6 Supplemental Materials..... 130

Chapter 6: Concluding Remarks..... 136
6.1 Summary of Key Findings and Interpretations..... 136
6.2 Limitations..... 139
6.3 Future Directions..... 140

Chapter 7: References..... 143

Chapter 8: Appendix..... 164

List of Tables

Chapter 3

Table 3.1: List of antibodies used in endothelial characterization..... 43

Table 3.S1: Blood sample data sheet I..... 61

Chapter 4

Table 4.1: R^2 values for each PLSR model..... 91

Table 4.S1: Patient blood sample datasheet II..... 101

Table 4.S2: Patient blood sample datasheet III..... 102

Table 4.S3: Percent of variance explained in occlusion result by PLSR..... 103

Table 4.S4: Variable importance in projection scores of PLSR analysis..... 104

Chapter 5

Table 5.S1: RNA sequencing quality control assessment..... 135

Appendix

Table A.1: Normal reference ranges for clinical metrics..... 164

List of Figures

Chapter 1

Figure 1.1: SCD acute and chronic complications..... 4

Figure 1.2: Mechanisms of SCD pathophysiology..... 7

Chapter 3

Figure 3.1 Schematic of endothelialization procedure..... 41

Figure 3.2: Experimental setup for oxygen control and device observation..... 46

Figure 3.3: Microfluidic device geometry and arrangement..... 50

Figure 3.4: Confocal imaging of three-dimensional endothelial lumen..... 52

Figure 3.5: Characterization of the endothelium..... 53

Figure 3.6: On-chip hypoxia treatment of vascularized channels..... 56

Figure 3.7: Red blood cell perfusion and occlusion in microfluidic devices..... 57

Figure 3.S1: Visualization of device geometry using dyes..... 62

Figure 3.S2: Microvascular endothelial cells cultured on-chip..... 62

Figure 3.S3: Healthy and SCD red blood cell perfusion through endothelialized devices..... 63

Chapter 4

Figure 4.1: Visual summary of chapter 4 experimental timeline and workflow..... 67

Figure 4.2: Occlusion profiles for each patient sample..... 75

Figure 4.3: Hypoxia preconditioning prevents vaso-occlusion among varied cohort of SCD patient samples..... 78

Figure 4.4: Incidence of vaso-occlusion, comparison by sex..... 81

Figure 4.5: Spearman correlation of clinical predictor variables with occlusion..... 83

Figure 4.6: PLSR analysis of occlusion results among endothelium pretreated with atmospheric control..... 85

Figure 4.7: PLSR analysis of occlusion results among endothelium pretreated with physiologic control..... 86

Figure 4.8: PLSR analysis of occlusion results among endothelium pretreated with cyclic hypoxia..... 87

Figure 4.9: PLSR analysis of occlusion results among endothelium pretreated with sustained hypoxia..... 88
Figure 4.S1: Hypoxia preconditioning prevents vaso-occlusion among varied cohort of SCD patient samples (with patient-specific labeling)..... 94
Figure 4.S2: Hypoxia preconditioning prevents vaso-occlusion among non-transfused SCD patient samples..... 95
Figure 4.S3: Significance charts for spearman correlation..... 96
Figure 4.S4: PLSR analysis of occlusion results among endothelium pretreated with atmospheric control (non-transfused samples only)..... 97
Figure 4.S5: PLSR analysis of occlusion results among endothelium pretreated with physiologic control (non-transfused samples only)..... 98
Figure 4.S6: PLSR analysis of occlusion results among endothelium pretreated with cyclic hypoxia (non-transfused samples only)..... 99
Figure 4.S7: PLSR analysis of occlusion results among endothelium pretreated with sustained hypoxia (non-transfused samples only)..... 100

Chapter 5
Figure 5.1: Visual summary of chapter 5 experimental timeline and workflow..... 108
Figure 5.2: Comparison of RNA extraction methods..... 112
Figure 5.3: Comparison of extracted RNA across treatment groups..... 115
Figure 5.4: Global gene expression profile due to hypoxia preconditioning..... 118
Figure 5.5: Pathway analysis of RNA sequencing results..... 119
Figure 5.6: Visualization of global transcriptional changes due to hypoxia preconditioning..... 123
Figure 5.7: Global gene expression profile due to hypoxia preconditioning in the extended incubation group..... 127
Figure 5.S1: Heatmap of highly regulated genes in the standard incubation group.... 131
Figure 5.S2: Pathway analysis of RNA sequencing results for the extended incubation group..... 132
Figure 5.S3: Visualization of global transcriptional changes due to hypoxia preconditioning in the extended incubation group..... 133
Figure 5.S4: Heatmap of highly regulated genes in the extended incubation group... 134

List of Abbreviations

Abbreviation	Definition
AAT	*Alpha 1-antitrypsin protein*
ACS	*Acute chest syndrome*
BSA	*Bovine serum albumin*
DEG	*Differentially expressed gene*
DV200	*Distribution value 200*
EGM-2	*Endothelial cell growth medium-2*
F-actin	*Filamentous actin*
FBS	*Fetal bovine serum*
GO	*Gene ontology*
Hb or HGB	*Hemoglobin*
HbA	*Adult hemoglobin*
HbF	*Fetal hemoglobin*
HbS	*Sickle hemoglobin*
HCT	*Hematocrit*
HIF1-alpha	*Hypoxia-inducible factor 1-alpha*
HMVEC-L	*Human microvascular endothelial cell from lung*
HU	*Hydroxyurea*
HUVEC	*Human umbilical vein endothelial cell*
ICAM-1	*Intercellular adhesion molecule-1*
IVF	*Intravenous fluid*

ISC	*Irreversibly sickled cell*
MCHC	*Mean corpuscular hemoglobin concentration*
MCV	*Mean corpuscular volume*
NGS	*Next generation sequencing*
NOX2	*NADPH oxidase protein-2*
PBS	*Phosphate-buffered saline*
PDMS	*Polydimethylsiloxane*
PECAM-1	*Platelet endothelial cell adhesion molecule-1*
PFA	*Paraformaldehyde*
PLSR	*Partial least squares regression*
PLT	*Platelet count*
RDW	*Red blood cell distribution width*
RIN	*RNA integrity number*
ROS	*Reactive oxygen species*
SCA	*Sickle cell anemia*
SCD	*Sickle cell disease*
SCT	*Sickle cell trait*
VCAM-1	*Vascular cell adhesion molecule-1*
VE-Cadherin	*Vascular endothelial cadherin*
VEGFR	*Vascular endothelial growth factor receptor*
VIP	*Variable importance in projection*
VOC	*Vaso-occlusive crisis*
WBC	*White blood cell count*

Chapter 1: Comprehensive Review of Sickle Cell Disease and Its Impact

1.1 An Introduction to Sickle Cell Disease: Inheritance and Incidence

Sickle cell disease (SCD) is the one of the most prevalent monogenic disorders, affecting approximately 100,000 Americans and millions worldwide.[1–4] Each year, over 300,000 infants are born with homozygous SCD, which is projected to rise to at least 400,000 by the year 2050.[4–6] Disease prevalence is highest throughout sub-Saharan Africa, largely due to the protection offered by sickle cell trait (SCT) against malaria.[7] In the United States, African American communities are most affected with around 1 in 365 black infants being born with SCD, or 1 in 13 born with SCT.[8–10] In the United States alone, SCD accounts for over 230,000 hospital admissions and at least $2.4 billion in expenses each year.[11,12]

SCD is an inherited autosomal-recessive disorder caused by a mutation in the gene encoding hemoglobin subunit β. Sickle cell anemia (SCA), the most common symptomatic form of SCD, is caused by homozygosity of the beta-S allele (β^S, HbSS) which differs from the wild type allele by a single nucleotide polymorphism. This mutation results in replacement of a hydrophilic glutamic acid residue (Glu) with a hydrophobic valine residue (Val).[13–16] Individuals may be homozygous for β^S (HbSS), but may also coinherit a single β^S allele with a separate mutant allele such as β^C, β^D , β^O, or β^{thal} that results in alternate SCD genotypes

(HbSC, HbSD, HbSO, and HbSβ^{thal}, respectively). Sickle hemoglobin SC disease is caused by inheritance of the HbSC genotype. It is the second most common hemoglobinopathy after homozygous SCD (HbSS) and globally around 55,000 infants are born each year with HbSC.[1,2,17] Though it is driven by similar pathophysiology, the HbSC genotype of SCD is generally considered to be milder than the homozygous HbSS genotype.[17] HbSC is poorly researched and much of the evaluation and treatment for patients with HbSC is inferred from studies examining cohorts of mostly HbSS patients.[18] Inheritance of a single β^S allele results in SCT, a carrier form that has some clinical presentation but is often asymptomatic.[16] Overall, SCD can present with substantial phenotypic heterogeneity, due in part to these genetic modifiers but also to a complex underlying pathophysiology.[6,19,20] Our understanding of SCD and its complex disease mechanisms have evolved over time.

SCD was first described in 1910, acquiring its name from the “thin, elongated, sickle-shaped and crescent-shaped” red blood cells observed by physician James Herrick.[21] Under deoxygenated conditions, unbound sickle hemoglobin (HbS) has been shown to polymerize into rigid fibers, distorting red blood cell morphology into the characteristic “sickle” or crescent cell shape. Hemoglobin polymerization initiates a cascade of downstream effects and often culminates in vaso-occlusive crisis (VOC). During VOC, the microcirculation becomes obstructed by sickled red blood cells and other blood components causing tissue ischemia and organ injury.[22–24] The remaining sections of this

chapter will review complications experienced by patients, examine the complex pathophysiology driving SCD, and discuss currently available therapeutic interventions.

1.2 Clinical Presentation and Complications

In SCD, hemoglobin polymerization and red cell sickling initiate a cascade of downstream effects including endothelial dysfunction, inflammation, nitric oxide deficiency, hypercoagulability, oxidative stress, and reperfusion injury. Collectively, these complex processes contribute to a multisystem disorder marked by lifelong acute and chronic complications throughout the body. The pathophysiology of this disorder contributes to significant mortality as well as decreased quality of life. Most children with SCD in high-income countries survive to adulthood, however an estimated 50-80% of infants born in Africa with SCD die before age 5.[25] In a recent study, the projected life expectancy of an American with SCD was estimated to be just 54 years, compared to 76 years for someone without SCD.[26] Improved life expectancy in the U.S. is due in part to early diagnosis, increased access to care and education, and improved disease management.[27] A number of significant SCD complications contributing to morbidity and early mortality are reviewed here, though not every complication could be included for brevity. A more exhaustive list has been included in the schematic below, which includes material adapted from Kato et al. (Figure 1.1).[20]

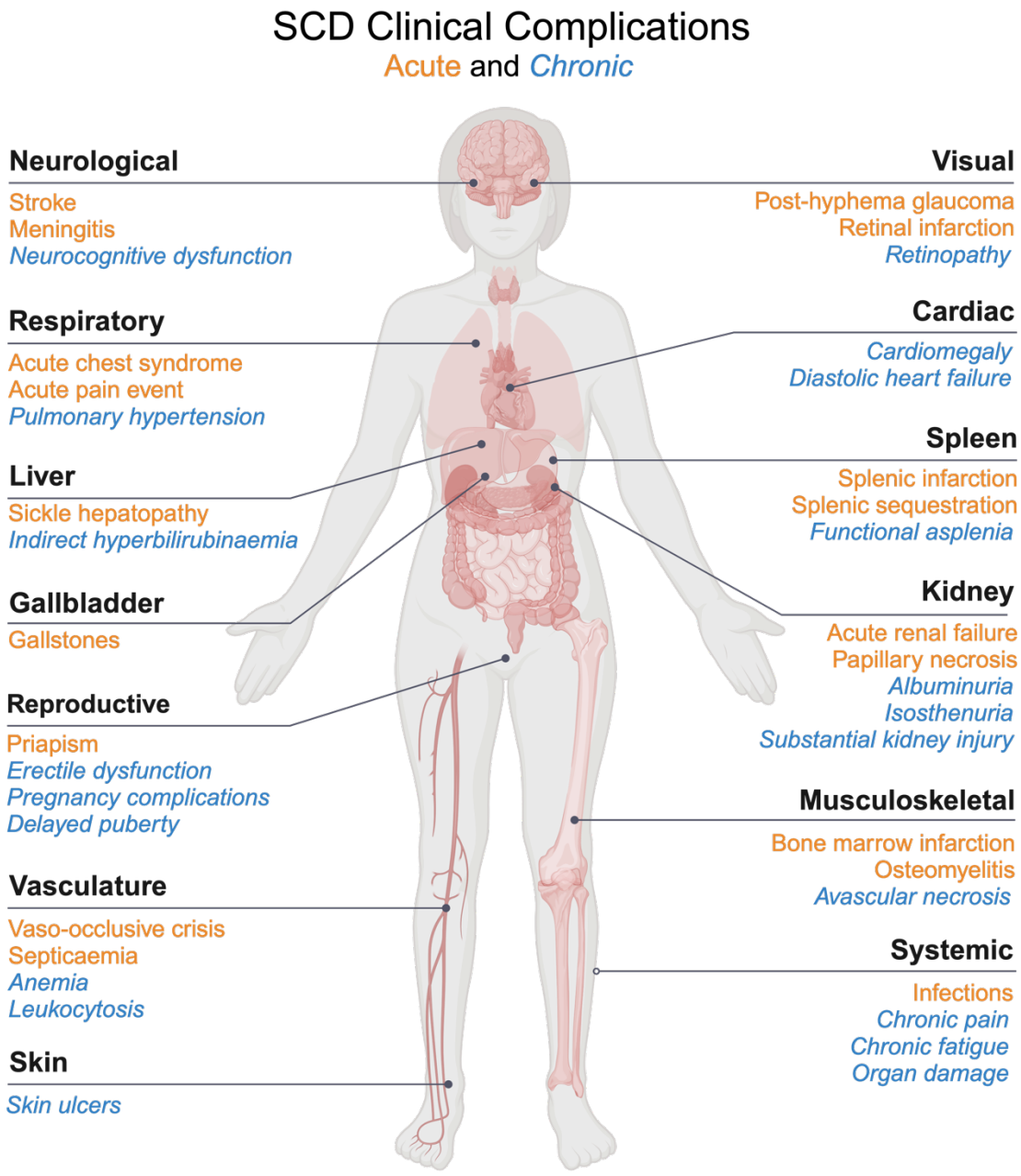


Figure 1.1: SCD acute and chronic complications. SCD is a multisystem disorder in which patients experience a wide range of complications throughout the body. Highlighted acute (orange) and chronic (blue, italicized) complications are included. Created using BioRender and adapted from Kato et al.[20]

Vaso-occlusive crisis (VOC), or sickle cell pain crises, are responsible for the most SCD-related hospitalizations.[28] VOC are usually sudden in onset and are

associated with throbbing, sharp pain often located in the lower back, joints, and extremities. VOC are also often correlated with other clinical manifestations including acute chest syndrome, cerebrovascular complications, and organ damage.[29]

Acute chest syndrome (ACS) is a form of acute lung injury involving obstruction of the pulmonary vasculature. ACS is often triggered by infection or pulmonary fat embolism[30,31] and symptoms can include fever, cough, chest pain, and shortness of breath.[30,32,33] One study suggested that nearly half of all ACS episodes for adults with SCD occurred between 24 to 72 hours after admission for severe VOC, suggesting a correlation between the pathophysiology of VOC and ACS.[30,33] Recurrent episodes of ACS are often accompanied by prolonged hospitalization and can present an increased risk for development of debilitating sickle cell chronic lung disease or sickle cell-related mortality.[34] In fact, ACS is the leading cause of death and the second most likely cause of hospitalization for adults with SCD.[30,31,33,35,36]

SCD increases risk for several neurologic complications including acute ischemic and hemorrhagic stroke. Most pediatric cases are of ischemic stroke, with intercranial hemorrhage being more common among adults. The risk of acute stroke is 300 times higher for children with SCD than for children without SCD[37] and in one study 7.8% of children with untreated SCD had at least one stroke by age 14.[38] Patients with ischemic stroke typically present with sudden weakness, loss of consciousness, or transient ischemic attack. Hemorrhagic stroke presents

with severe headache or loss of consciousness.[20,37,39] High incidence of stroke and other neurologic complications put SCD patients at risk of cognitive impairment that can significantly affect quality of life.[40,41]

Acute anemic episodes are characterized by rapid falls in hemoglobin levels and are related to a range of clinical complications. In particular, splenic sequestration crisis occurs when an excessive amount of red blood cells become trapped in the spleen, causing a dangerous drop in blood volume. This complication is associated with abdominal pain, sudden enlargement of the spleen, and fatigue. Splenic sequestration crisis has been estimated to affect between 7-30% of children with SCD and has been a long-standing leading cause of infant mortality.[42–44] However, early detection and treatment with blood transfusion and splenectomy have markedly reduced mortality rates in some studies from 15-44% to <1% with treatment.[42,43,45]

Overall, SCD presents a significant burden to patients. The acute and chronic complications highlighted in this section are just a few of many that patients with SCD experience. Additionally, day-to-day symptom load can be severe, including pain crises, fatigue, swelling, infection, and organ damage, among numerous others. The complex pathophysiology driving these biological effects will be further described in the next section of this chapter.

1.3 A Complex Pathophysiology

The multisystem pathophysiology of SCD is first initiated by hemoglobin polymerization and ultimately results in VOC. In order to best treat patients suffering from recurrent VOC, it is critical to thoroughly understand the mechanisms driving microcirculation obstruction in SCD. More specifically, these mechanisms include hemoglobin polymerization, membrane damage, red cell sickling, hemolysis, endothelial activation, inflammation, hypoxia reperfusion injury, adhesion, and vaso-occlusion as highlighted in the schematic below (Figure 1.2). Many of these mechanisms are interconnected and can occur simultaneously throughout the body, as they reinforce each other and can cause the disease to worsen over time.

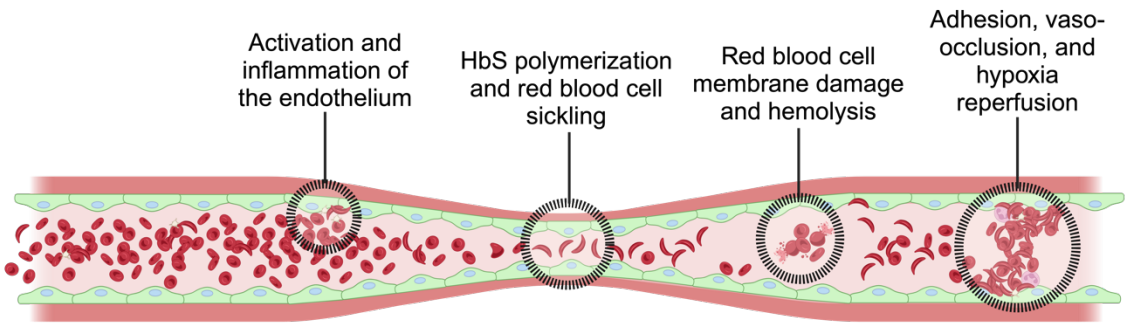


Figure 1.2: Mechanisms of SCD pathophysiology. Highlighted SCD mechanisms including sickle hemoglobin polymerization, red blood cell sickling, membrane damage, hemolysis, endothelial activation, inflammation, adhesion, vaso-occlusion, and hypoxia reperfusion injury are visualized here. Created using BioRender.

1.3.1 Hemoglobin polymerization

Under deoxygenated conditions, unbound sickle hemoglobin can polymerize into rigid fibers causing a series of changes to red blood cell morphology and membrane function. The most readily observable of which is the key morphological change from a biconcave disk to the “sickled” cell shape.[21–24] Sickled red blood cells suffer from poor deformability and are highly susceptible to trapping and adhesion in circulation. Moreover, it is clear that HbS polymerization alters not only cellular morphology but also cellular function. In sickled red blood cells, molecular transport via membrane ion channels is altered which leads to a significant dehydrating effect that further favors cell sickling.[46–48] Additionally, the polymerization of sickle hemoglobin further reduces its affinity for oxygen, helping to stabilize the deoxygenated form.[49] Collectively, altered membrane biology is correlated with poor hydration, reduced deformability, increased hemolysis, and accelerated cell death.[46,47] Meanwhile clinically, HbS polymerization and red blood cell membrane damage are correlated with incidence of VOC in SCD. Studies have shown a link between percentage of sickled cells in the blood and incidence of pain crises, with proportion of sickled cells spiking 1-3 days before clinical presentation of VOC.[50,51]

1.3.2 Red blood cell membrane damage and hemolysis

In SCD, red blood cells undergo membrane damage that results in a wide range of membrane abnormalities and downstream contributions to the vaso-occlusive cascade.[52,53] Some sickled red blood cells may become irreversibly sickled as a result of HbS polymerization-induced membrane damage. These irreversibly sickled cells (ISCs) are poorly deformable and exceedingly dehydrated. Their contribution to the pathophysiology of SCD is further emphasized because they retain sickled morphology even under fully oxygenated conditions. For example, increased oxidative stress has been correlated with proportion of ISCs in SCD.[54–56] Additionally, frequent and repeated damage to sickle red blood cells increases hemolytic risk.

Sickled red blood cells are highly susceptible to hemolysis. In fact, the lifespan of a sickled red blood cell is substantially reduced (≥75%) compared to that of a standard red blood cell.[57,58] Hematocrit (a measure indicating the volume percentage of red blood cells in the blood) of patients with SCD has been reported to be approximately 25.7 ± 4.4%, substantially lower than the average for healthy adults which nears 40%.[32] Hemolysis leads to release of free heme and other red blood cell components into the bloodstream, contributing to inflammation, oxidative stress, and endothelial dysfunction in SCD.[59] This proinflammatory, high oxidative stress environment further affects membrane properties by promoting activation of red blood cell NADPH oxidase and consequently increasing production of intra-erythrocyte reactive oxygen species (ROS). This results in additional damage to

red blood cell membranes, further modifying the deformability, aggregation, and adhesion properties of the red blood cells.[60,61]

1.3.3 Endothelial activation, inflammation, and adhesion

Clinically, inflammation is a hallmark of SCD pathogenesis and is driven by several key mechanisms. First, studies have shown elevated levels of many pro-inflammatory cytokines in the blood of SCD patients including tumor necrosis factor-alpha (TNF-a), IL-1, IL-3, IL-6, GM-CSF, endothelin-1, and prostaglandin E2.[62–67] These proinflammatory cytokines promote activation of endothelial cells, platelets, and leukocytes which results in upregulation of the endothelial adhesion molecules P-selectin, E-selectin, intercellular adhesion molecule-1 (ICAM-1), and vascular cell adhesion molecule-1 (VCAM-1). This further increases likelihood of adhesion and VOC.[62–67] In particular, P-selectin has been identified as a major therapeutic target, as it has been shown to contribute to both endothelial adhesion and occlusion.[68–70] P-selectin is stored in Weibel-Palade bodies of endothelial cells and alpha-granules of platelets and is translocated to either surface during activation or inflammation.[71–74] In SCD, increased levels of free heme, thrombin, and histamine are also known to induce endothelial P-selectin expression.[72,75–77] Elevated expression of P-selectin on activated endothelial cells in SCD promotes leukocyte adhesion and motivates vaso-occlusion.[70,78] P-selectin has also been shown to mediate formation of platelet-neutrophil aggregates, which is further enhanced by hypoxia/reoxygenation in SCD.[69,70]

Hemolysis of sickle red blood cells results in activation of endothelial cells leading to increased expression of pro-adhesive molecules, such as P-selectin, ICAM-1, and E-selection. Free heme released during intravascular hemolysis in SCD activates endothelial toll-like receptor-4 signaling, resulting in Weibel-Palade body degranulation and NF-kB pathway activation.[79] Furthermore, hemolysis results in increased release of von Willebrand factor and other pro-coagulopathic proteins from the endothelium, which results in increased adhesion of not only sickle red blood cells, but also neutrophils, monocytes and platelets.[69,70,80] Plasma heme concentrations are also related to neutrophil extracellular trap formation, which significantly contributes to SCD pathogenesis.[81,82] Additionally, a significant amount of microparticles are released from red blood cells, white blood cells, endothelial cells, and platelets that further elevate inflammation and oxidative stress in SCD.[83]

1.3.4 Hypoxia reperfusion injury

Recurrent episodes of vaso-occlusion in SCD results in recurrent hypoxia reperfusion injury and, consequently, a chronically inflamed state. This process is defined in two parts: initial vaso-occlusion causing hypoxic conditions and tissue ischemia, and a secondary state of reperfusion that restores blood flow. Hypoxic conditions in the microvasculature activate the anerobic metabolism and lactic acid production, which contribute to calcium overload, ROS production, and endothelial P-selectin activation. Functionally, these processes are known to initiate apoptosis,

elevate levels of inflammatory stimuli, modify cell surface marker expression on leukocytes and endothelial cells, and affect nitric oxide availability.[84–88] Reperfusion injury further contributes to a proinflammatory environment and adds to microvascular dysfunction and damage. The biologic process of hypoxia reperfusion injury may manifest clinically to patients as ACS, priapism, pulmonary hypertension, or acute kidney injury. Patients with SCD undergo many cycles of hypoxia and reperfusion, which is a significant contributor to overall morbidity.[85,87,88] In recent years, increased attention has been paid to hypoxia/ischemia reperfusion injury as a driving mechanism of SCD pathology.[62,86–88] While hypoxia and reperfusion are classically thought to induce harmful inflammatory responses associated with apoptosis and symptom onset, a remarkable trait of reperfusion injury is that certain mild or cyclic periods of low oxygen may instead provoke a conditioning effect that ameliorates subsequent severe reperfusion injury.[84,87,89,90] Previous attempts to identify mechanisms that initiate this pro-survival phenotype are incomplete and contradictory.[87,88,91,92] Although some studies have begun to examine the effect of hypoxia/ischemia preconditioning on various organs and tissue compartments,[93,94] the effect on the microvasculature itself is largely unexplored. A better understanding of hypoxia reperfusion's conditioning effect on the endothelium in SCD may inform our overall understanding of SCD pathophysiology and offer insight towards therapeutic intervention.

1.3.5 Vaso-occlusion

Collectively, the mechanisms discussed above work together to prime small microvasculature (such as post-capillary venules) for endothelial adhesion and subsequent microvascular occlusion in SCD.[95,96] The microvasculature in SCD may be chronically inflamed due to hypoxia reperfusion, oxidative stress, and cellular activation, further increasing adhesivity and promoting vaso-occlusion. In particular, increased endothelial expression of selectins (P-selectin and E-selectin), vascular cell adhesion molecules (VCAM-1 and ICAM-1), and leukocyte chemo-attractants (IL-8) are observed in SCD, characterizing an activated/inflamed state that has profound effects on adhesion and occlusion.[70,97–99] Additionally, sickle red blood cells have been shown to overexpress several adhesion molecules (including alpha-4β1 integrin, platelet glycoprotein 4, and Lutheran/basal cell adhesion molecule), which results in a highly adhesive membrane.[20,100] Activation of other circulating blood components in SCD further encourages adhesion to the endothelium. For example, activated neutrophils express high levels of alpha-MB2 integrin[101] and activated platelets express high levels of both P-selectin and αIIbβ3 integrin, all of which enhance adhesivity.[69] VOC can be initiated in a multitude of ways: adhesion of a sickled red blood cells or platelets to the endothelium, formation of platelet-neutrophil aggregates in circulation that are more likely to become adhered, sticking between rolling neutrophils and an activated endothelium, or other variations.[20] Each small event

can add to the state of chronic inflammation and activation in the microvasculature, demonstrating the complexity and redundancy of SCD pathophysiology.

The complex pathophysiology of SCD is initiated by changes in the hemoglobin and red blood cell membrane, but modern research has demonstrated that the endothelium and other biological factors also contribute considerably to VOC onset. The work in this thesis strives to better understand the occlusive relationship between hypoxia, the endothelium, and red blood cells in SCD. It is critical to better understand VOC and the factors contributing to its incidence to best prevent its occurrence in the patient population.

1.4 Therapeutic Challenges Underscore Need for Further Research

Despite decades of research, treatment options for SCD remain extremely limited. The chemotherapy agent hydroxyurea was FDA-approved for SCD in 1998 and has remained the most effective disease modifying drug since. After two decades of minimal progress, three additional pharmaceuticals (L-glutamine, Crizanlizumab, and Voxelotor) were approved under orphan designation between 2017 and 2019 with variable success.[102] In addition to these drugs, patients often rely on intravenous fluid (IVF), pain management, and transfusion therapy. Advancing technologies such as hematopoietic stem cell transplant and gene therapy offer curative hope yet remain out of reach for most with the disease. The available SCD therapies and interventions are discussed below.

1.4.1 Pharmaceutical agents

Hydroxyurea (HU, also referred to as hydroxycarbamide) (Hydrea, Droxia) is a ribonucleotide reductase inhibitor used to induce fetal hemoglobin (HbF) production in patients with SCD. Hydroxyurea has been the most effective disease modifying therapy since it was first tested in SCD in 1984.[103,104] Induction of HbF counteracts HbS, reducing HbS polymerization, cell sickling, and VOC. Hydroxyurea has also been shown to reduce expression of inflammatory adhesion molecules that contribute to adhesion and occlusion, notably E-selectin, P-selectin, ICAM-1, and VCAM-1,[104] as well as alpha4beta1 integrin and CD36.[104] HU use can be associated with mild toxicity involving cytopenia and bone marrow suppression. Other adverse effects can include dermatologic changes, headache, and gastrointestinal symptoms such as nausea or abdominal discomfort.[104,105] There are additional concerns regarding the effect of HU on fertility for both men and women, and there is insufficient data to conclude that it is safe to take during pregnancy.[106] Patient compliance with HU is generally low (with estimates between 49% and 85%), and may be attributed to a variety of factors including provider-related prescription bias, patient-related fear of toxicities and adverse effects, and socio-economic-related inability to obtain and afford treatment.[106]

L-glutamine (Endari) is a pharmaceutical agent used to reduce oxidative stress and, consequently, the incidence of VOC in SCD. L-glutamine is an essential amino acid critical in the production of nicotinamide adenine dinucleotide (NAD) and required in high levels by sickle red blood cells. It is thought to raise the

NAD redox ratio in sickled red blood cells and reduce painful VOC.[107,108] In 2017, the FDA approved L-glutamine to reduce acute complications of SCD. The phase III trial showed significantly fewer pain crises and hospitalizations in the L-glutamine group than the placebo (3:4 pain crises and 2:3 hospitalizations, respectively). However, patients treated with L-glutamine did experience low-grade nausea, fatigue, noncardiac chest pain, musculoskeletal pain.[108,109]

Crizanlizumab (Adakveo) is a humanized monoclonal antibody used in the prevention of VOC in SCD patients. Crizanlizumab functions as an anti-adhesion therapy by selectively binding P-selectin and blocking interaction with associated P-selectin glycoprotein ligand-1.[110,111] Crizanlizumab acts by binding to and inhibiting P-selectin in a dose-dependent manner, thereby reducing adhesion to the endothelium and lowering incidence of VOC. In November 2019, the FDA granted accelerated approval for Crizanlizumab as an orphan drug based on the results of the phase II SUSTAIN trial. Initial reports suggested a reduction in median time to VOC (4.1 vs. 1.4 months) and annual rate of VOC (1.63 vs. 2.98 per year) for the treatment group when compared to placebo.[109,111–114] However, Novartis was forced to recall Crizanlizumab in the U.K. in February 2024 after the U.K. Medicines and Healthcare products Regulatory Agency revoked its conditional approval due to failure to significantly reduce annual incidence of VOC.[115] Adverse effects due to crizanlizumab were uncommon, but included headaches, nausea, and back pain.[116,117] Additionally, crizanlizumab is delivered

as a monthly intravenous infusion, which adds an additional barrier to treatment compared to oral/pill delivery.[116]

Voxelotor (Oxybryta, previously GBT440) is a hemoglobin oxygen affinity modulator that has been used to treat SCD. By increasing the affinity of hemoglobin for oxygen, Voxelotor inhibits HbS polymerization under hypoxic conditions. It was shown to reduce incidents of intravascular hemolysis while increasing hemoglobin levels in Phase I/II studies.[26,111,118] However, Pfizer voluntarily withdrew all lots of Voxelotor worldwide and discontinued all ongoing trials in September 2024 due to indications that the benefits of treatment no longer outweighed the risks.[119] Side effects could also be significant, with many patients reporting adverse effects such as headaches, gastrointestinal upset, joint pain, fatigue, and rashes.[117]

Perfusion of saline or IVF can also be used to help mitigate SCD-related complications such as VOC by reducing incidence of red blood cell sickling.[120,121] A number of studies have demonstrated the importance of saline composition in SCD, including some studies performed in microfluidic devices.[122–124] However, there is limited clinical evidence supporting the use of IVF in SCD and more randomized controlled trials could be done to better clarify their safety and efficacy as disease management.[121]

1.4.2 Pain management

Due to the lack of effective treatments, many patients with SCD require pain management to cope with VOC. Opioids, acetaminophen, and NSAIDs are commonly used to control pain and reduce inflammatory load.[29] In particular, the use of NSAIDs has been suggested to control mild-to-moderate pain while counteracting elevated inflammatory markers in SCD and also providing an opioid-sparing effect.[125] The use of pain management comes with additional risks including organ damage and opioid dependence.

1.4.3 Transfusion therapy

In addition to pharmaceutical interventions, blood transfusion is widely used to mitigate VOC in SCD. Transfusion usage for SCD patients has increased in recent years due to improved transfusion safety and increased evidence of efficacy.[126] Transfusions provide temporary disease improvement by increasing the oxygen-carrying capacity of the blood and decreasing the concentration of HbS in relation to HbA. Collectively, these modifications can prevent or reverse the complications of vaso-occlusive events.[126–128]

Transfusions may be utilized in a number of indications, such as pre-operative treatment and symptom prevention.[129] Surgery and general anesthesia present an increased risk of complications for many SCD patients.[35] Compared to non-transfused SCD patients, preoperative transfusions were shown to

significantly reduce incidence of clinically important complications (15% vs. 39%) with a particularly noticeable reduction in ACS (3% vs. 27%).[130] Transfusion therapy can also be used as a preventative or therapeutic measure against ACS. Patients undergoing chronic transfusions showed a decrease in hospitalization rate for ACS (2.2 vs. 15.7 events per 100 patient-years).[131] Separate studies have verified these conclusions: Miller et al. concluded that patients undergoing chronic transfusions experienced fewer ACS adverse events (1.81 vs. 14.35 events per 100 patient-years, $p<0.001$) than patients in the observation group,[132] and Hankins et al. demonstrated that children with recurrent or unusually severe cases of sickle-related ACS saw a significant improvement in ACS frequency after undergoing chronic transfusion.[133] Additionally, transfusion therapy may be used as a preventative measure for patients with a high risk of stroke. Stroke has been shown to recur in 60-90% of SCD patients with no therapeutic intervention,[134] but chronic transfusions can provide a significant reduction in stroke recurrence.[131,135–137]

Transfusion therapy provides substantial benefit in the prevention and treatment of SCD-related complications, but unfortunately it carries its own risk of complications such as alloimmunization, infection, and iron overload. Alloimmunization is a complication of red blood cell transfusion in which the body induces an immune response to foreign antigens from a blood donor. This complication can expose the patient to increased risk of delayed hemolytic transfusion reactions, which can further incite SCD pathophysiology. Furthermore, accumulation of antigens increases difficulty in finding appropriate blood units for

future transfusions.[138,139] The risk for alloimmunization is particularly high for patients who are undergoing chronic transfusion therapy.[140] In observational studies, only about 1-5% of the general population have reported alloimmunization, whereas upwards of 50% of transfused SCD patients have been shown to develop significant alloantibodies[139–142] Unfortunately, many patients with SCD in the United States are at an especially heightened risk for alloimmunization due to antigenic differences between patients (predominantly of African descent) and blood donors (predominantly of European descent).[138,143]

Transfusion presents several risks, including the potential for donor transmitted infection. Improved donor screening has substantially reduced the risk of transfusion-transmitted infections in the U.S. (less than one in a million units of blood); however, it remains a potential adverse effect for those receiving chronic or frequent transfusions, especially those in developing countries without the assurance of advanced screening procedures.[144] Frequent transfusion therapy also results in an accumulation of iron in the blood, which can lead to severe complications.[145] SCD patients with iron overload have been shown to have an increased risk of organ failure (71% vs 19%), pain episodes (64% vs 38%), and mortality (64% vs. 5%) compared to patients with low serum ferritin and percent transferrin saturation levels.[146] Iron overload may also present a proinflammatory effect in some patients that has the potential to aggravate other SCD pathologies.[146,147] Overall, these risks highlight the drawbacks and limitations of transfusion therapy for SCD treatment.

1.4.4 Emerging technologies

A number of developing technologies are now being tested for SCD including stem cell transplantation and gene therapy/gene editing. Hematopoietic stem cell transplantation (HSCT) with allogenic or haplo-identical donors is currently the only curative strategy for SCD. Gene therapy, including CRISPR-Cas methodologies, is also an active and growing area of translational research with encouraging results. Two cell-based gene therapies (Casgevy and Lyfgenia) have recently been FDA-approved in the treatment of SCD. Casgevy employs CRISPR-Cas9 genome editing technology to modify the DNA of patient hematopoietic stem cells. Specifically, this editing results in increased production of HbF and therefore reduced red blood cell sickling.[149] Lyfgenia uses a lentiviral vector to genetically modify a patient's blood stem cells to product HbA^{T87Q}, a form of hemoglobin that functions similarly to HbA, therefore reducing red blood cell sickling and VOC.[149] While these treatments are truly groundbreaking, both HSCT and gene therapy treatments have significant limitations including high cost, poor donor availability, and potentially fatal complications. Access to these treatments also remains extremely limited, especially in low-income countries where most patients with SCD reside.[96,150,151]

SCD is a complex, multi-system disorder characterized by lifelong acute and chronic complications. It is critical to understand the pathophysiology of SCD at the molecular and cellular levels in order to design more effective therapies. In this chapter, we provided a comprehensive review of SCD and its impact. In the

next chapter, we will examine technologies and methodologies that have been used to study hematologic disorders like SCD and identify the gaps in literature that this thesis aims to address.

Chapter 2: Overview of Existing Models and Methodologies

2.1 Microfluidic Models to Study Hematologic Disease

Microfluidic technology offers a unique approach to simulate micro-scale physiologic environments while allowing for precise control of fluid flow and shear stress. It offers numerous benefits over in vivo animal research including optical accessibility, higher throughout, customization, and simplicity of fabrication. In vivo animal models are exceedingly complex, but often fail to reliably inform human trials.[152,153] Studies have suggested that merely one third of highly cited animal research translates to human randomized trials, despite the significant cost and burden associated with in vivo research.[152,153] Unlike animal models, microfluidic devices can easily integrate patient-derived cell lines or blood samples to better capture patient heterogeneity and improve relevance to human studies. Whereas imaging in vivo can be extremely challenging and often requires the use of specialized imaging tools, microfluidic technology is compatible with modern microscopy methods. As a result, microvascular processes can be visualized in real-time using standard laboratory microscopes. Additionally, device geometry, fluid flow rates, shear stresses, etc. may be directly controlled and modified by the researcher which allows for highly customizable experimental conditions. Microfluidic fabrication is also high throughput and cost-effective compared to expensive, lengthy animal studies.

The first evidence of SCD research being performed in microfluidics dates back to 2007, in which Higgins et al. modeled sickle vaso-occlusion and rescue in a microfluidic device.[154–156] They demonstrated that it is possible to "evoke, control, and inhibit" SCD vaso-occlusive or jamming events on-chip using an oxygen-tunable microfluidic platform.[154] This study laid the groundwork for more complicated microfluidic models of SCD. Since 2007, use of microfluidics to study SCD has increased rapidly, growing from just 3 publications by 2010 to 43 publications by 2020.[156] Numerous types of microfluidic models have become essential in the study of hematologic diseases. In particular, the use of oxygen-tunable microfluidics, occlusion/thrombosis microfluidics, and endothelialized "vessel-on-a-chip" microfluidics have been well documented. A brief review of relevant literature in this field is summarized below.

2.2 Oxygen-Tunable Microfluidics

The ability to control oxygen concentration within a microfluidic device has substantial value when investigating SCD. As discussed in Chapter 1, hemoglobin polymerization and red blood cell sickling are oxygen-dependent processes that occur more readily in low oxygen/hypoxic environments. Due to this, low oxygen microvasculature such as the capillaries and post-capillary venules are often associated with cell sickling, adhesion, and vaso-occlusion. When modeling these microvascular systems, oxygen concentration may be controlled to better mimic the native environment. In doing so, researchers can induce hemoglobin

polymerization, red cell sickling, and resultant vaso-occlusion in a microfluidic device. Additionally, hypoxia reperfusion injury is a key process in SCD's complex pathophysiology. Hypoxia reperfusion injury occurs in two parts: (1) initially, a vaso-occlusive event blocks blood flow and cuts off oxygen to surrounding vasculature and tissues, then (2) during reperfusion oxygen is restored, resulting in an inflammatory response. The ability to control oxygen in a microfluidic device could also be useful in simulating periods of hypoxia and reperfusion.

Researchers have developed multiple methods to control oxygen in microfluidic platforms in order to better study SCD. For example, Kim et al. introduced a microfluidic device in 2017 that utilized a tubing-based micro-gas exchanger to deliver various oxygen concentrations. The micro-gas exchanger was comprised of two concentric tubes – the inner, gas-permeable and the outer, gas-impermeable – which allowed for mixing of gas within the exchanger and delivery of gas at either complete hypoxia or normoxia.[157] In their study, they concluded that sickle red blood cells exhibited greater adhesion under hypoxia than normoxia.[157] However, these experiments were only performed in fibronectin or laminin coated devices and therefore only quantified the adhesion of sickle red blood cells to extracellular matrix proteins, neglecting the complex factor of endothelial cells. Similarly, Papageorgiou et al. showed that environmental hypoxia significantly enhanced sickle red blood cell adhesion via hypoxia-driven red cell sickling, but their work was performed in devices without any biological factors.[158]

As mentioned above, Higgins et al. pioneered the space of oxygen-tunable microfluidics in the study of SCD. They utilized a multi-layer polydimethylsiloxane (PDMS) microfluidic device that integrated a gas reservoir layer, diffusively coupled to an attached microvascular layer. These layers were separated only by a 100 μm PDMS membrane. Since PDMS is gas-permeable, an injected gas mixture could diffuse rapidly from the gas reservoir through the PDMS membrane and into the microvascular layer. This design was fundamental for a number of ensuing studies[159–161] and provided the basis for our group's oxygen-tunable microfluidic designs as well.[162–169] Many of these studies specifically investigated sickle red blood cells under hypoxia, answering questions about rheology, viscosity, and therapeutic effect of SCD drugs on red blood cells. For example, Wood et al. utilized a similar device in 2012 to assess fluidic conductance as a measure of blood rheology and correlated this with SCD severity.[160] In our group specifically, Valdez et al. utilized an oxygen-tunable platform for the quantification of oxygen-dependent viscosity and shear thinning in sickle blood[165] while Hansen et al. investigated effect of several therapies on blood rheology and oxygen saturation.[166,167] However, little work has been done to examine the relationship between hypoxia, red blood cells, and the endothelium in SCD.

2.3 Occlusion Microfluidics

Since Higgins et al. first demonstrated recapitulation of VOC on-chip in 2007, a number of groups have developed microfluidic devices to more thoroughly

investigate vaso-occlusion. Man et al. introduced the OcclusionChip in 2020 which presented a new microfluidic platform for the investigation of the occlusion index, a metric indicative of red blood cell deformability and associated microcapillary occlusion frequency.[170] The OcclusionChip was designed to mimic capillary bed architecture so that it could measure red blood cells' ability to navigate through microcapillaries. Their study included modulation of hypoxia and ultimately concluded that hypoxia treatment is correlated with higher occlusion index in SCD. Their group went on to use the OcclusionChip in several other works, demonstrating its use as an alternative to ektacytometry for detection of small-fraction red blood cell populations with abnormal deformability.[171] The OcclusionChip showed promise as a means of deformability measurement, but only examined occlusion at the capillary level and did not account for any other biological components contributing to occlusion (endothelial cells, white blood cells, platelets, or activation of any of these components).

On the other hand, some groups have developed endothelialized models to study occlusion in SCD. In 2011, Tsai and Kita et al. introduced an endothelialized microfluidic model and used it to model microvascular occlusion and thrombosis of hematologic disease. In the context of SCD, they showed that samples from SCD patients actively taking HU exhibited lower average red blood cell velocity on-chip and also resulted in significantly more microchannel obstruction.[172] These experiments were groundbreaking in the endothelialized microfluidic space, inspiring a number of later studies and helping to direct the work presented in this

thesis. In response to the spike in microfluidic-based occlusion assays, Fay et al. developed an open-source software tool for analyses of adhesion and occlusion on-chip, further demonstrating the emerging appeal of this field.[173]

2.4 Endothelialized Microfluidics

Recently, the use of endothelialized or “vessel-on-chip” microfluidic devices has become more common. This is largely due to their ability to more accurately recapitulate the cellular, physical, and hemodynamic environment of the microvascular system in the body. In 2012, Myers et al. published an article in Journal of Visualized Experiments (JoVE) detailing a method to produce endothelialized models, inspiring numerous others in the field.[174] The group went on to develop a series of several different types of endothelialized models, including the endothelialized occlusion model by Tsai and Kita mentioned above.[172] They effectively used this platform to investigate platelet aggregation and thrombus formation in hematologic disease. This platform offered a more physiologically relevant platform for the investigation of thrombosis in disease.

Vascularized microfluidics have been widely used to investigate adhesion to the endothelium. In 2018, Kucukal et al. demonstrated that sickle red blood cells adhere more often to heme-activated endothelial cells compared to non-activated endothelial cells.[175] Additionally, they showed that two distinct patient subpopulations could be identified, stratifying adhesion incidence with clinical

phenotype. However, it should be noted that these results were generated from a 2-dimensional endothelial monolayer, rather than a 3D endothelial-lined microvascular system. Additional insight could be gained by performing these experiments under 3-dimensional physiologic conditions.

Endothelialized microfluidics have also been extensively used to study other hematologic disorders. In 2023, Beckman et al. used endothelialized microfluidics to investigate the effect of JAK-STAT inhibitors. Ultimately, they showed that these inhibitors prevented increased leukocyte-endothelial adhesion and reduced upregulation of prothrombotic pathways in myeloproliferative neoplasms.[176] Moreover, Sakurai et al. published a vascularized bleeding model in 2018 that effectively integrated multiple components of hemostasis.[177] In their model, they were able to visualize and characterize vascular injury, showing that hemophilia A blood exhibits unstable hemostatic plug formation and altered fibrin architecture.[177] Overall, these endothelialized microfluidic devices show the ability of physiologic models to more accurately investigate underlying mechanisms of hematologic disease.

2.5 Leveraging Next Generation Sequencing with Microfluidic Technology

The field of next generation sequencing (NGS) has been advancing rapidly over the last few decades, enabling investigation into biological pathways and uncovering numerous factors that contribute to disease. In the field of SCD, RNA

sequencing ("RNA-seq") has been utilized to investigate modulation of whole blood gene expression profiles between those with SCD and healthy controls,[178] and also between SCD samples taken amid crisis (ACS or VOC) with those taken at baseline.[179] In particular, these studies showed pathway enrichment of hemoglobin associated genes and ubiquitin-proteasome genes in SCD compared to control,[178] and also demonstrated that IL-10 signaling, inducible nitric oxide synthase (iNOS) signaling, IL-6 signaling, and B cell signaling pathways were most modulated during VOC.[179] These studies indicate that RNA sequencing can be a powerful tool to uncover changes in gene expression in the disease state.

In 2021, Mathur et al. performed RNA sequencing on blood outgrowth endothelial cells (BOECs) in parallel to endothelialized microfluidic studies to investigate SCD.[180] They compared differential gene expression results from RNA sequencing to platelet adhesion readouts from their endothelialized microfluidic device, ultimately correlating severity of SCD phenotype with extent of endothelial activation. However, the RNA was extracted from BOECs cultured in 2D on flasks, rather than from microfluidic devices. It is well known that culturing endothelial cells under flow and shear stress modulates their gene expression and endothelial phenotype.[181] Therefore, a more accurate differential gene analysis result could have been gained via RNA extraction of cells cultured on-chip.

Only recently has NGS been leveraged to examine the gene expression profile of cells cultured on-chip in a microfluidic platform. In November of 2024, Caruso et al. published work in which endothelial cells were extracted from

microfluidic devices to undergo single cell RNA sequencing.[182] In their study, researchers examined the differential gene expression of an endothelium exposed to a less deformable heterogenous red blood cell perfusion compared to a healthy homogenous red blood cell perfusion.[182] This study was the first of its kind to extract cells from endothelialized microfluidic devices to perform RNA sequencing, paving the way for more to come.

2.6 Gaps in Knowledge

Together, it is noted that endothelialized microfluidics, occlusion chips, and oxygen-tunable devices each offer distinct advantages in the study of SCD. However, no model exists that combines each of these key biological components, and therefore researchers are unable to fully recapitulate the native environment in SCD. Therefore, we anticipated significant value in the development of a novel platform that collectively merged these features, successfully integrating multiple physiologic characteristics of SCD. In particular, we set out to develop a microfluidic platform that included three-dimensional endothelial-lined microchannels with physiologically relevant shear stresses in an oxygen-tunable environment, thus enabling simulation of hypoxia reperfusion and red blood cell sickling/occlusion. Additionally, we sought to develop a method for RNA sequencing of cells cultured on-chip to explore hypoxia-induced endothelial modulation. Our proposition is that development of a more physiologically relevant model will also yield more accurate conclusions about the underlying mechanisms

and biological processes driving SCD. Ultimately, these conclusions could be more informative in the development of effective therapies for SCD patients.

Historically, red blood cells (and specifically, hemoglobin), have been recognized as the driving force of SCD pathology, but new research is drawing attention to the critical role of the endothelium in adhesion and vaso-occlusion. Conclusions from a number of previous studies have excluded this critical biological component in their modeling; consequently, drawing less reliable conclusions from acellular or protein-coated microchannels. Only recently have researchers begun to add endothelial cells to their models to better mimic the biological environment. However, even fewer of these models incorporate full 3D microvascular channel lumens (as opposed to a 2D monolayer) or are designed at relevant size scales with appropriate fluid flow and shear stresses. Our model intends to improve upon foundational work in this field, creating a more physiologically accurate model that will ultimately yield more reliable and informative biological results.

It was also noted that the research surrounding hypoxia reperfusion injury in SCD was incomplete and often contradictory. Being a predominant and complex component of SCD pathophysiology, hypoxia reperfusion must be properly understood in order to design effective therapies. We set out to better comprehend the effects of hypoxia reperfusion on the endothelium and its corresponding contributions to VOC. Our goals, detailed below, focus on the investigation of hypoxia-induced endothelial modulation and its effect on vaso-occlusion in SCD

using our novel microfluidic platform. The results from these studies will offer a better understanding of the mechanistic changes affecting the endothelium during hypoxia reperfusion injury and also support the hypothesis that hypoxia reperfusion may offer a protective effect against vaso-occlusion in SCD.

2.7 Goals and Hypotheses

The objectives of this work are centered around gaining a better understanding of the underlying mechanisms of VOC in SCD. In particular, this thesis takes a direct look at hypoxia reperfusion injury to better understand its contribution to SCD severity. To do so, it was necessary to develop a more physiologically relevant microfluidic model that incorporates key biological components of SCD. This microfluidic platform has been used to examine the effects of hypoxia preconditioning on the endothelium and associated changes in VOC incidence. The specific aims guiding this work are consist of:

Aim 1: Develop a more physiologically relevant microfluidic model of SCD that integrates pertinent biological features of the disease. We hypothesize that the incorporation of three-dimensional endothelial-lined microchannels with physiologically relevant shear stresses in an oxygen-tunable environment will enable more accurate recapitulation of the SCD microvasculature and therefore offer a more informative tool for research. This aim will be discussed in Chapter 3.

Aim 2: Design and implement an occlusion assay on-chip to examine the effects of hypoxia preconditioning on the likelihood of VOC in SCD. We hypothesize that hypoxia preconditioning (either sustained or cyclic hypoxia) will condition the endothelium, making it less susceptible to microvascular occlusion. This aim will be discussed in Chapter 4.

Aim 3: Leverage NGS technology to investigate hypoxia-induced endothelial modulations that affect occlusive likelihood in SCD. We hypothesize that hypoxia preconditioning will modulate a number of genes in key gene ontology pathways affecting VOC such as cellular adhesion, blood coagulation, and inflammation. This aim will be discussed in Chapter 5.

This chapter has effectively synthesized relevant literature on existing microfluidic models and methodologies to study SCD. The work presented in the remainder of this thesis aims to address the limitations of previously established models and also to better inform our understanding of SCD pathophysiology. The following chapters will outline the methodologies, results, and insights gained from each of these studies.

Chapter 3: A Novel Microfluidic Platform to Study Sickle Cell Disease

3.1 Introduction

Sickle cell disease (SCD) is an inherited autosomal-recessive disorder caused by a point mutation in the gene encoding hemoglobin subunit β that affects millions of people worldwide.[1,3,5] When deoxygenated, unbound sickle hemoglobin can polymerize into rigid fibers, distorting red blood cell morphology and resulting in cell sickling.[22–24] Hemoglobin polymerization and red blood cell sickling initiate a cascade of downstream effects in SCD including impaired hemorheology, hypoxia/ischemia reperfusion injury, endothelial dysfunction, inflammation, nitric oxide deficiency, oxidative stress, hypercoagulability, and painful vaso-occlusion.[20,98] Together, these complex processes contribute to a multisystem disorder, marked by lifelong acute and chronic complications throughout the body.[28–30,32,37,43] This contributes to significant morbidity, diminished quality of life, and decreased life expectancy.[25,26]

Despite its discovery over a century ago, treatment options for the millions of SCD patients worldwide remain remarkably limited. Existing models have failed to reliably inform clinical trials, with only 11.8% of orphan drug studies in the last 20 years bringing about approvals.[102] Therefore, a better understanding of the underlying mechanisms of SCD is needed to discover how these complex processes can be modulated to further reduce morbidity and mortality.

Numerous types of microfluidic models have become essential in the study of hematologic diseases including SCD due to their optical accessibility, high throughput, cost effectiveness, and ease of integration with human cell samples. Microfluidic models that are humanized (those that include human cell types in physiologic environments) have the potential to more reliably inform clinical trials than 2D in vitro studies, animal work, or microfluidic systems lacking biological relevance. Recently, the use of endothelialized microfluidics and vasculature-on-a-chip methods have been well documented as a means of investigating endothelial contribution to disease.[172,174,177,183–190] For example, Tsai et al. presented a novel endothelialized microfluidic platform in 2012 that simulated thrombosis and microvascular occlusion in SCD and other hematologic diseases.[172] They used this platform to investigate the role of platelet aggregation, thrombus formation, and also effects of various treatments. Additionally, a number of groups have utilized acellular devices in the study of microvascular occlusion.[161,170,171,191] Man et al. introduced the OcclusionChip in 2020 which presented a new microfluidic platform for the investigation of the occlusion index, a metric indicative of both red blood cell deformability and associated microcapillary occlusion frequency.[170] Their study incorporated elements of hypoxia, and ultimately correlated hypoxia treatment with a higher occlusion index for SCD samples. Separately, our group has recently pioneered hypoxia-tunable microfluidics for the study of red blood cell rheology in SCD.[162,165–167,169] In particular, Valdez et al. utilized this platform for the quantification of oxygen-

dependent viscosity and shear thinning in SCD blood,[165] while Hansen et al. investigated the effects of several therapies on blood rheology and oxygen saturation.[166,167] Together, it was recognized that endothelialized microfluidics, occlusion chips, and oxygen-tunable devices each offer distinct advantages in the study of SCD.

Overall, these studies show the ability of physiologic models to more accurately investigate underlying mechanisms of hematologic disease, but currently, no model exists that integrates each of these key biological components to effectively study the underlying contributors to vaso-occlusive crisis (VOC) in SCD. Accordingly, we developed a microfluidic platform that includes three-dimensional endothelial-lined microchannels with physiologically relevant shear stresses in an oxygen-tunable environment, thus enabling simulation of hypoxia reperfusion and vaso-occlusion in one unified system.

In this chapter, we detail the methodologies used and the validation studies performed to assess the utility of our microfluidic platform in SCD research. In particular, we show that this model is capable of culturing endothelial cells in physiologic vessel structures. Additionally, these vascular networks can survive treatment with hypoxia to simulate incidences of low oxygen in the body or localized hypoxia reperfusion. And lastly, these endothelialized models can be used to model blood flow, adhesion, and vaso-occlusion using SCD patient blood samples.

3.2 Materials and Methods

3.2.1 Microfluidic device design

The microfluidic device consists of three layers: (1) a gas layer to modulate oxygen tension in the device, (2) a hydration layer to maintain humidity and prevent cell dehydration, and (3) an endothelialized cell layer that mimics a network of microvascular channels (Figure 3.S1). The branching vascular network resolves into 32 individual channels, each measuring 60 μm wide by 50 μm tall. The cell layer geometry is inspired by similar vascular networks on-chip, which allow for observation of a large number of microchannels in parallel.[154,174,183,186] The gas and hydration layer geometries are modified from our lab's previous designs, in which hypoxia has been used to examine sickle cell rheological properties in microfluidics lacking endothelium.[162,165–167,169] These two layers directly overlap the cell layer's vascular network. Oxygen tension in the gas layer is diffusively coupled to the cell layer via the gas permeability of PDMS. Because of this, oxygen level can be rapidly modulated in real-time to initiate red cell sickling or simulate localized hypoxia within the device. The geometry for each layer was designed in AutoCAD (Autodesk) and printed onto mylar photomasks (Fineline Imaging). The diffusive properties of similar devices have been previously validated with modeling software (COMSOL Multiphysics).[165]

3.2.2 Microfabrication

The microfluidic device is composed of polydimethylsiloxane (PDMS) and is fabricated from silicon wafer molds using photolithography and soft lithography techniques. Individual silicon wafers were first fabricated using SU-8 negative photoresist (SU-8 2100, SU-8 3050, Kayaku Advanced Materials) and mylar photomasks at the Minnesota Nano Center. The gas layer was placed in a petri dish and cast with a 1:10 ratio of PDMS curing agent to base (Sylgard 184, Dow Corning) at a thickness of approximately 6 mm. The dish was placed in a desiccator to degas any air bubbles, then the PDMS was cured by baking in an oven at 75°C for 2 hours.

Meanwhile, the hydration and cell layers were cast via PDMS compression molding as previously described by our lab,[165] creating 100 μm PDMS membranes between each layer. Briefly, this process involved (1) modifying silicon wafers by attaching 100 μm-thickness microscope slides with cyanoacrylate adhesive, (2) fastening of silicon wafers to plastic transparency sheets via double sided adhesive tape, (3) pouring a thin layer of degassed liquid PDMS over the wafer, (4) rolling of plastic transparency sheeting over exposed PDMS, (5) transferring the wafer to a hotplate and covering with a cylindrical weight to apply compression, (6) setting the hotplate to 75°C for 2 hours or alternatively at 55°C overnight to fully cure the PDMS. Once cured, PDMS layers were punched with either 18-gauge needles (gas layer) or 1mm biopsy punches (hydration and cell layers) to create inlet/outlet ports. The layers were adhered to each other and affixed to a glass microscope

slide via oxygen-plasma bonding. Each layer was plasma bonded at an oxygen flow rate of 100 cc per minute with 100 W power for either 60 seconds (PDMS to glass) or 120 seconds (PDMS to PDMS) (PE-50, PlasmaEtch).

3.2.3 Cell culture

Pooled donor human umbilical vein endothelial cells (HUVECs) were obtained from ATCC. HUVECs were maintained in a humified incubator at 37°C with 5% CO_2 and cultured aseptically with endothelial cell growth medium-2 (EGM-2) (Lonza). EGM-2 culture media contained basal medium, appropriate supplement kit, 2% fetal bovine serum (FBS), and antibiotic-antimycotic (Gibco). In addition to HUVECs, human lung microvascular endothelial cells (HMVEC-Ls) obtained from Lonza were also used in a small number of studies to validate methodology across multiple cell types (Figure 3.S2). HMVEC-L culturing conditions were identical except for the use of microvascular endothelial cell growth medium-2 supplement kits (EGM-2 MV) in place of EGM-2 supplement kits. Cells were handled according to manufacturer's recommended techniques. All cells were verified to be mycoplasma contaminant-free via the LookOut Mycoplasma Detection Kit (Sigma-Aldrich) and were used between passages 3-7.

3.2.4 Microfluidic device endothelialization

Microfluidic endothelialization methodology was optimized for this device's specific geometry and scaling. A schematic overview of the endothelialization process is included below (Figure 3.1).

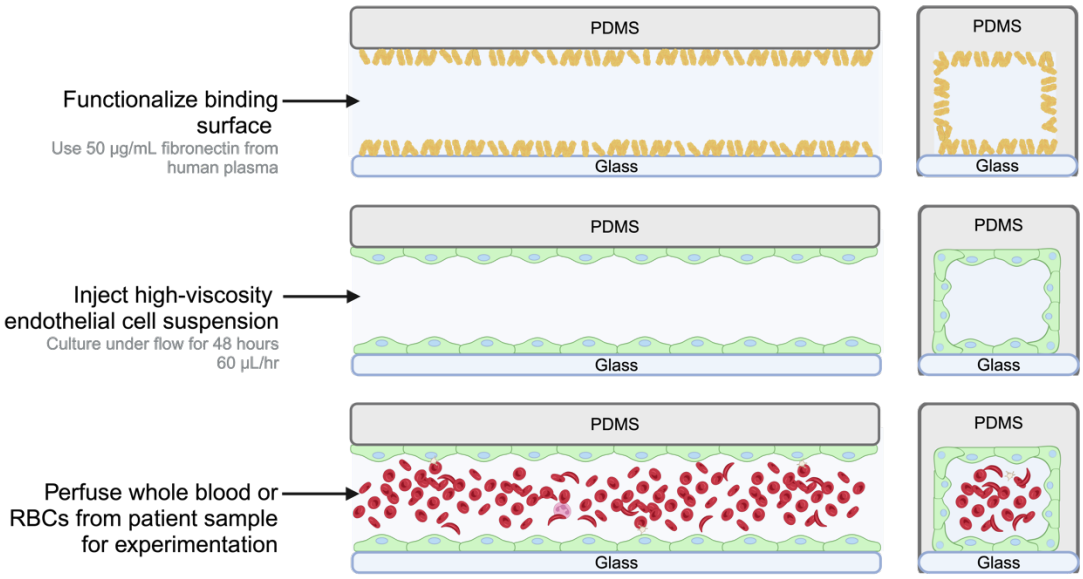


Figure 3.1: Schematic of endothelialization procedure. A visual summary of the device endothelialization process is included here, including functionalization, cell seeding, and incubation under flow. After a confluent, aligned cell monolayer has been formed, endothelialized devices may undergo experimental treatments or blood perfusion. Schematics of microchannel side view (center) and cross-sectional view (right) are included at each step. Created using BioRender.

Microfluidic devices were first sterilized via UV treatment for 30 minutes. Then, a solution of 50 µg/mL fibronectin from human plasma in PBS was added to the device's cell layer via pipetting. Fibronectin is a native extracellular glycoprotein commonly expressed in blood and tissues that makes the device's microchannel walls more amenable to cell attachment. The devices were incubated with fibronectin for approximately 60 minutes, then rinsed twice with HBSS. HUVECs

were grown in cell culture flasks to approximately 80% confluency, then trypsinized and resuspended at a concentration of 15 x 10^6 cells/mL in a solution of 8% dextran-EGM-2 media. The inclusion of dextran in the cell resuspension increases the loading viscosity, thus increasing contact time between endothelial cells and the microfluidic channel walls.[174]

Cell suspension was added via pipette tip, reseeding between 4 to 6 times to achieve desired cell density. Devices were incubated for approximately 90 minutes under static conditions to allow proper cell attachment and spreading. After sufficient cell attachment, syringe pumps (New Era Pump Systems) were used to perfuse EGM-2 media at a consistent flow rate of 60 µL/hr. Initially, flow conditions were based on a publication by Mannino et al, who utilized a flow rate of 73.8 µL/hr to mimic the postcapillary venules and approximate a wall shear stress of ~1 dyne/cm^2 for blood in 30 µm-wide channels.[174] In our system, perfusion at 60 µL/hr approximates a flow rate of 1.875 µL/hr in each of the smallest 60 µm-wide channels, which corresponds to a wall shear stress of ~1 dyne/cm^2 for blood. Endothelialized devices were cultured under these flow conditions for 48 hours to establish a confluent monolayer and encourage cell alignment under physiologic shear.[192]

3.2.5 Immunofluorescence staining of the endothelium

A number of fluorescent stains, probes, and antibodies were used to thoroughly characterize the endothelium (Table 3.1). These materials included

Hoechst 33258 (nucleic acid stain, Invitrogen), CellMask Deep Red (plasma membrane stain, Invitrogen), CD31 conjugated monoclonal antibody (PECAM-1 antibody, Bio-Rad), CD144 monoclonal antibody (VE-Cadherin antibody, Invitrogen), CD106 recombinant antibody (VCAM-1 antibody, Invitrogen), Phalloidin CruzFluor 594 (F-actin stain, Santa Cruz), and cell permeable DAF-2 DA (nitric oxide probe, Santa Cruz). Secondary antibodies such as anti-mouse or anti-rabbit Alexa Fluor 555 and 647 (Invitrogen) were utilized when appropriate.

Antibody	Alias	Source	Catalog Number	Identifier
PECAM-1	CD31	Bio-Rad	MCA1738PE	Clone ID: WM59
VE-Cadherin	CD144	Invitrogen	348513	Clone ID: BV9
VCAM-1	CD106	Invitrogen	MA5-31965	Clone ID: SA05-04
Secondary Alexa Fluor 555	AF 555	Invitrogen	A21422	RRID: AB_2535844
Secondary Alexa Fluor 647	AF 647	Invitrogen	A31573	RRID: AB_2536183

Table 3.1: List of antibodies used in endothelial characterization. Table includes antibody names, aliases, companies of purchase, catalog number, and identifying numbers (either clone ID or resource research identifier).

Blocking buffers were prepared using 1-5% bovine serum albumin (BSA) or 10% FBS in PBS. Where needed, 0.1% TritonX100 or 0.1% Tween20 surfactant was used for permeabilization. DAF-2DA staining was performed on live endothelial cells, while CellMask imaging has been performed on both live and fixed cell cultures. All other stains were performed on cells fixed via 4% paraformaldehyde (PFA). Briefly, endothelialized devices were gently rinsed via pipette with PBS several times. Then, they were incubated with cold 4% PFA for 8

minutes, pipetting every 1-2 minutes to flush new fixative agent through the device. Devices were rinsed with PBS and stored at 4°C prior to staining.

Individualized protocols for each fluorescent material are included below. General care was taken to protect each from exposure to light. Hoechst was used to stain cell nuclei, highlighting cell density and location in microchannels. Hoechst was prepared at a concentration of 1:1000 in PBS and applied for 20 minutes before imaging. Endothelial confluency and alignment were visualized using the CellMask plasma membrane stain. CellMask solution was prepared at a 1:1000 dilution in EGM-2 media or PBS for live or fixed cells, respectively. Staining solution was perfused across endothelium for 15 minutes, then imaged immediately. Devices undergoing antibody staining were blocked overnight, as appropriate. Conjugated (CD31), primary (CD144 and CD106), and secondary antibodies (Alexa Fluor 555 and 647) were prepared at 1:100 - 1:250 in blocking buffer and incubated in blocked endothelialized devices at 4°C overnight. For all staining, redundant wash steps were included throughout to minimize background. Phalloidin was used to label F-actin. Phalloidin solution was made at 1:100 in blocking buffer and incubated in blocked endothelialized devices at 4°C overnight. Nitric oxide production was visualized with the DAF-2 DA fluorescent probe. DAF-2 DA solution was produced at dilution of 1:250 in EGM-2 media and perfused via syringe pump to live endothelialized devices at a rate of 60 μL/hour for 1 hour.

3.2.6 Microscopy and image processing

Microscopy was performed on either a Zeiss Axio Observer widefield microscope or a Nikon AX R confocal microscope. The widefield scope was equipped with an incubation chamber that maintained the environmental temperature to 37°C. Image processing was performed in Zen software (Zeiss), NIS Elements software (Nikon), and FIJI/ImageJ software. Secondary only antibody control and corresponding background subtraction was performed when appropriate.

3.2.7 Hypoxia treatment

A gas mixing system from previous studies[165] was adapted to control oxygen in the microfluidic device and thus treat the cell layer with hypoxia. The gas mixer added compressed air (21% O_2, 5% CO_2, balance N_2) to compressed nitrogen (0% O_2, 5% CO_2, balance N_2) in a solenoid valve-controlled mixing chamber to achieve a user-specified oxygen concentration between 0 and 21%. A custom Python code was used to control oxygen setpoints. Then, the pre-mixed gas at the desired oxygen concentration was perfused into the gas layer of the device for 60 minutes. Oxygen gas tension was monitored via a calibrated fiber optic oxygen sensor (NeoFox-GT, Ocean Optics). To maintain a physiologic environment, the environmental chamber was heated to 37 °C and EGM-2 was perfused through the cell layer during hypoxia treatment. Endothelialized devices

were returned to the incubator and assessed after 4 hours, a period of time that allowed the endothelium to respond to the preconditioning treatment based on previous studies on delay of genomic response in endothelial cells.[92,193] A visual reference of the experimental setup is included below (Figure 3.2).

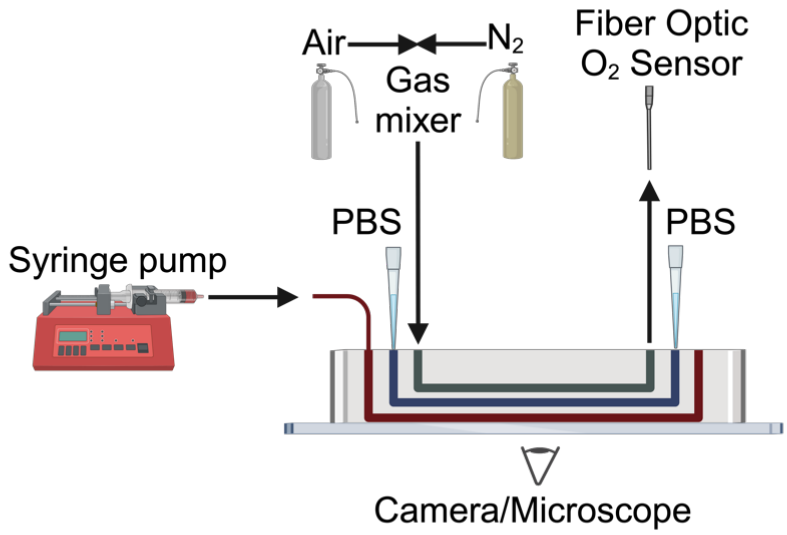


Figure 3.2: Experimental setup for oxygen control and device observation. Microfluidic devices were placed on the stage of a Zeiss Axio Observer widefield microscope within an environmental chamber heated to 37°C. A gas mixing system of pressurized air and N_2 was employed to directly control partial pressure of oxygen entering the device's gas layer. Gas rapidly diffused through the device, modulating oxygen tension in the cell layer in real-time. Local oxygen percentage in the device was validated via a fiber optic O_2 sensor. Hydration in the device was maintained via PBS in the hydration layer. A syringe pump or pipettes were used to add various materials (endothelial cells, cell culture media, red blood cells, etc.) to the cell layer for endothelialization, maintenance, and blood perfusion. Observation was performed via the microscope and high-speed camera. Schematic not to scale, created using BioRender.

3.2.8 Blood sample collection

Blood samples from patients with SCD were collected into citrate vacutainer tubes at Massachusetts General Hospital and Children's Hospitals and Clinics of Minnesota under Institutional Review Board approved protocols. Control blood

samples from non-sickle patients with hemoglobin AA were collected from Massachusetts General Hospital under approved protocol. All patients gave informed consent before participating in the study. Blood analyses including complete blood count and hemoglobin variant analysis were performed on samples whenever possible, either by the collection hospital or by Mayo Clinic (Rochester, MN). Relevant information is included in the supplemental materials (Table 3.S1) and normal reference ranges for these metrics are included in the appendix (Table A.1). Prior to use, blood samples were stored at 4°C for a minimum of 2 hours and a maximum of 3 days.

3.2.9 Blood sample preparation and perfusion

Immediately before an experiment, blood plasma and buffy coat was removed by fractionating blood in a centrifuge (400g, 5 minutes x 3 cycles) and replaced with PBS without calcium or magnesium (Corning). Washed red blood cells were gently loaded into a syringe with attached 0.015” inner diameter tubing (BD Intramedic) and mounted on a syringe pump (Harvard Apparatus). Washed red blood cells were used in this experiment to isolate just the contribution of the endothelium and red blood cells in vaso-occlusion, decoupling variability from platelets, leukocytes, etc. While these protocols have been used successfully to isolate RBCs in other experiments, direct validation of white blood cell and platelet removal were not validated at the time of experiment via complete blood count testing or blood smear, which is a limitation of this study. Samples were loaded

into new syringes for each microfluidic trial to limit effect of red cell packing. Red blood cells were perfused into each device's endothelialized cell layer at 60 μL/hr for perfusion studies.

In several cases, red blood cells were fluorescently labeled using the PKH26 red fluorescent cell linker kit (Sigma-Aldrich) to better visualize blood perfusion. Cell staining methodology was based on manufacturer recommendations and relevant literature sources.[194] Briefly, whole blood was centrifuged and rinsed three times to isolate red blood cells. Red blood cells were then incubated with PKH26 dye solution for 4 minutes. The reaction was subsequently stopped with 1% BSA and the red blood cells were rinsed via centrifugation in PBS four times to remove background before perfusion and imaging.

3.3 Results and Discussion

In this chapter, we present a novel microfluidic device for the study of SCD. More specifically, this section introduces the microfluidic platform, validates its physiologic relevance, and tests its ability to simulate two key biological processes in SCD. The results presented here lay the foundation for studies in subsequent chapters that will delve deeper SCD's underlying pathophysiology.

3.3.1 Development of an endothelialized, oxygen-tunable microfluidic model

Lack of effective treatment methods in SCD necessitates the development of more physiologically relevant, predictive models that accurately recapitulate underlying disease pathophysiology. Existing models fall short by oversimplification and do not reliably inform clinical trials.[102] We hypothesized that integration of three-dimensional, endothelial-lined microchannels with relevant shear stresses in an oxygen-controllable environment would allow for a more accurate simulation of SCD processes, therefore providing a more valuable research tool. An overview of the device development process is included here while more detailed methodologies and protocols can be found in the Materials and Methods section above.

After several optimization steps, a multi-layer microfluidic device was designed and fully refined within this work. The final design of the device incorporated multiple layers to control oxygen tension and culture endothelial cells on the same chip. The first layer was designed to act as a gas reservoir to regulate oxygen tension in the device and initiate hypoxia and/or red cell sickling. The second layer provided the necessary hydration to prevent cells from becoming dehydrated. The third and most critical layer consisted of a fully endothelialized network of channels to mimic a microvascular network (Figure 3.3; Figure 3.S1). Considerations were made to ensure the experimental flexibility of this device, allowing for its application in a variety of protocols.

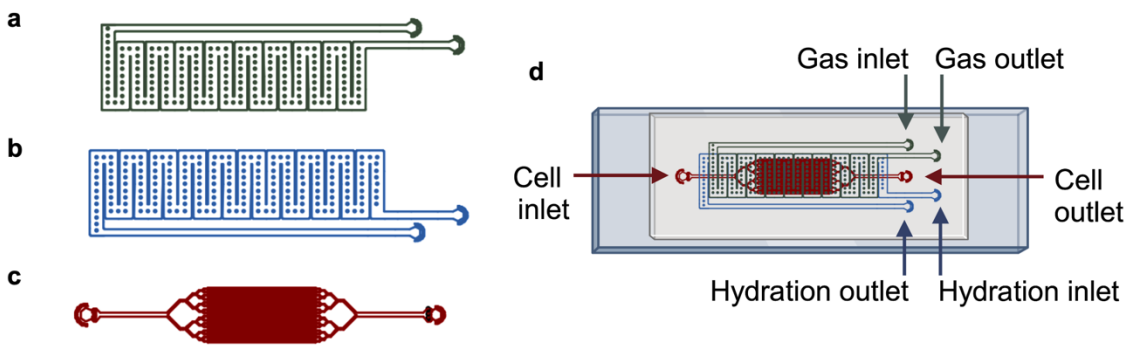


Figure 3.3: Microfluidic device geometry and arrangement. The microfluidic device is composed of three layers: (a) a gas reservoir to deliver oxygen, which initiates hypoxia and/or red cell sickling, (b) a hydration layer that prevents cell dehydration, and (c) a cell layer which is fully endothelialized to mimic the native microvascular system. The cell layer includes a branching network of 32 individual channels measuring 50 μm x 60 μm that can be observed under the microscope. (d) The multi-layer microfluidic device is assembled via plasma bonding. Inlet/outlet ports allow access for gas delivery, oxygen sensing, hydration delivery, device endothelialization, media perfusion, blood perfusion, and staining. Created using AutoCAD, Inkscape, and BioRender.

The endothelium represents a key component of SCD biology, and much optimization was done to develop an effective endothelialization method. Due to the challenging nature of the branching vessel geometry and small size scales, established protocols[174] for device endothelialization were incapable of fully endothelializing this geometry's thin branching network without frequent clogs or bare regions. Through a series of optimizations, a unique protocol was developed that resulted in a confluent, aligned microvascular system that mimics post-capillary venules in vivo. In particular, key advancements included: (1) increasing endothelial cell seeding density to 15 x 10^6 cells/mL from commonly used ranges of 0.5 to 2.0 x 10^6 cells/mL, (2) repeated, intermittent seedings via pipette tip instead of via syringe pump to improve cell contact time with microchannel walls, and (3) additional 90-minute incubation period before adding flow to allow cells to fully attach and spread throughout channels. With these optimizations, a revised

methodology was developed that resulted in a confluent, aligned microvasculature system that mimics post-capillary venules in vivo.

This protocol was optimized using HUVECs, which are well characterized and widely used in vascular biology research. However, these methodologies also proved effective with a small number of studies using HMVEC-Ls (Figure 3.S2). The successful endothelialization of microfluidic devices with HMVEC-Ls emphasizes the versatility of this protocol across multiple endothelial cell types. Also notable, this protocol is especially suitable for small microfluidic channels (less than 100 μm in width and height) which are often more difficult to fully endothelialize than larger channels. These protocol modifications make it possible to study numerous diseases that involve small microvasculature, whereas much of the literature in the vessel-on-chip space has historically focused on simulation of larger vasculature.

3.3.2 Microfluidic platform recapitulates SCD microvasculature

Fluorescent microscopy was used to evaluate the endothelium, including visualization of the vascular network and also confirmation of key physiologic attributes. In the body, microvasculature is cylindrical or tubular in structure and aligned in the direction of flow.[195] It was critical that our model system recapitulated these traits: confluency along the cylindrical channel, presence of a lumen, and alignment horizontally through the channel. Confocal microscopy was utilized to

verify that endothelial cells in our microfluidic device effectively coated the top, bottom, and side walls of each microchannel while supporting a central lumen (Figure 3.4). Visualization of the fluorescently labeled endothelium also revealed sufficient endothelial confluency and alignment.

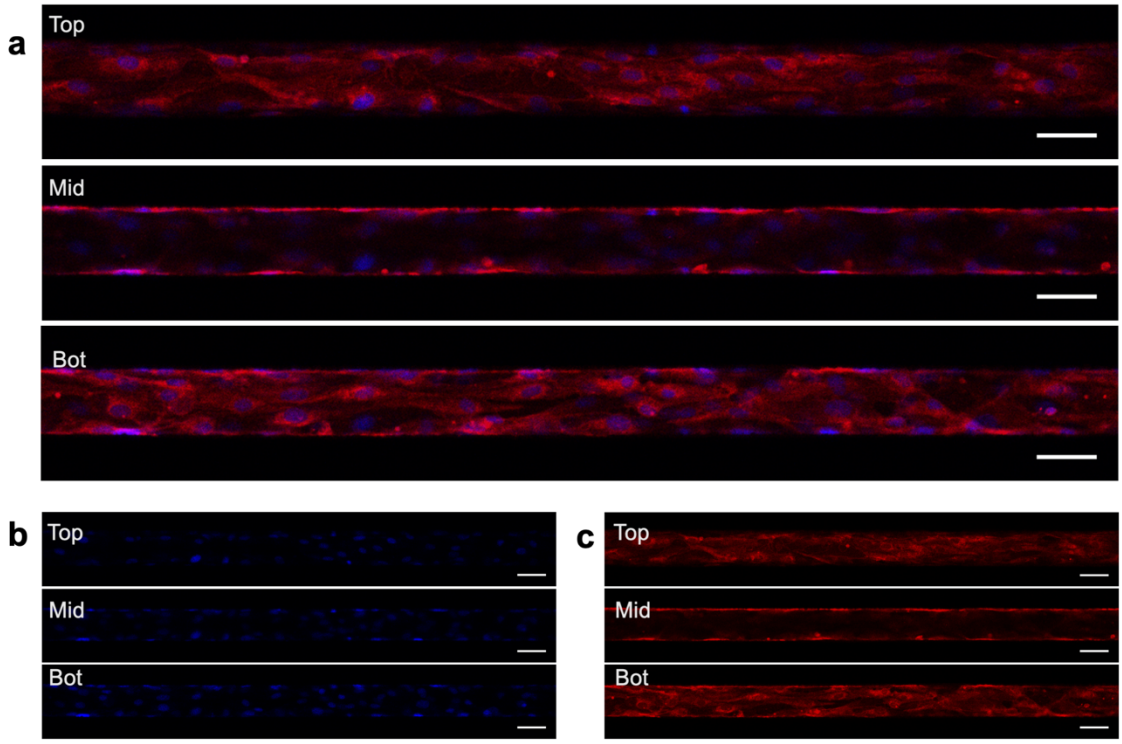


Figure 3.4: Confocal imaging of three-dimensional endothelial lumen. Confocal microscopy was used to image vertically through the microfluidic device, verifying 3-dimensional lumen structure and confluent microchannel lining. (a) Top, middle ("mid"), and bottom ("bot") sections of the microchannel were fluorescently imaged after staining for nuclei (Hoechst 33258, blue) and plasma membrane (CellMask, red). HUVECs adequately cover the top, bottom, and side walls of the microchannel while maintaining a central lumen. Cells also align with flow in the horizontal direction. (b-c) Individual channel images pre-merge for nuclei (b, left) and plasma membrane (c, right) are also shown. All scale bars indicate 50 μm.

It is also critical that the device's vascular network exhibits key functional characteristics such as the expression of adhesion molecules, the ability to synthesize essential biological factors, and the ability to form cytoskeletal

components. Fluorescent microscopy was used to characterize the endothelium and identify the presence of these physiologically relevant features (Figure 3.5).

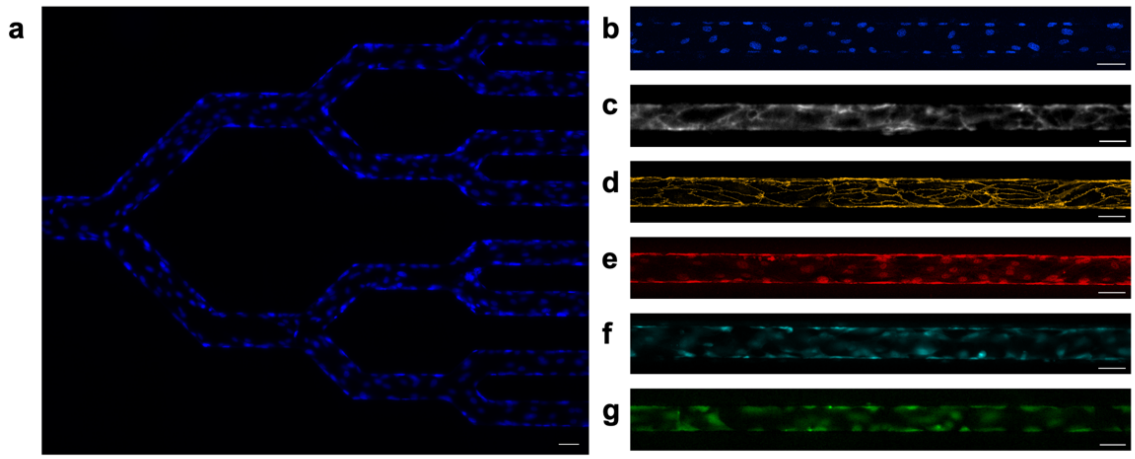


Figure 3.5: Characterization of the endothelium. Numerous fluorescent probes and techniques were used to visualize the endothelial cells and examine their physiologic. (a) Bifurcating network and (b) straight channel of HUVECs were fluorescently labeled for nuclei (Hoechst 33258) to identify cell locations within microchannels. HUVECs were shown to express a number of relevant adhesion markers, including (c) platelet endothelial cell adhesion molecule-1 (PECAM-1/CD31), (d) vascular endothelial cadherin (VE-Cadherin/CD144), and (e) vascular cell adhesion protein-1 (VCAM-1/CD106). HUVECs cultured in microchannels also demonstrated appropriate (f) F-actin structures (via Phalloidin) and (g) nitric oxide production (via DAF-2 DA), indicating vascular function. Fixation and staining was performed after 48 hours of flow. Cells were used within passages 4-6. All scale bars indicate 50 μm.

Adhesion molecules such as platelet endothelial cell adhesion molecule-1 (PECAM-1) and vascular endothelial cadherin (VE-cadherin) are associated with formation and maintenance of tight junctions between endothelial cells. These adhesion molecules contribute to barrier function and help maintain vascular homeostasis.[196] Vascular cell adhesion molecule-1 (VCAM-1) also contributes to vessel wall integrity, while separately being shown to facilitate adhesion and recruitment of leukocytes to the endothelium.[196] PECAM-1, VE-cadherin, and VCAM-1 all play critical roles in endothelial function, and therefore it was

necessary to confirm their presence in our endothelialized system. Each of these adhesion molecules have been successfully identified in our endothelialized microfluidics via fluorescent staining (Figure 3.5 c-e).

To further validate the model, we confirmed the presence of filamentous actin (F-actin) via phalloidin staining (Figure 3.5 f). HUVECs normally express F-actin, a key component of the cytoskeleton. F-actin contributes to endothelial structural support, cell barrier function, and cell-cell adhesion.[197] Lastly, we confirmed that HUVECs cultured in microfluidic devices produce nitric oxide, another indicator of vascular function (Figure 3.5 g). Nitric oxide, a soluble gas synthesized by endothelial cells in the body, modulates vascular homeostasis, vascular tone, and even protects blood vessels from injury.[198]

Overall, these results demonstrate that the endothelium in our microfluidic devices morphologically and functionally resembles that of an in vivo environment. These results validate the physiological relevance of this work by showcasing the endothelial confluency, alignment, adhesion molecule expression, cytoskeletal development, and production of synthesized factors within our microfluidic model.

3.3.3 Endothelium on-chip tolerates hypoxia preconditioning

As previously mentioned, hypoxia is a critically important variable affecting hemoglobin polymerization, red blood cell sickling, endothelial activation, inflammation, and vaso-occlusion. The platform presented in this chapter

effectively includes the ability to control oxygen in order to initiate these processes on-chip, however it was not yet known how hypoxia would affect an endothelium cultured in 3D. Particularly, it was unknown if the endothelium on-chip would be able to tolerate hypoxic exposure without significant loss of viability, detachment from microchannel walls, or morphological change. Much of the existing knowledge focused on endothelial exposure to hypoxia in two-dimensional cell culture plates[199,200] or non-human in vivo studies.[201–203] Therefore, we compared the morphology of endothelium in devices that had undergone various types of oxygen/hypoxia conditioning to ensure this model would be functional for future studies.

To validate the endothelium's ability to tolerate drops in oxygen, devices were exposed to various levels of oxygen with the gas mixing system. Endothelialized devices were exposed to one of the following treatments for 60 minutes: (1) atmospheric control: 21% oxygen, (2) physiologic control: 12% oxygen, (3) cyclic hypoxia: alternating between 12% oxygen and 5% oxygen at 10-minute intervals, or (4) sustained hypoxia: 5% oxygen. After treatment with one of the four conditions, endothelialized devices were returned the incubator (37°C, 5% CO_2) and cultured under media flow for 4 additional hours to accommodate temporal delay in cellular response to stimuli. It was confirmed that no loss of cells, detachment from microchannel walls, or significant morphological change occurred (Figure 3.6). This conclusion was critical, revealing the robustness of

vasculature-on-chip systems and their ability to sustain environmental stimuli such as hypoxia.

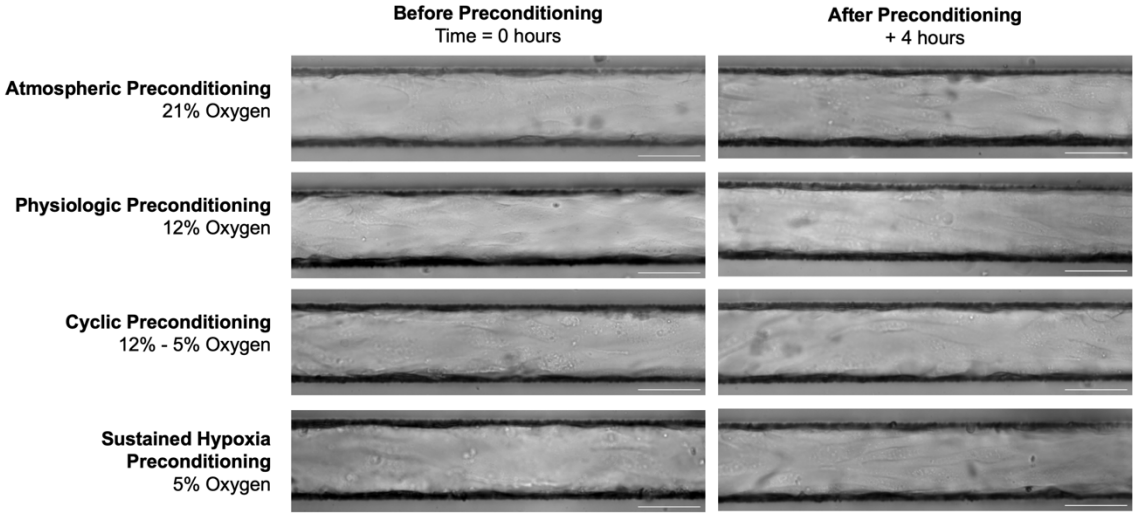


Figure 3.6: On-chip hypoxia treatment of vascularized channels. The endothelialized microchannels were treated with one of four oxygen/hypoxia conditions for 60 minutes, then incubated under flow at normoxia for 4 hours to assess morphologic change due to treatment. Brightfield imaging shows that HUVECs tolerated various types of oxygen/hypoxia conditioning on-chip without significant morphological damage. All scale bars indicate 50 μm.

3.3.4 Blood perfusion and occlusion modeling on-chip

This microfluidic platform was established with the goal of modeling SCD blood flow, adhesion, and occlusion to investigate the processes contributing to VOC. Preliminary work was done to validate the use of this microfluidic system for future blood perfusion/occlusion experimentation (Figure 3.7).

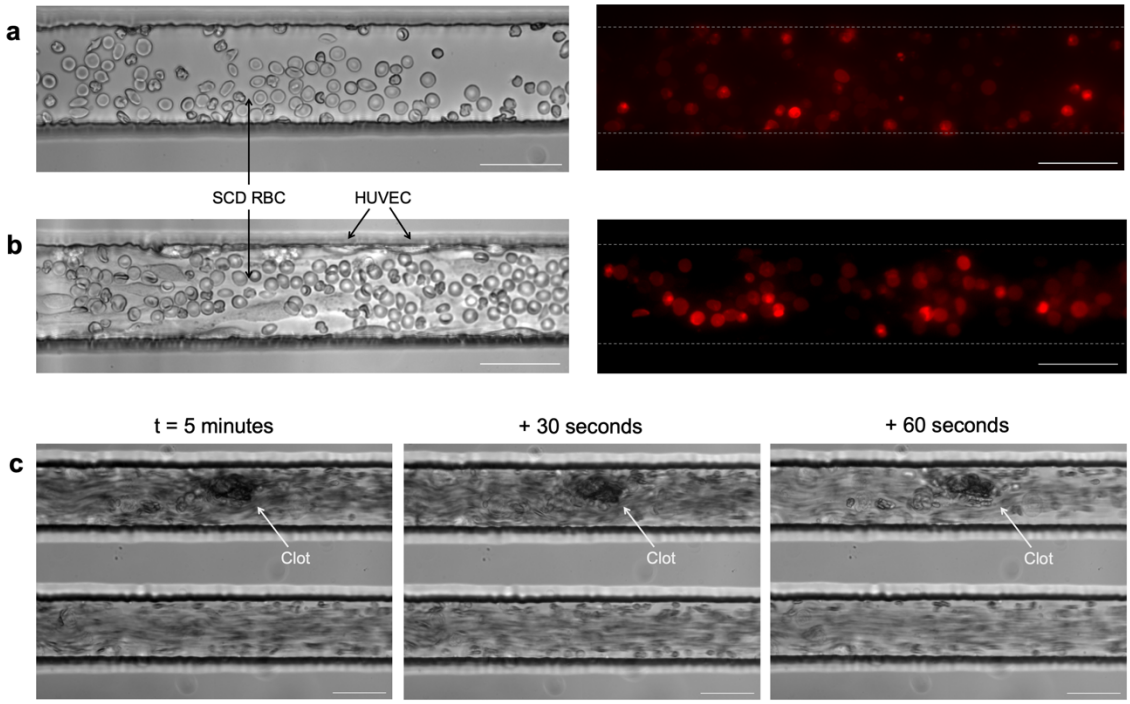


Figure 3.7: Red blood cell perfusion and occlusion in microfluidic devices. Brightfield and fluorescence microscopy were utilized to visualize blood perfusion through microfluidic devices at normoxia. (a) Red blood cells (RBCs) from a patient with SCD (Patient ID #14) were first perfused through non-functionalized, acellular devices. Brightfield imaging (left) and fluorescence microscopy (right) highlight presence of red blood cells in devices after perfusion. A red fluorescent cell membrane labeling kit was used to mark red blood cells. (b) Red blood cells from SCD patients were then perfused through fully endothelialized devices, also shown via brightfield (left) and fluorescence (right). Endothelial cells (HUVECs) can be observed at channel walls as indicated above. (c) During perfusion, the red blood cells adhere to the endothelium as shown. Red cell/endothelial cell adhesion can lead to clot formation and vaso-occlusion, which can be observed in real-time over the course of an experiment. All scale bars indicate 50 μm.

Specifically, red blood cells from patients with homozygous SCD were perfused through acellular (Figure 3.7 a) and endothelialized (Figure 3.7 b) devices at standard atmospheric oxygen levels (21%). Brightfield microscopy was used during blood perfusion to visualize the red blood cells as they interacted with endothelial cells. Labeling methods (such as PKH26 general membrane tagging) were implemented to fluorescently tag red blood cells and provide an alternative form of visualization. Additionally, preliminary tests were performed to compare

blood flow of non-sickle control samples (hemoglobin AA) with that of SCD patient samples (hemoglobin SS) (Figure 3.S3). Further inquiry into non-sickle blood perfusion was not investigated at this time but could be explored in future work. Even without manipulation of oxygen concentration, perfusion of SCD red blood cells resulted in some instances of red blood cell-endothelial cell adhesion and clot development within 5 minutes (Figure 3.7 c). A significant advantage of this platform is its optical accessibility, allowing for observation of clot development in real-time as they progress from small adhesive events to large-scale obstructions in the vascular network. Future work will be done to incorporate hypoxia with blood studies and investigate contributing factors to microvascular occlusion in endothelialized devices.

3.4 Conclusion

SCD is a complex multisystem disorder that has yet to be fully understood. Many unanswered questions remain about the underlying pathophysiology of the disease and potential opportunities for therapeutic intervention. Current treatment options are limited and the development of new drugs in the SCD field has been underwhelming despite decades of active research.[102] Many recent models of SCD fall short due to oversimplification and therefore do not reliably inform clinical trials. We recognized the need for a more physiologically relevant model of SCD that integrated numerous biological attributes of disease processes. In this chapter, we detailed the design and optimization of a multi-layer microfluidic platform that

contains a fully endothelialized microvascular system with the ability to initiate hypoxia on-chip.

Importantly, the endothelium cultured in our microfluidic system was shown to morphologically and functionally mimic native microvasculature. Fluorescence microscopy was leveraged to visualize the endothelium and stain for key biological components present in the native environment. Specifically, nuclear and plasma membrane staining was performed to evaluate the confluency, alignment, and lumen structure of endothelialized microchannels. Additionally, antibodies and fluorescent probes were used to confirm the presence of key adhesion molecules, synthesized factors, and cytoskeletal components in the endothelial network. Taken together, validation of these components confirm that the endothelium functionally and morphologically resembles that of in vivo.

In addition to validating the on-chip endothelium's physiologic relevance, we also demonstrated the utility of this platform in modeling several fundamental SCD processes. First, we showed that the endothelium cultured on-chip is able to tolerate sustained and cyclic periods of hypoxia without loss of viability or detachment from microchannel walls. This conclusion supports the use of hypoxia in endothelialized microfluidics in future work. Second, we showed that endothelialized devices may be perfused with patient blood samples to simulate adhesion, clot formation, and vaso-occlusion. Taken together, this system offers a more physiologically relevant microfluidic model of SCD that can be used to investigate underlying pathophysiology and better inform clinical trials.

This chapter effectively introduced a novel microfluidic platform for the study of SCD. The next chapter will expand upon the foundational model presented here, investigating the role of hypoxia reperfusion injury in SCD vaso-occlusion and considering other factors that may make patients more susceptible to VOC.

3.5 Acknowledgements

Valuable endothelialization advice and expertise was provided by Yumiko Sakurai and Dr. Wilbur Lam's lab at Emory University and Georgia Institute of Technology, which helped set this project in motion. Portions of this work were conducted in the Minnesota Nano Center (MNC). The MNC afforded access to photolithography and microfabrication equipment, enabling the development of this microfluidic platform. The MNC is supported in part by the National Science Foundation (NSF) through the National Nano Coordinated Infrastructure Network (NNCI) under Award Number ECCS-1542202. We also acknowledge Dr. José Valdez and Dillon Williams for their contributions in coding the oxygen control software tools in MATLAB and Python. Lastly, the University Imaging Center (UIC) at the University of Minnesota provided valuable access to confocal microscopy, facilitating high quality imaging of the endothelialized devices.

3.6 Supplemental Materials

The supplemental materials included below consist of one additional table and three additional figures to be referenced in context with Chapter 3.

ID	Recent Trans-fusion?	HU Usage?	Genotype	Hemoglobin Variant Analysis				
				HbS	HbF	HbA	HbA2	HbC
14	Yes	No	HbSS	*Insufficient sample to perform test*				
15	No	No	HbAA	0.0%	0.0%	97.5%	2.5%	0.0%
16	Yes	Yes	HbSS	46.1%	6.9%	44.4%	2.6%	0.0%

ID	Age	Sex	Complete Blood Count Analysis						
			HGB	HCT	MCV	MCHC	RDW	WBC	PLT
14	11	F	7.7	23.9	101.0	32.2	26.5	14.4	289
15	88	M	14.7	44.6	92.7	33.0	12.7	6.84	204
16	24	F	7.2	21.7	97.7	33.2	19.8	12.48	489

Table 3.S1. Blood sample data sheet I. Table includes patient ID number, history of recent transfusion, hydroxyurea (HU) usage, genotype (HbSS for homozygous SCD, HbAA for control/non-SCD), hemoglobin variant analysis results if available, age, sex, and complete blood count results (HGB: hemoglobin (g/dL), HCT: hematocrit (%), MCV: mean corpuscular volume (fL), MCHC: mean corpuscular hemoglobin concentration (g/dL), RDW: red blood cell distribution width (%), WBC: white blood cell count (k/μL), PLT: platelet count (k/μL)). Normal reference ranges can be found in the appendix (Table A.1).

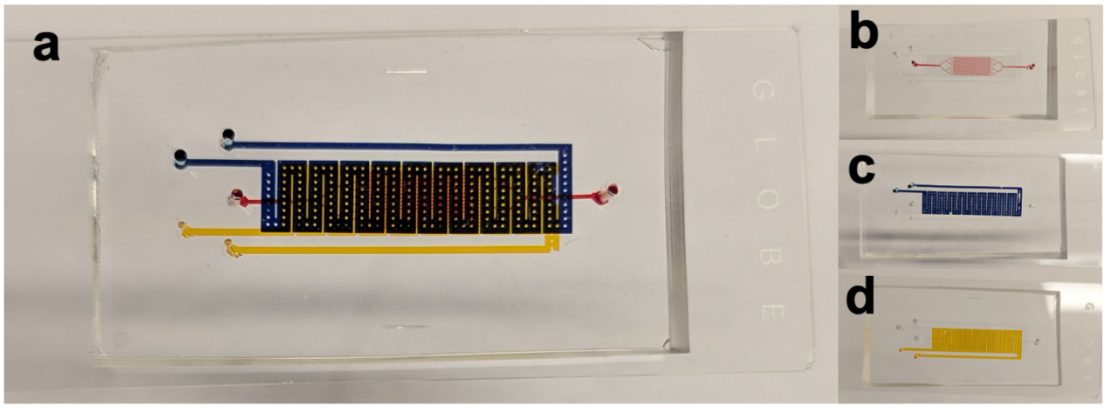


Figure 3.S1: Visualization of device geometry using dyes. (a) Microfluidic device was injected with three color variants of dye to visualize individual layer geometries, including (b) cell layer, (c) hydration layer, and (d) gas layer. Devices measure approximately 25 mm in width, 50 mm in length, and 6 mm in height.

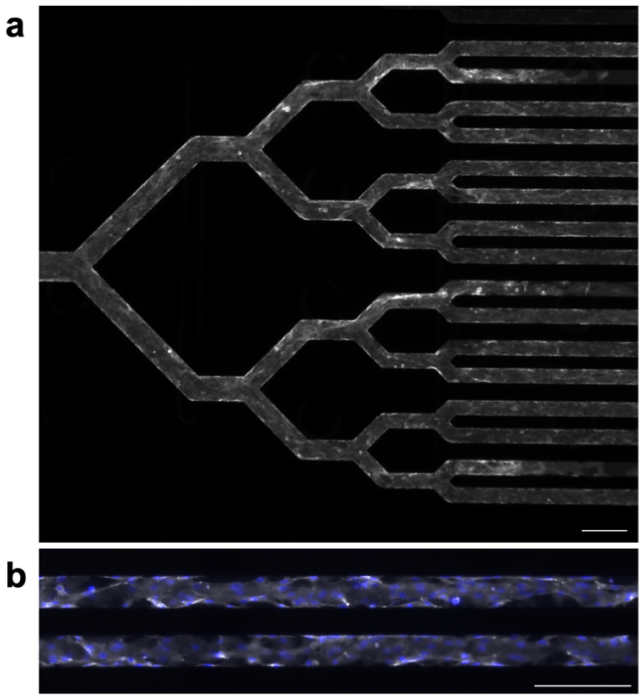


Figure 3.S2: Microvascular endothelial cells cultured on-chip. Preliminary studies demonstrate successful culture of human lung microvascular endothelial cells (HMVEC-Ls) cultured under flow conditions in a microfluidic device. (a) Bifurcating network of HMVEC-Ls, fluorescently labeled for plasma membrane. (b) Straight channels of HMVEC-Ls, fluorescently labeled for plasma membrane (grey) and nuclei (blue). All scale bars indicate 200 μm.

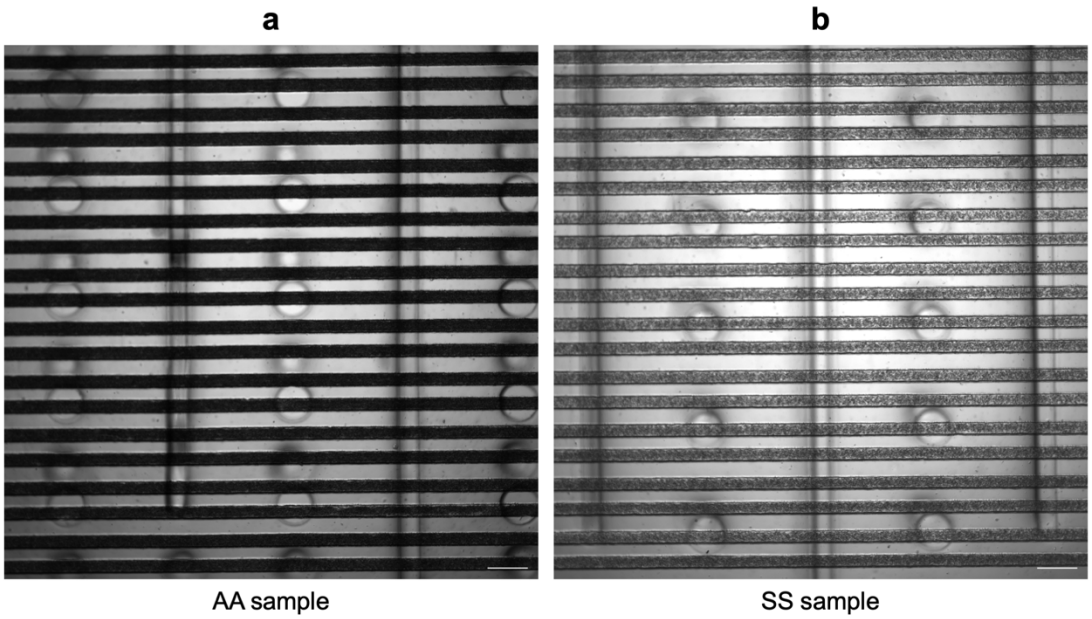


Figure 3.S3: Healthy and SCD red blood cell perfusion through endothelialized devices. Preliminary experimentation confirmed ability to perfuse donor red blood cells through endothelialized microfluidics under normoxic conditions. (a) Red blood cells from non-sickle donor (Patient ID #15, hemoglobin AA) and (b) patient with SCD (Patient ID #16, hemoglobin SS) were perfused through endothelialized microfluidic devices without adjusting patient hematocrit. Higher intensity in the AA samples is indicative of higher hematocrit and more densely packed microchannels. All scale bars indicate 200 μm.

Chapter 4: Implementation of an Occlusion Assay on-Chip to Explore Effects of Hypoxia Preconditioning and Contributors to VOC

4.1 Introduction

Sickle cell disease (SCD) is a hematologic disorder caused by a mutation in the hemoglobin β gene, leading to hemoglobin polymerization, red blood cell sickling, and a cascade of pathophysiological events culminating in painful vaso-occlusive crisis (VOC). SCD can present with substantial phenotypic heterogeneity which is only partially understood.[6,19,20] Despite decades of research, treatment options for the millions of SCD patients worldwide remain remarkably limited, highlighting the need for a better understanding of underlying SCD mechanisms.[1,3] Additionally, investigation into the factors causing increased occlusion rates among a subset of patients may present an opportunity for therapeutic intervention.

Recently, increased attention has been paid to hypoxia/ischemia reperfusion injury as a driving mechanism of SCD pathology.[62,86–88] Hypoxia reperfusion injury in SCD is characterized by an initial hypoxic or ischemic event attributed to vaso-occlusion, followed by a reperfusion of oxygen that triggers a significant pro-inflammatory response. While hypoxia and reperfusion are classically thought to induce harmful inflammatory responses associated with apoptosis and symptom onset, a notable trait of reperfusion injury is that certain mild or cyclic periods of low oxygen may instead provoke a conditioning effect that

ameliorates subsequent severe reperfusion injury.[84,87,89,90] Previous attempts to identify mechanisms that initiate this pro-survival phenotype are incomplete and contradictory.[87,88,91,92] Although some studies have begun to examine the effect of hypoxia/ischemia preconditioning on various organs and tissue compartments, the effect on the microvasculature itself is largely unexplored.[93,94,204] A better understanding of hypoxia reperfusion's conditioning effect on the endothelium may inform our overall understanding of SCD pathophysiology and offer insight towards therapeutic intervention.

To better understand what causes VOC in the body, occlusion microfluidics have been used by several labs to simulate and quantify incidences of microchannel clotting or obstruction on-chip. These previous studies include several unique models, each with their own advantages and disadvantages. For example, the OcclusionChip was introduced by Man et al. in 2020. This acellular platform was used to quantify red blood cell deformability and occlusion index, ultimately concluding that hypoxia treatment is correlated with higher occlusion index in SCD.[170] While many similar studies utilize acellular devices, a few labs have published endothelialized models that are able to model vaso-occlusion in vascularized networks to capture the contribution of endothelial cells in the vaso-occlusive cascade. In particular, Tsai et al. presented a platform in 2012 that simulated microvascular occlusion and thrombosis in various hematologic diseases.[172] Inspired by these existing models, we developed a more physiologically relevant model that incorporates both hypoxia control and

endothelialized microchannels at relevant size scales. These features allowed us to properly investigate the relationship between hypoxia reperfusion injury and VOC in SCD.

In this chapter, we examine the effect of hypoxia preconditioning on incidence of vaso-occlusion on-chip. We hypothesized that pre-treatment of the endothelium with mild hypoxia or hypoxia cycling may provoke a conditioning effect, protecting against VOC. We also anticipated that clinical variables obtained from laboratory screening (hemoglobin analysis and complete blood count testing) may inform patient-to-patient heterogeneity in response. Together, these results demonstrate the utility of an occlusion assay on-chip to investigate the underlying pathophysiology of SCD and uncover key contributors to VOC.

4.2 Materials and Methods

The following experiments utilize the microfluidic platform that was first introduced in Chapter 3 of this document. A brief review of pertinent method details is included here; however, reference may also be made to Chapter 3.2 Materials and Methods for a more thorough description of device design, microfabrication, and endothelialization. Generally, the methodology of this chapter includes microfluidic device fabrication, endothelialization, incubation, hypoxia preconditioning, and the occlusion assay. A visual summary of the methods,

highlighting hypoxia preconditioning and the occlusion assay in particular, is included below (Figure 4.1).

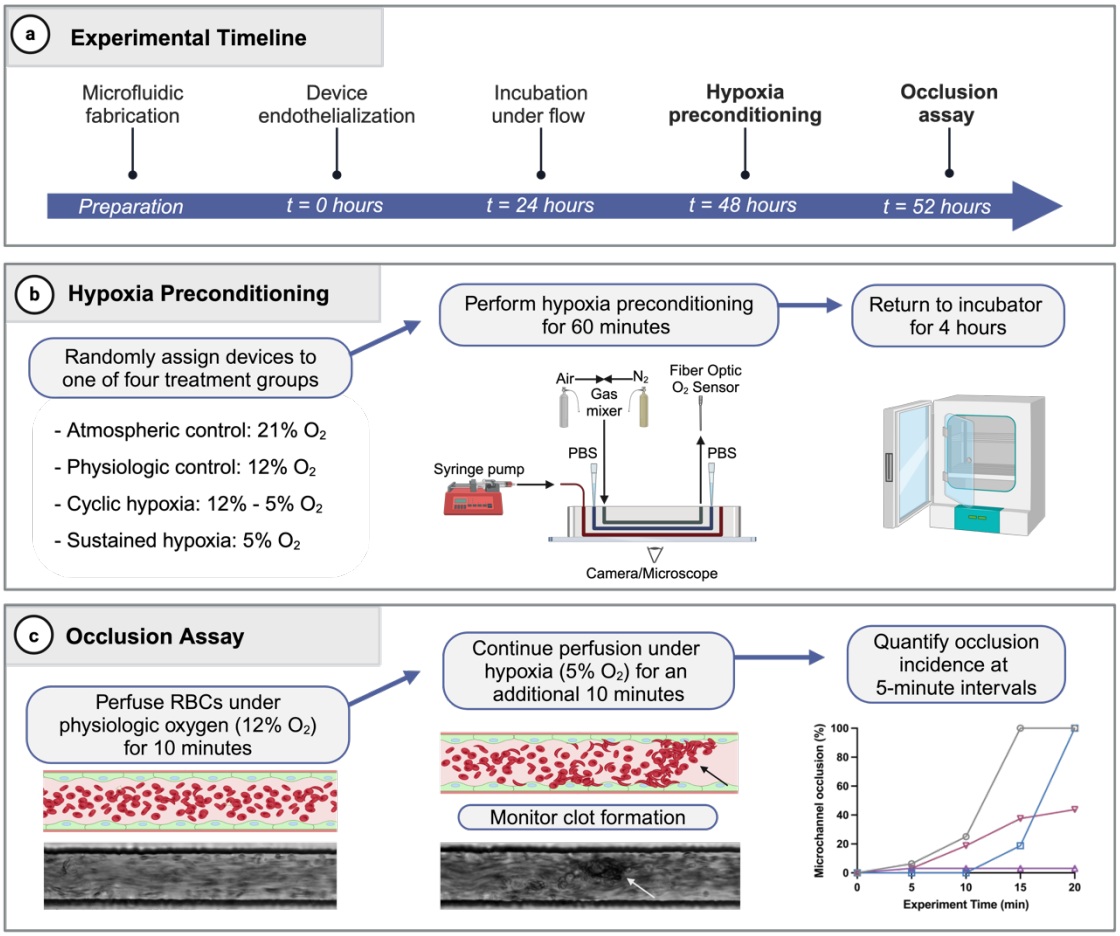


Figure 4.1: Visual summary of chapter 4 experimental timeline and workflow. Schematic featuring (a) experimental timeline of the major steps in chapter 4 with panels highlighting the workflow of (b) hypoxia preconditioning and (c) the occlusion assay. Created using BioRender.

4.2.1 Microfluidic device design, fabrication, and endothelialization

A multi-layer microfluidic platform was designed and optimized, consisting of (1) a gas reservoir to regulate oxygen tension in the device and initiate hypoxia and red cell sickling, (2) a hydration layer to prevent cell dehydration, and (3) a fully endothelialized cell layer to mimic a network of microvascular channels. The

device geometry was designed in AutoCAD (Autodesk) and printed on mylar photomasks for fabrication (Fineline Imaging). The PDMS microfluidic devices were fabricated from silicon wafer molds using photolithography, soft lithography, compression molding, and oxygen-plasma bonding techniques. Oxygen tension can be directly manipulated in the cell layer of this device due to the gas-permeable nature of PDMS. Punching of inlets and outlets in each layer allowed for delivery of various materials, including oxygen gas, phosphate-buffered saline (PBS), endothelial cell suspensions, cell media, and blood samples.

Human umbilical vein endothelial cells (HUVECs) were cultured aseptically per manufacturer's recommendations using endothelial cell growth medium-2 (EGM-2, Lonza). Devices were endothelialized as previously described, refer to Chapter 3.2 of this document for more detailed instruction. Briefly, microfluidic devices were coated with 50 μg/mL fibronectin from human plasma in PBS. Then, HUVECs were resuspended to a concentration of 15 x 10^6 cells/mL in a solution of 8% dextran-EGM-2 media. Cell suspension was loaded into devices by pipetting, then incubated to allow for cell attachment. Finally, syringe pumps (New Era Pump Systems) were connected to endothelialized devices via tubing, allowing media to be flowed through microchannels at a consistent flow rate of 60 μL/hr.

4.2.2 Hypoxia preconditioning

Hypoxia preconditioning of the endothelium was achieved using a solenoid valve gas mixing system based on one used in previous works.[162,165] Briefly, the gas mixer combined compressed air (21% O_2, 5% CO_2, balance N_2) with compressed nitrogen (0% O_2, 5% CO_2, balance N_2) in a solenoid valve-controlled mixing chamber to obtain a user-specified oxygen concentration between 0 and 21%. A calibrated fiber optic oxygen sensor (NeoFox-GT, Ocean Optics) was used to validate the oxygen delivery. The oxygen/hypoxia treatment was performed in a 37°C environmental chamber and EGM-2 was perfused at a flow rate of 60 µL/hr during preconditioning to maintain cell viability and alignment.

Endothelialized devices were exposed, or "preconditioned," to one of the following treatments for 60 minutes: (1) atmospheric control: 21% O_2, (2) physiologic control: 12% O_2, (3) cyclic hypoxia: alternating 12% O_2 and 5% O_2 at 10-minute intervals, or (4) sustained hypoxia: 5% O_2. Experiments performed at normal atmospheric oxygen levels (21% or 160 mmHg) do not replicate oxygen tension in vivo. Arterial blood oxygen tension is typically between 75 and 100 mmHg, whereas venous blood oxygen tension is typically between 30 and 40 mmHg.[205,206] Because of this, we chose to include both an atmospheric control (21% O_2, 160 mmHg) and a physiologic control (12% O_2, ~90 mmHg) alongside our experimental conditions. A custom Python code was used to set the desired oxygen level and control the gas mixing system in real-time. After 60 minutes of hypoxia preconditioning, endothelialized devices were returned to the incubator

and maintained for an additional 4 hours at 37°C, 5% CO_2 under media flow. This window of time allowed the endothelium to respond to the preconditioning treatment and was chosen based on previous studies on delay of genomic response in endothelial cells.[92,193]

4.2.3 Blood sample collection and preparation

Massachusetts General Hospital, Children's Hospitals and Clinics of Minnesota, and the University of Minnesota Medical Center performed blood sample collection from patients with SCD using citrate vacutainer tubes. Patients consented and the procedures were performed under Institutional Review Board approved protocols. Complete blood count and hemoglobin variant analysis testing were performed on all samples, either via the collection hospital or by Mayo Clinic (Rochester, MN). Relevant patient metrics including hemoglobin (HGB), hematocrit (HCT), mean corpuscular volume (MCV), mean corpuscular hemoglobin concentration (MCHC), red cell distribution width (RDW), white blood cell count (WBC), platelet count (PLT), hemoglobin variant percentages, and patient demographic information are included in the supplement (Table 4.S1 and Table 4.S2). Normal reference ranges for these metrics can be found in the appendix (Table A.1). Prior to use, blood samples were stored at 4°C for no longer than 3 days. The occlusion assay was performed using washed red blood cells rather than whole blood to specifically isolate the interaction between endothelial

cells and red blood cells during the vaso-occlusive process and decouple the involvement of additional variables such as platelets, leukocytes, etc.

Immediately prior to experimentation, red blood cells were isolated from whole blood and washed to remove the plasma, white blood cells, and platelets. Briefly, blood was fractionated in a centrifuge (400g, 5 minutes x 3 cycles) and blood plasma was removed then replaced with PBS. During this process, care was taken to minimize red blood cell damage or lysis. Gently, washed red blood cells were loaded into a syringe with attached 0.015-inch inner diameter tubing (BD Intramedic). Loaded syringe was mounted on a syringe pump (Harvard Apparatus) to allow for precise, consistent perfusion.

4.2.4 Occlusion assay

The goal of this assay was to quantify incidence of occlusion, investigating whether certain preconditioning regimes prevent or promote vaso-occlusion. One at a time, devices were loaded onto the microscope stage within the heated environmental chamber. Several preliminary steps were performed to prepare for the occlusion assay, including: (1) calibration of oxygen mixing system, (2) injection of PBS via pipetting into the hydration layer, (3) delivery of 12% oxygen into gas layer via solenoid mixing system, and (4) validation of accurate oxygen tension delivery via NeoFox oxygen sensor. Finally, red blood cells were perfused into the cell layer at a flow rate of 60 μL/hr via syringe pump (Harvard Apparatus).

To perform the occlusion assay, microfluidic devices first underwent red blood cell perfusion under physiologic oxygen levels (12% O_2) for 10 minutes, establishing a baseline. Then, perfusion was continued under hypoxia (5% O_2) for an additional 10 minutes. Throughout the testing, the device was monitored via brightfield microscopy for evidence of clot formation and occlusion in real-time. For the purpose of this study, occlusion was defined as complete microchannel obstruction and blockage of flow. Quantity of fully occluded microchannels was recorded at 5-minute intervals. Occlusion incidence was presented as a percentage of the 32 total microchannels that were fully obstructed within each device.

4.2.5 Microscopy and image processing

Microscopy was performed on a Zeiss Axio Observer widefield microscope equipped with a temperature-controlled chamber preset to 37°C. The microscope and accompanying incubation chamber were used for both the hypoxia preconditioning and the occlusion assay procedures. A high-speed camera (Hamamatsu) was used to capture pictures and videos of the microfluidic device. Image processing was performed in Zen software (Zeiss).

4.2.6 Statistical analyses

Prism (GraphPad) and MATLAB (MathWorks) were used to conduct multiple statistical analyses. Occlusion incidence significance results were determined via one-way or two-way ANOVA testing, where appropriate. Geisser-Greenhouse correction was used to account for lack of sphericity/unequal variability of differences as recommended. A Tukey test for multiple comparison analysis was performed at a confidence interval of 95%.

Two statistical analyses methods were used to correlate clinical predictors with the vaso-occlusive outcome on-chip for each preconditioning treatment: first, a Spearman nonparametric correlation and second, a partial least squares regression analysis (PLSR). Unlike a typical Pearson correlation, Spearman correlation makes no assumption about the distribution of values and does not require data to be samples from a Gaussian distribution. Significance was indicated via p-value, in which *$p<0.05$ and **$p<0.01$. In parallel, statistical regression modeling was performed using a PLSR analysis. The model was generated with 7 features in the X-block (the biological predictors: hemoglobin, hematocrit, MCV, MCHC, RDW, WBC, and PLT) and 1 feature in the Y-block (the response variable: microchannel occlusion incidence). Variable importance in projection (VIP) scores above 1 indicate significant contribution to the model. The coefficient of determination R^2 indicates how well the regression model explains the variance in the response variable.

4.3 Results and Discussion

In this chapter, we present an application of the novel microfluidic platform that was presented in Chapter 3. Specifically, we introduce an occlusion assay that was used to explore the relationship between hypoxia reperfusion injury and vaso-occlusion in SCD. The results presented here better inform our current understanding of hypoxia's effects on the endothelium and its contributions to VOC in SCD.

4.3.1 Measurement of vaso-occlusive incidence on-chip

The lack of effective treatment options for SCD highlights the need for more physiologically relevant, predictive models to better understand the underlying contributors to VOC. To investigate our hypothesis that pre-treatment of the endothelium with mild hypoxia or hypoxia cycling may protect against VOC, we first developed a methodology to quantify likelihood of a patient sample to occlude on-chip.

To test the effect of hypoxia preconditioning on probability of microchannel occlusion, a cohort of patient samples were perfused through endothelialized devices that had been preconditioned to each of the four conditions: atmospheric control, physiologic control, cyclic hypoxia, or sustained hypoxia. Throughout the course of the experiment, total occlusion incidence was quantified. Microchannel occlusion percentage for each device, with associated hypoxia preconditioning treatment and patient identifiers, were reported at 5-minute intervals (Figure 4.2).

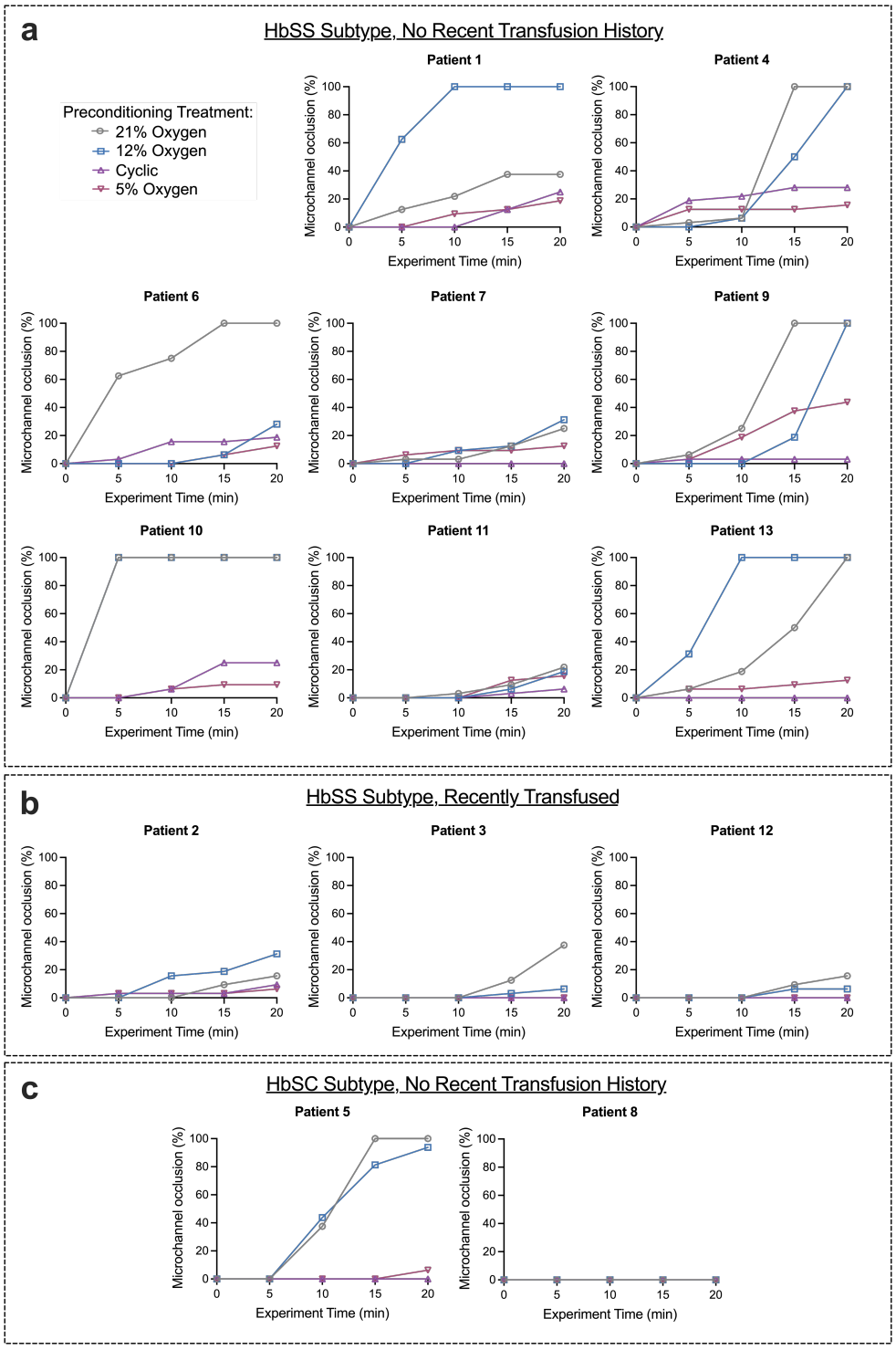


Figure 4.2: **Occlusion profiles for each patient sample.** Microchannel occlusion percentage at 5-minute intervals are presented for each of the 13 patient samples perfused through preconditioned endothelialized devices. The cohort included samples from patients with the following genotypes and histories: (a) SS, no recent transfusions, (b) SS, recent transfusions, (c) SC, no recent transfusions.

Review of individual patient occlusion profiles over time draws attention to several conclusions. First, the occlusion assay can be used to make deductions about vaso-occlusive likelihood of individual patient samples on-chip, which may correspond to SCD severity and clinical risk of VOC. In general, both sustained and cyclic hypoxia-pretreated endothelialized devices exhibited less propensity for vaso-occlusion compared to either control condition. Lastly, while these trends are regularly conserved for each patient, significant patient-to-patient occlusion variability exists. Further investigation into patient-specific characteristics like genotype, transfusion history, and clinical laboratory predictor variables can be of use in explaining this heterogeneity.

It should be noted that this patient cohort includes a varied group of patient samples, which likely contributed to heterogeneity in response. It was not always possible to control for these variables before receiving and running samples. First, all blood samples were obtained from patients diagnosed with SCD, but 11 were identified as genotype HbSS (the most common symptomatic form of SCD) whereas the remaining 2 (patient ID numbers 5 and 8) were identified as the genotype HbSC (sickle hemoglobin HbSC disease). Though driven by a similar pathophysiology, hemoglobin SC disease generally presents with less clinical severity[17] and is poorly researched, which may explain the abnormal complete lack response from patient 8. Patient 8 was completely protected from vaso-occlusion regardless of treatment condition. Future work should be done to more thoroughly

characterize the sickle hemoglobin SC variant in our devices, as a larger sample size is needed draw any significant conclusions.

In addition to genotype variability, it was not possible to control for patient therapeutic/transfusion history. Several of the patients within this cohort (patient ID numbers 2, 3, and 12) had a recent history of transfusion with moderate levels of HbA as evidenced by their hemoglobin variant analyses (ranging between 13.3 and 18.7% HbA). Just as transfusions manage VOC and other disease complications, it would be expected that transfused blood in a patient sample might reduce incidence of occlusion on-chip. Closer inspection of these transfused patient samples confirms this theory, as all three were minimally occlusive. Regardless of treatment condition, not a single transfused sample experienced full device occlusion. Additionally, we were unable to obtain full medication lists for all patients. In possible future studies, it could be valuable to stratify results based on active medication lists to investigate therapeutic effectiveness in VOC management.

4.3.2 Hypoxia preconditioning reduces probability of vaso-occlusion

Occlusion results from each patient were pooled to analyze trends across the cohort of SCD samples with varied expression profiles. (Figure 4.3; Figure 4.S1). Across samples, a bimodal distribution was observed in which endothelium preconditioned with either cyclic or sustained hypoxia exhibited a lower likelihood

of vaso-occlusion compared to either control. This trend was initially observed to a lesser, not statistically significant, extent within the first 10 minutes of the experiment under 12% O_2 (Figure 4.3 a). The trend then became statistically significant after the 5% O_2 period, in which incidence of adhesion, occlusion, and full device obstruction became more common (**p<0.01) (Figure 4.3 b). We observed average vaso-occlusion rates of 8.89% and 11.78% after cyclic and sustained hypoxia preconditioning compared to 57.93% and 55.05% for atmospheric and physiologic controls, respectively. There were no significant differences between control conditions or between hypoxic conditions.

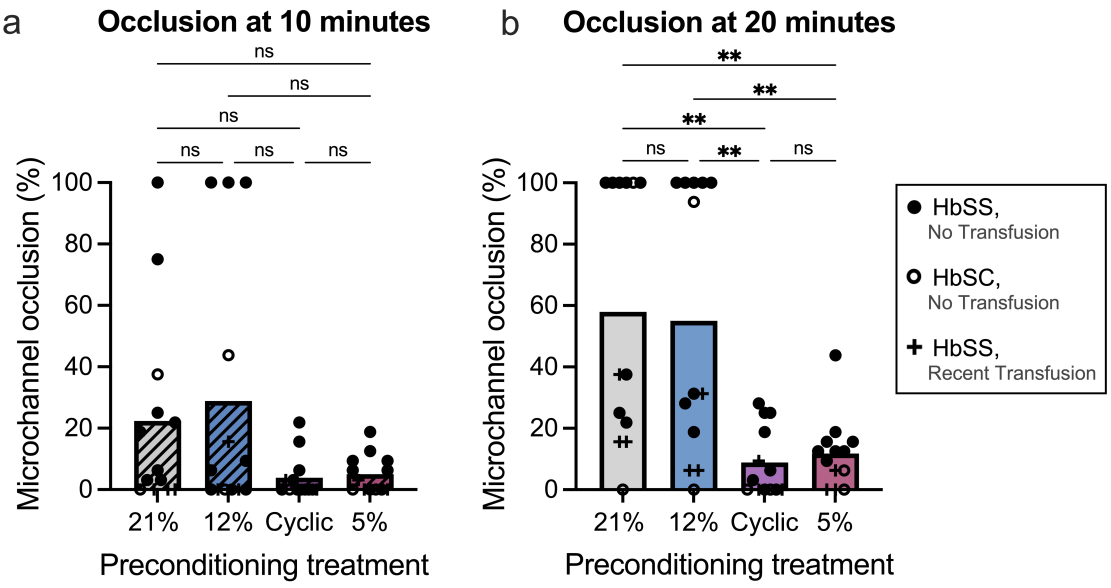


Figure 4.3: Hypoxia preconditioning prevents vaso-occlusion among varied cohort of SCD patient samples. Blood occlusion assay can be used to examine the effect of hypoxia preconditioning on occlusion incidence of a varied cohort of SCD patient samples (n=13) after (a) initial 10 minutes of red blood cell perfusion at 12% oxygen and after (b) subsequent 10 minutes of red blood cell perfusion at 5% oxygen. Filled circles indicate samples from non-transfused patients with the HbSS genotype, empty circles indicate samples from non-transfused patients with the HbSC genotype, pluses indicate samples from patients with the HbSS genotype who had recently been transfused. One-way ANOVA statistical testing was performed, *p<0.05, **p<0.01. An alternate form of this plot marking individual patients with unique shape identifiers is available in the supplement (Figure 4.S1).

To assess any potential effect due to recent transfusion history, the data was also statistically tested and plotted excluding patients 2, 3, and 12 (Figure 4.S2). Exclusion of the transfused sample data did not affect the significance of this result, in fact there was only a slight change in magnitude for each treatment group while the trends remained the same. Exclusion of transfused samples increased the average microchannel occlusion percentage from 57.9% to 68.4%, 55.0% to 67.2%, 8.9% to 10.6%, and 11.8% to 14.7% for the atmospheric control, physiologic control, cyclic hypoxia, and sustained hypoxia preconditioning treatments, respectively.

These results support the hypothesis that hypoxia reperfusion may offer a protective effect against vaso-occlusion by preconditioning the endothelium in SCD. It also draws attention to the critical importance of incorporating physiologic features in model systems. When integral to the disease mechanisms, neglecting to account for biological components such as hypoxia may lead to unreliable conclusions that misinform clinical study.

4.3.3 Samples from male patients exhibit higher occlusion incidence

The occlusion assay presented in this chapter effectively concluded that hypoxia preconditioning of the endothelium reduces incidence of occlusion; however, we found the patient-to-patient variability to be especially compelling. SCD can present with significant phenotypic heterogeneity which is not completely

understood. To better understand what may be causing some patient samples to occlude more readily than others, we compared the occlusion outcomes and the patient clinical data set (Table 4.S1; Table 4.S2). First, we performed a statistical analysis to determine if samples from either male or female patients were more likely to occlude. It should be noted that this cohort included a narrow age range of female patients (n=5, ages 21-29) and a wider age range of male patients (n=8, ages 7-39). In girls, hormonal changes during puberty are known to have some clinical effect on SCD,[207] however, this potentially confounding variable is not relevant to our study due to all females being in the adult category. Based on our limited sample size, samples from male patients trended towards higher occlusion likelihood (Figure 4.4). In the case of the physiologic control, samples from male patients were significantly more likely to occlude ($p=0.0497$ when analyzing all samples, or $p=0.0227$ when analyzing only non-transfused samples). These results aligned with what has been reported in the literature. In pediatrics, male SCD patients reported higher pain crisis frequency compared to female patients (1.6 vs. 0.6 per year) and also experienced more severe infectious and cardiovascular complications.[208] Worse morbidity and mortality rates have also been observed in adult male patients compared to female patients.[36] Additional samples are needed to further validate this claim in devices, but these initial conclusions prompt significant interest for future studies. Moreso, uncoupling why male patients may experience more severe SCD could present opportunities for therapeutic intervention.

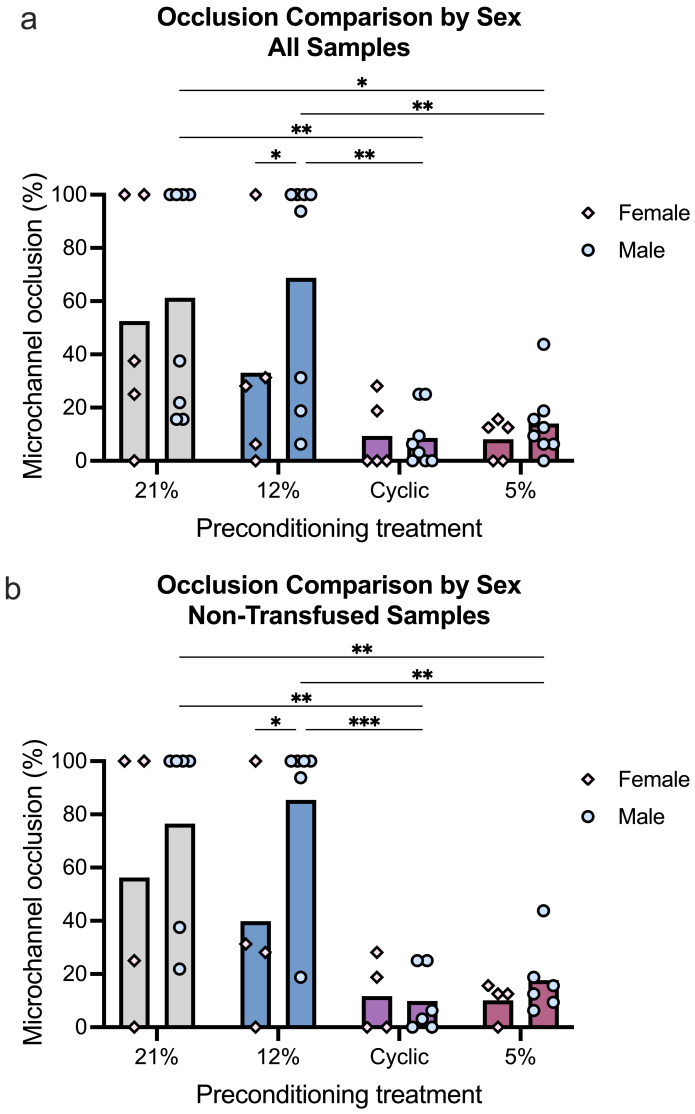


Figure 4.4: Incidence of vaso-occlusion, comparison by sex. Incidence of microchannel occlusion in preconditioned devices was analyzed for all patient samples, separated by sex. Analysis was performed for (a) entire cohort of varied samples, and (b) only non-transfused samples. Diamonds indicate samples from female patients, circles indicate samples from male patients. Two-way ANOVA statistical testing was performed, *p<0.05, **p<0.01, ***p<0.001.

4.3.4 Investigation of clinical predictor variables' contributions to occlusive outcomes

We leveraged multiple statistical methods to test our hypothesis that clinical predictor variables may be correlated occlusion incidence. Each of these methods

– the nonparametric Spearman correlation and partial least squares regression analysis (PLSR) – are unique, offering distinct advantages and disadvantages.

A nonparametric Spearman correlation was performed to investigate the relationship between clinical predictor variables and percent occlusion in response to each type of hypoxia preconditioning treatment (Figure 4.5; Figure 4.S3). Separately, statistical testing was performed on the entire patient sample set, and also the cohort of only non-transfused samples to isolate the potentially confounding variable of donor blood. Across both analyses, a number of significant trends were observed. Hemoglobin and hematocrit demonstrated a weak inverse correlation with occlusion percentage across all groups except the atmospheric control. Generally, HbS, MCV, WBC, and PLT exhibited moderate correlation with occlusion percentage across all groups. When analyzing the entire patient sample set (n=13), the results show significant correlation between HbS and percent occlusion in the 5% preconditioning group (r_s=0.769, p=0.003), between PLT and percent occlusion in the 5% preconditioning group (r_s=0.735, p=0.006), and between WBC and percent occlusion in the 5% and 12% oxygen preconditioning groups (r_s=0.696, p=0.01, and r_s=0.612, p=0.03, respectively).

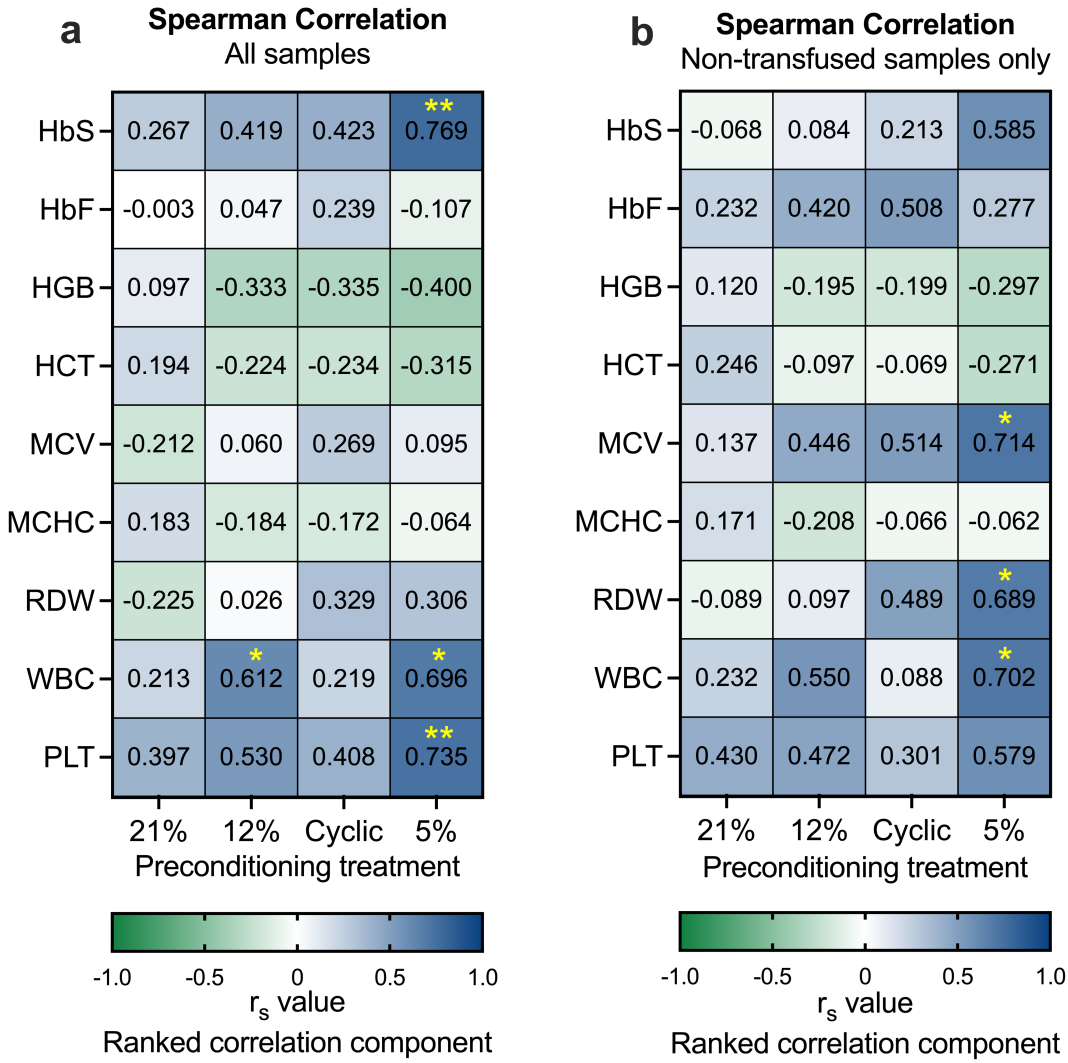


Figure 4.5: Spearman correlation of clinical predictor variables with occlusion. A nonparametric Spearman correlation was used to quantify correlation between clinical predictor variables and percent microchannel occlusion after various hypoxia preconditioning treatments. Spearman correlation r value was calculated for (a) all samples (n=13) and (b) only non-transfused samples (n=10). Clinical metrics were obtained from hemoglobin variant analysis and complete blood count testing, and consist of hemoglobin S (HbS), hemoglobin F (HbF), hemoglobin (HGB), hematocrit (HCT), mean corpuscular volume (MCV), mean corpuscular hemoglobin concentration (MCHC), red blood cell distribution width (RDW), white blood cell count (WBC), and platelet count (PLT). Ranked correlation coefficient "r_s" ranges from -1 to 1 as indicated in the legend, with 0 indicating that the variables do not vary together, 1 indicating perfect correlation, and -1 indicating perfect inverse correlation. Significance is indicated by asterisks, *p<0.05, **p<0.01.

Analysis of the non-transfused patient cohort minimally affected interpretation. Notedly, the non-transfused analysis demonstrated a stronger correlation between both MCV and RDW with occlusion, but a weaker trend between HbS and occlusion. In particular, a significant correlation was observed in the 5% preconditioning group between MCV and percent occlusion (r_s=0.714, p=0.024), between RDW and percent occlusion (r_s=0.689, p=0.028), and between WBC and percent occlusion (r_s=0.702, p=0.085). These results indicate that patients with high levels of WBC, PLT, HbS, MCV, or RDW, as well as low levels of hemoglobin or hematocrit may exhibit a more occlusive, severe SCD phenotype.

In parallel, a partial least squares regression analysis (PLSR) was conducted to investigate the relationship between clinical predictor variables and percent occlusion for each type of hypoxia preconditioning treatment (Figures 4.6, 4.7, 4.8, and 4.9; Tables 4.1, 4.S3, and 4.S4). In a similar manner to the Spearman analysis, statistical testing was repeated on only the cohort of non-transfused samples in order to remove the potentially confounding variable of donor blood. The results of the analysis on the non-transfused patients are available in the supplemental materials (Figures 4.S4, 4.S5, 4.S6, and 4.S7; Tables 4.1, 4.S3, and 4.S4). Interpretation of the PLSR analysis is less straightforward than the Spearman test; however, comparison across treatment groups allows for several conclusions.

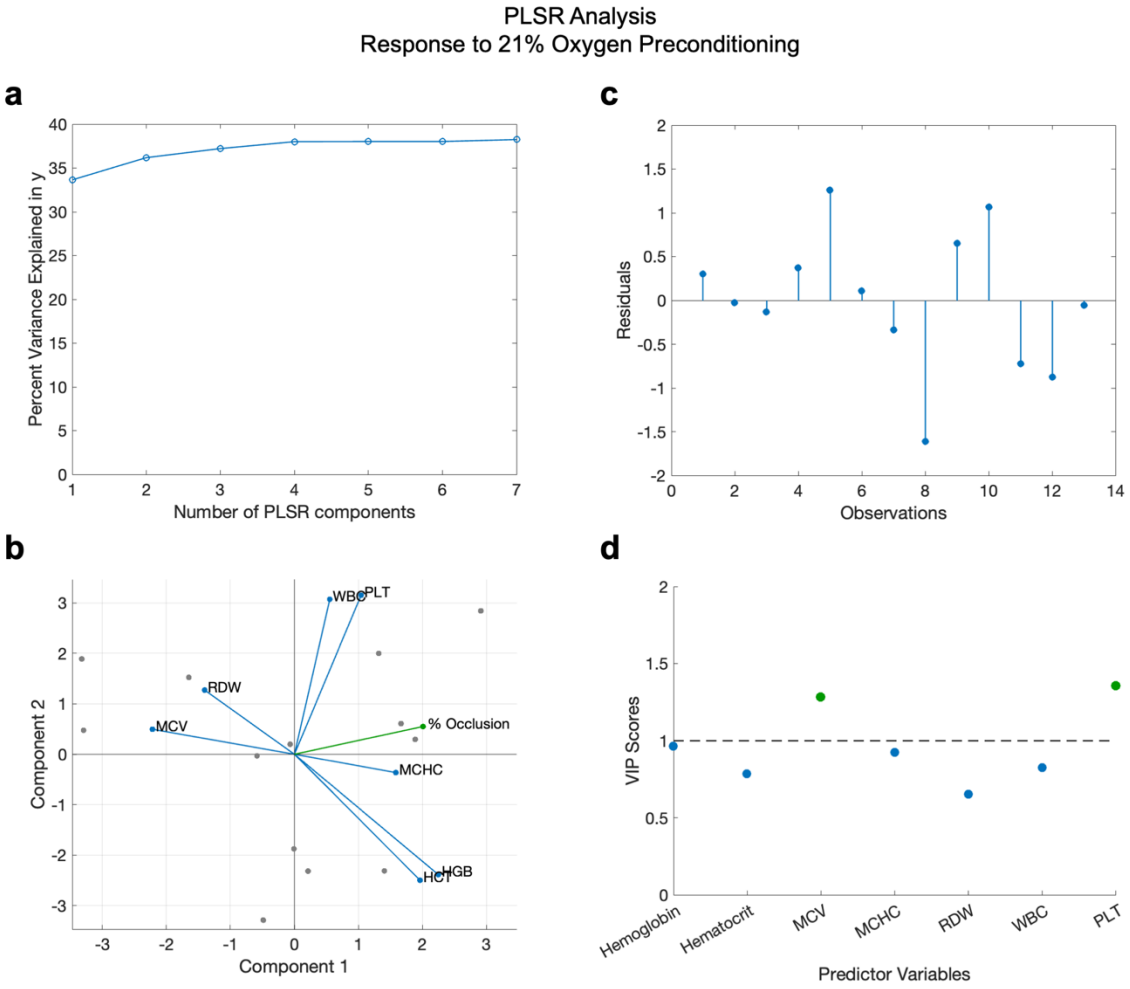


Figure 4.6: PLSR analysis of occlusion results among endothelium pretreated with atmospheric control. PLSR analysis was performed using only the devices that had been preconditioned with 21% O_2. (a) Percent of variance explained in the y-value (occlusion result) increases with increasing number of PLSR model components. (b) Loading biplot demonstrates clustering of variables along first two components of the model. (c) Random distribution of residual plot confirms PLSR model goodness of fit. (d) Variable importance in projection (VIP) scores of the clinical variables MCV and PLT show significant predictive contribution to the model. VIP scores greater than 1 indicate significant contribution to the model. VIP scores between 0.8 and 1.0 indicate marginal contribution.

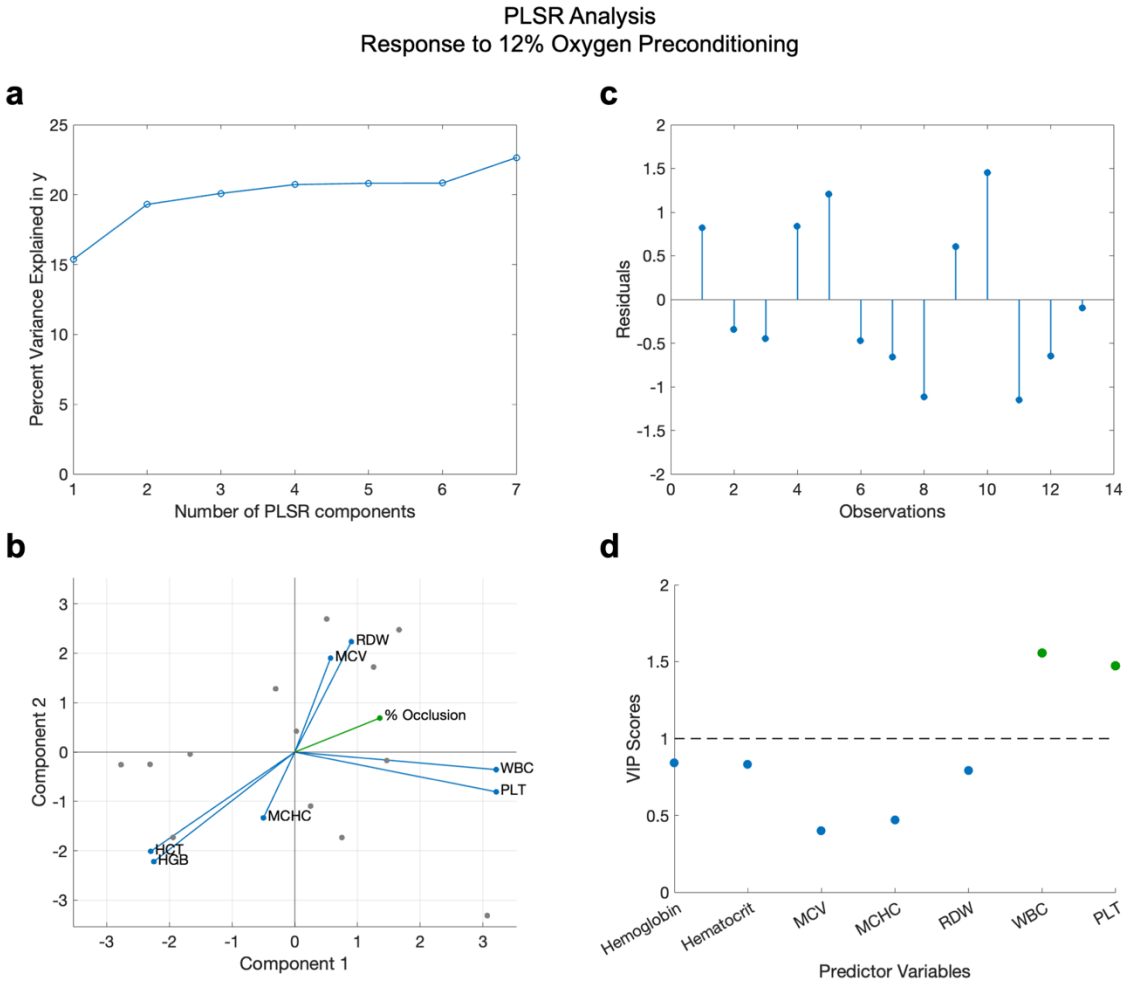


Figure 4.7: PLSR analysis of occlusion results among endothelium pretreated with physiologic control. PLSR analysis was performed using only the devices that had been preconditioned with 12% O_2. (a) Percent of variance explained in the y-value (occlusion result) increases with increasing number of PLSR model components. (b) Loading biplot demonstrates clustering of variables along first two components of the model. (c) Random distribution of residual plot confirms PLSR model goodness of fit. (d) Variable importance in projection (VIP) scores of the clinical variables WBC and PLT show significant predictive contribution to the model. VIP scores greater than 1 indicate significant contribution to the model. VIP scores between 0.8 and 1.0 indicate marginal contribution.

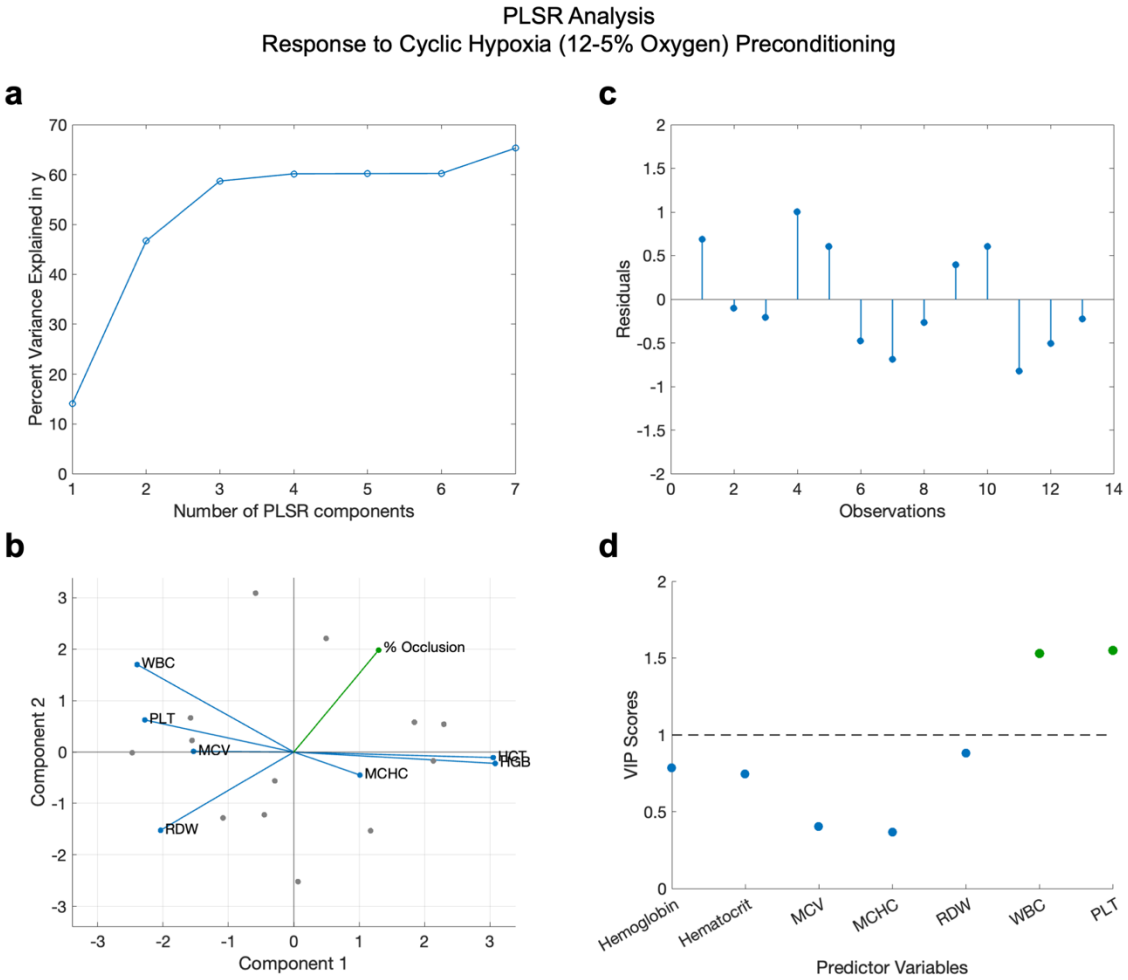


Figure 4.8: PLSR analysis of occlusion results among endothelium pretreated with cyclic hypoxia. PLSR analysis was performed using only the devices that had been preconditioned with cycling of 12% and 5% O_2. (a) Percent of variance explained in the y-value (occlusion result) increases with increasing number of PLSR model components. (b) Loading biplot demonstrates clustering of variables along first two components of the model. (c) Random distribution of residual plot confirms PLSR model goodness of fit. (d) Variable importance in projection (VIP) scores of the clinical variables WBC and PLT show significant predictive contribution to the model. VIP scores greater than 1 indicate significant contribution to the model. VIP scores between 0.8 and 1.0 indicate marginal contribution.

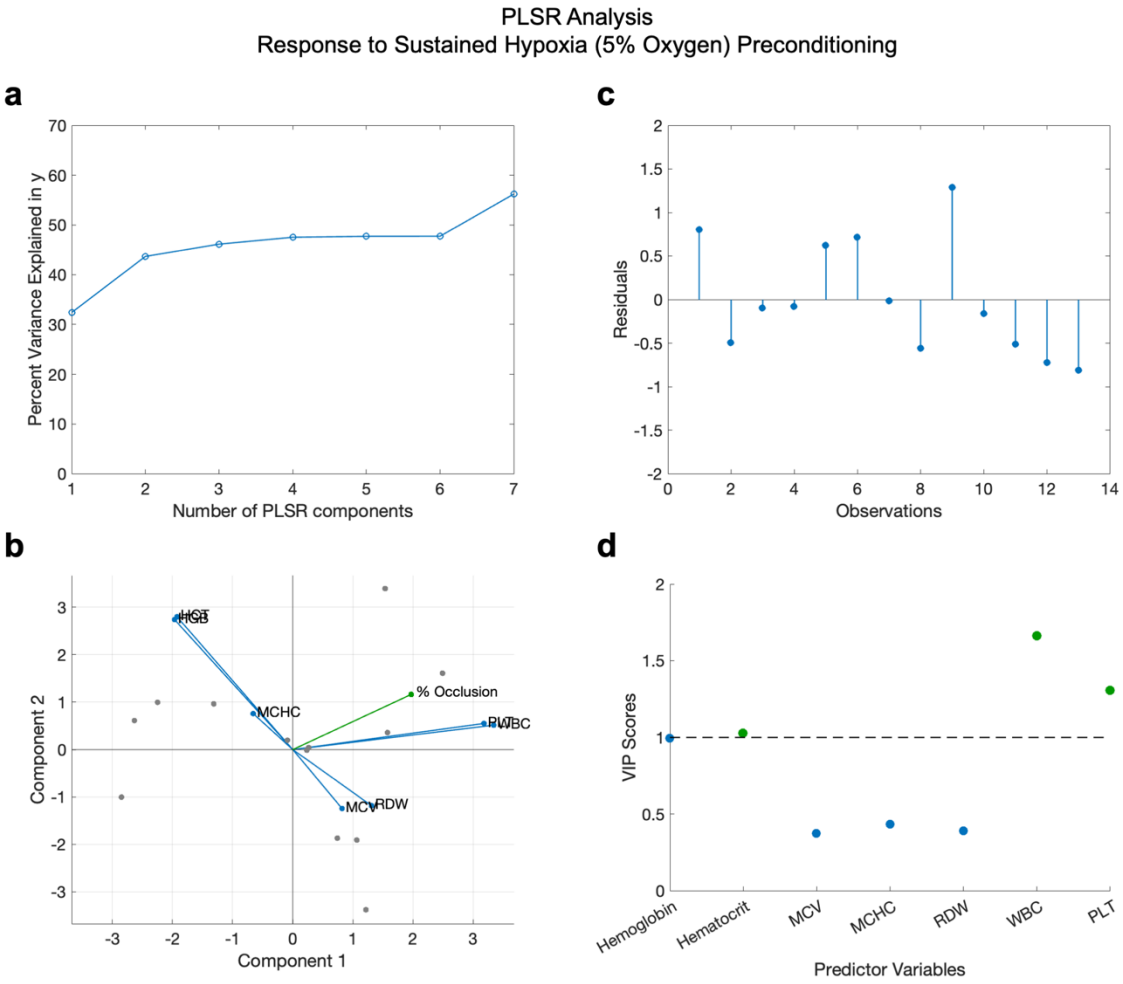


Figure 4.9: PLSR analysis of occlusion results among endothelium pretreated with sustained hypoxia. PLSR analysis was performed using only the devices that had been preconditioned with 5% O2. (a) Percent of variance explained in the y-value (occlusion result) increases with increasing number of PLSR model components. (b) Loading biplot demonstrates clustering of variables along first two components of the model. (c) Random distribution of residual plot confirms PLSR model goodness of fit. (d) Variable importance in projection (VIP) scores of the clinical variables hematocrit, WBC, and PLT show significant predictive contribution to the model. VIP scores greater than 1 indicate significant contribution to the model. VIP scores between 0.8 and 1.0 indicate marginal contribution.

First, it is evident that the PLSR model components explain a moderate portion of the variance in the occlusion result (Figures 4.6 a, 4.7 a, 4.8 a, and 4.9 a; Table 4.S3). When interpreting the PLSR models derived from all samples, the

average percent of variance explained was 36.46% for two components, 41.61% for four components, 41.71% for six components, and 45.61% for seven components. Meanwhile, interpretation of the PLSR models derived from only non-transfused samples yielded average percent of variance explained 41.01% for two components, 50.82% for four components, 51.27% for six components, and 74.40% for seven components (Table 4.S3). Accordingly, this means that the clinical variables used in this model offer some predictive power in the occlusion outcome. Further examination into specifically which variables, and how they inform a sample's likelihood to occlude, may better inform our understanding of VOC. However, it should be noted that these variables do not entirely explain the variance in the model. There are likely other factors apart from those tested here that explain the remaining variance.

Next, interpretation of variable clustering and variable importance in projection (VIP) scores of individual clinical predictors may elucidate how each component contributes to VOC in SCD. Generally, the PLSR loading plots showed clustering of clinical values that are associated with inflammation (WBC, PLT) and, separately, close clustering of clinical values associated with red blood cell indices (hemoglobin, hematocrit) along unique component axes (Figures 4.6 b, 4.7 b, 4.8 b, and 4.9 b). VIP scores indicate individual predictor variables' predictive contribution to the PLSR model, with a VIP>1 indicating significance. Consistently, WBC and PLT exhibited high VIP scores, indicating significant contribution to microchannel occlusion on-chip (Figures 4.6 d, 4.7 d, 4.8 d, and 4.9 d; Table 4.S4).

This result is particularly interesting, since the occlusion assay was performed using only red blood cells and not a whole blood solution containing white blood cells or platelets. This suggests that the chronic inflammation associated with high WBC and PLT activates not only the white blood cells and platelets but also exerts an effect on the red blood cells themselves. This inflammatory effect on the red blood cells appears to contribute to an increased occlusion incidence on-chip, aligning with existing literature. Studies have shown that WBC and PLT counts are significantly elevated during VOC, and high leukocyte counts have also been positively correlated with a number of SCD risk factors including early death, ACS, and stroke.[70] However, our study suggests that it may be white blood cell and platelets' effect on the red blood cells, rather than elevated WBC and PLT specifically, that increases vaso-occlusion during chronic periods of inflammation.

Lastly, various measures can be used to confirm the model's fit. The residual plots for each condition are randomly distributed, which indicates goodness of fit between the model results and the observed values from individual observations (Figures 4.6 c, 4.7 c, 4.8 c, and 4.9 c). When interpreting the PLSR models derived from all samples, the average R^2 value was 0.42 for two components, 0.46 for four components, 0.46 for six components, and 0.50 for seven components. Meanwhile, interpretation of the PLSR models derived from only non-transfused samples yielded average R^2 value of 0.47 for two components, 0.56 for four components, 0.56 for six components, and 0.77 for

seven components (Table 4.1). The results here show that a moderate amount of the variance was explained via incorporation of multiple components, however, additional factors could be included in order to better inform the model.

Preconditioning Treatment	**R^2 value** (all samples)						
	1C	2C	3C	4C	5C	6C	7C
21%	0.39	0.41	0.42	0.43	0.43	0.43	0.43
12%	0.22	0.26	0.26	0.27	0.27	0.27	0.29
Cyclic	0.21	0.51	0.62	0.63	0.63	0.63	0.68
5%	0.38	0.48	0.50	0.52	0.52	0.52	0.60
Preconditioning Treatment	**R^2 value** (non-transfused samples only)						
	1C	2C	3C	4C	5C	6C	7C
21%	0.34	0.36	0.37	0.38	0.38	0.38	0.72
12%	0.22	0.26	0.27	0.28	0.28	0.29	0.58
Cyclic	0.30	0.51	0.70	0.77	0.77	0.77	0.83
5%	0.54	0.74	0.78	0.80	0.80	0.80	0.95

Table 4.1: R^2 values for each PLSR model. PLSR analysis was performed in MATLAB, using both the entire cohort of samples (top) and only the cohort of samples from patients that had not recently undergone transfusion therapy (bottom). This table presents a summary of R^2 values from the PLSR model when including a given number of components (1C = 1 component, 2C = 2 components, etc.) for each treatment set. R^2 indicates how well the regression model explains the variance in the response variable. An R^2 of 0 indicates that the model explains none of the variance in occlusion and an R^2 of 1 indicates that the model completely explains all of the variance in the occlusion result.

4.4 Conclusion

Hypoxia reperfusion injury is a driving mechanism of SCD pathology; however, its contributions to VOC are not fully understood.[62,86–88] While hypoxia and reperfusion are traditionally associated with a negative inflammatory

response, recent studies have shown that certain periods of cyclic or mild hypoxia may in fact protect against subsequent reperfusion injury.[84,87,89,90] Gaining a better understanding of this mechanism improves our overall knowledge of SCD pathophysiology and could guide the development of targeted therapies in future studies.

Using the microfluidic platform developed in Chapter 3, we developed an occlusion assay to effectively measure occlusion incidence of individual samples on-chip. Moreover, we compared occlusion results between endothelialized devices preconditioned with different oxygen/hypoxia treatments to better understand the potential protective effect of hypoxia reperfusion injury. The results of this study demonstrate that mild sustained hypoxia and cyclic hypoxia preconditioning cause a protective effect, reducing incidence of vaso-occlusion on-chip. Additionally, various statistical methods were utilized to investigate patient-to-patient heterogeneity in occlusion result. In particular, several clinical predictor variables including sex, white blood cell count, and platelet count were correlated with occlusion outcome. These conclusions better inform our current understanding of VOC in SCD.

In this chapter, we applied the novel microfluidic platform developed in Chapter 3 to better understand the relationship between hypoxia reperfusion and vaso-occlusion. The next chapter will expand upon the conclusions gained here, leveraging next generation sequencing technologies to investigate the hypoxia-induced endothelial modifications that may affect occlusion incidence.

4.5 Acknowledgments

Portions of this work were conducted in the Minnesota Nano Center (MNC). The MNC provided access to photolithography and microfabrication equipment, facilitating the development of this microfluidic system and its use in SCD research. The MNC is supported in part by the National Science Foundation (NSF) through the National Nano Coordinated Infrastructure Network (NNCI) under Award Number ECCS-1542202. We also acknowledge Dr. Matthew MacEwen for his assistance performing the PLSR statistical analysis in MATLAB.

4.6 Supplemental Materials

The following supplemental materials include seven additional figures and four additional tables to be referenced in context with Chapter 4.

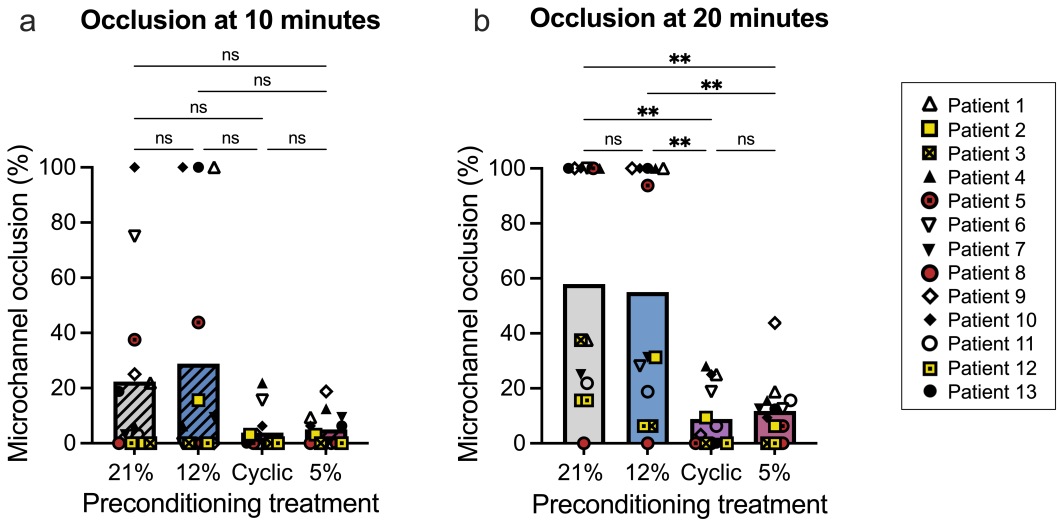


Figure 4.S1: Hypoxia preconditioning prevents vaso-occlusion among varied cohort of SCD patient samples (with patient-specific labeling). Alternate form of Figure 4.3, marking individual patients with unique shape identifiers to track patient-specific trends. Blood occlusion assay can be used examine effect of hypoxia preconditioning on occlusion incidence of a varied cohort of SCD patient samples (n=13). (a) After initial 10 minutes of red blood cell perfusion at 12% oxygen, a bimodal response began to emerge between preconditioning populations. (b) After subsequent 10 minutes of red blood cell perfusion at 5% oxygen, the data showed that endothelialized devices preconditioned with either cyclic hypoxia or sustained hypoxia were protected from vaso-occlusion on-chip compared to both controls. Refer to legend (right) to reference patient sample IDs. One-way ANOVA statistical testing was performed, *p<0.05, **p<0.01.

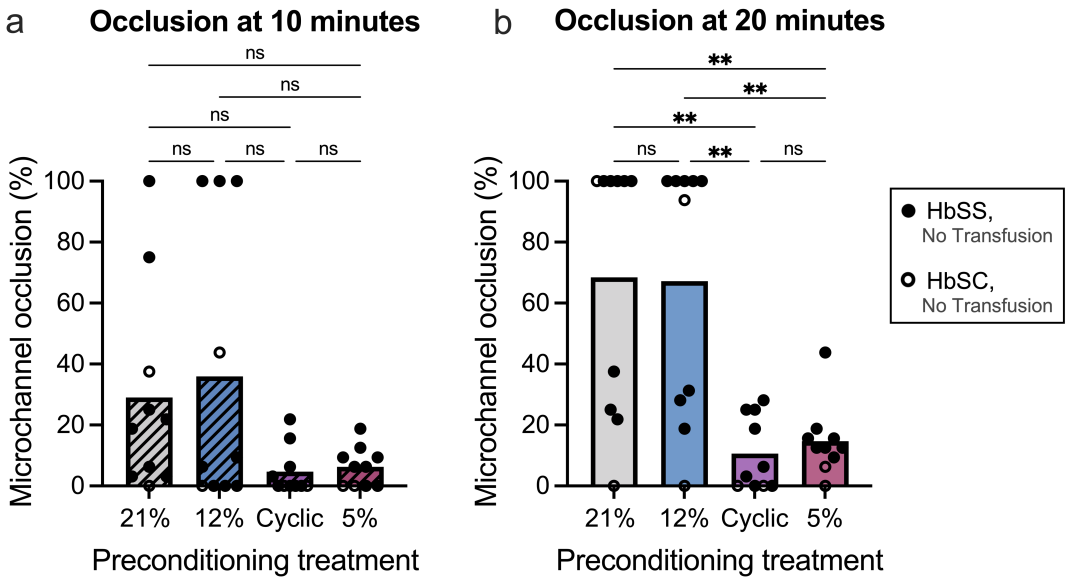


Figure 4.S2: Hypoxia preconditioning prevents vaso-occlusion among non-transfused SCD patient samples. Blood occlusion assay can be used examine effect of hypoxia preconditioning on occlusion incidence of a cohort of only non-transfused SCD patient samples (n=10). Marginal changes in magnitude, but not significance, are observed via exclusion of transfused samples when examining microchannel occlusion incidence over time. (a) After initial 10 minutes of red blood cell perfusion at 12% oxygen, a bimodal response began to emerge between preconditioning populations. (b) After subsequent 10 minutes of red blood cell perfusion at 5% oxygen, the data showed that endothelialized devices preconditioned with either cyclic hypoxia or sustained hypoxia were protected from vaso-occlusion on-chip compared to both controls. Filled circles indicate samples from non-transfused patients with the HbSS genotype, while empty circles indicate samples from non-transfused patients with the HbSC genotype. One-way ANOVA statistical testing was performed, *p<0.05, **p<0.01.

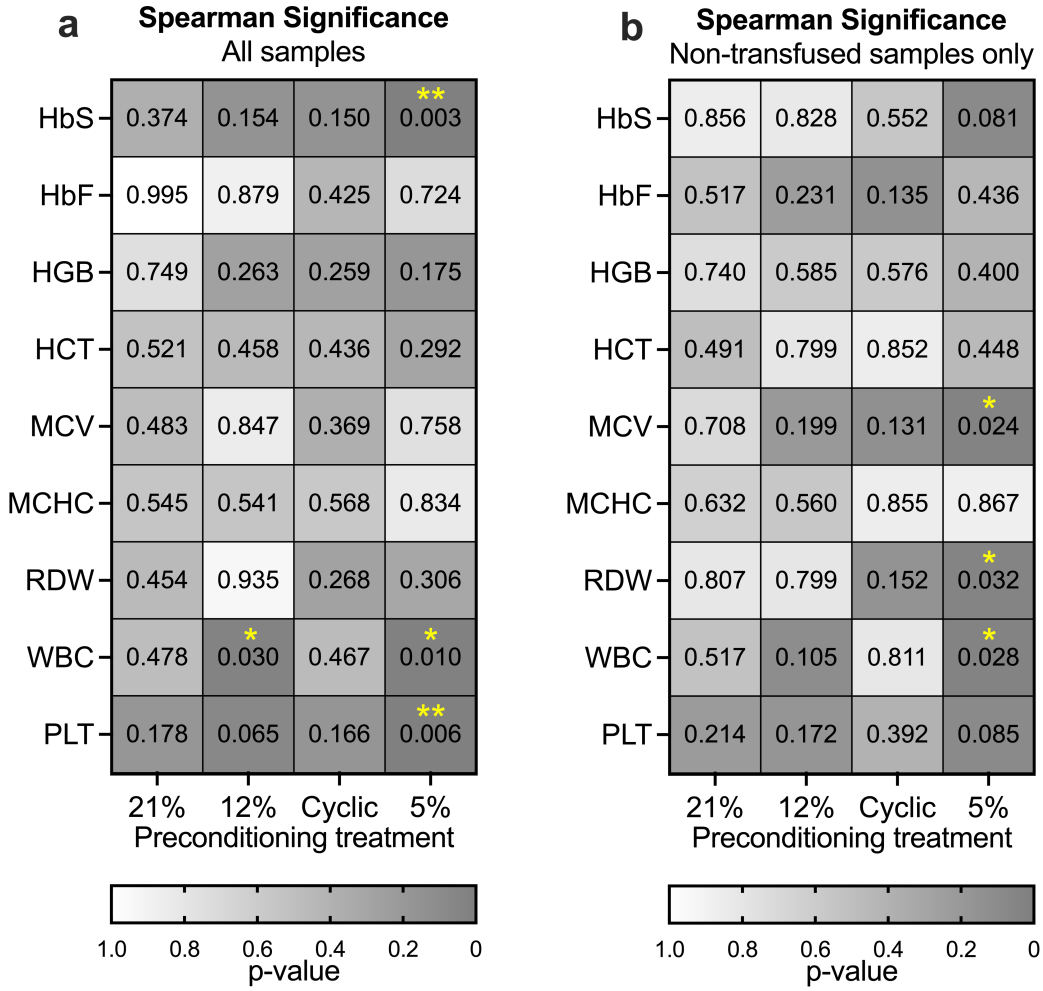


Figure 4.S3: Significance charts for spearman correlation. A nonparametric spearman correlation was used to quantify correlation between patient biomarkers and percent occlusion after various hypoxia preconditioning treatments. Spearman correlation p-values were calculated for (a) all samples (n=13) and (b) only non-transfused samples (n=10). Patient biomarkers were obtained from hemoglobin variant analysis and complete blood count testing, and consist of hemoglobin S (HbS), hemoglobin F (HbF), hemoglobin (HGB), hematocrit (HCT), mean corpuscular volume (MCV), mean corpuscular hemoglobin concentration (MCHC), red blood cell distribution width (RDW), white blood cell count (WBC), and platelet count (PLT). Significance is indicated by asterisks, *p<0.05, **p<0.01.

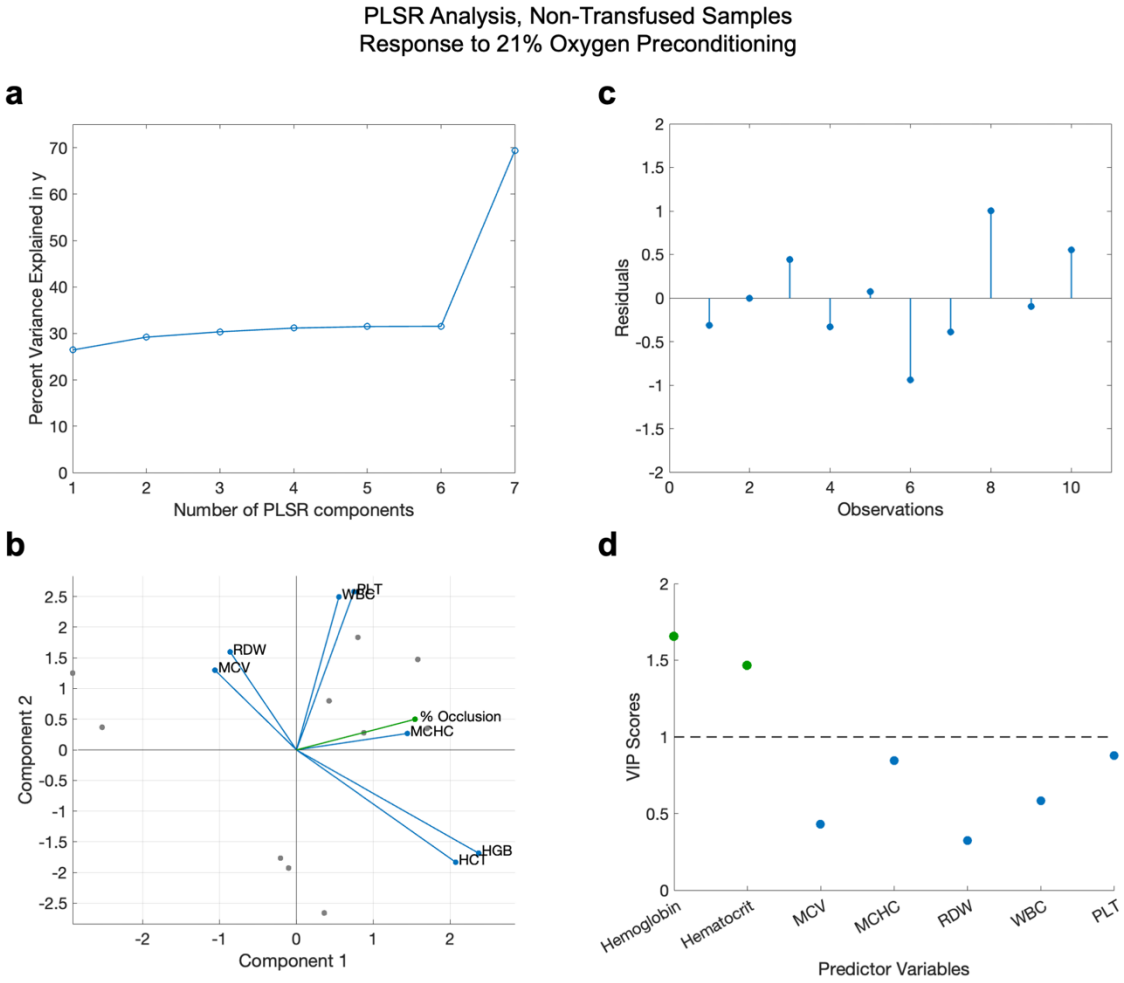


Figure 4.S4: PLSR analysis of occlusion results among endothelium pretreated with atmospheric control (non-transfused samples only). PLSR analysis was performed using only the cohort patients who had not recently undergone transfusion therapy and the device set that had been preconditioned with 21% O_2. (a) Percent of variance explained in the y-value (occlusion result) increases with increasing number of PLSR model components. (b) Loading biplot demonstrates clustering of variables along first two components of the model. (c) Random distribution of residual plot confirms PLSR model goodness of fit. (d) Variable importance in projection (VIP) scores of the clinical variables hemoglobin and hematocrit show significant predictive contribution to the model. VIP scores greater than 1 indicate significant contribution to the model. VIP scores between 0.8 and 1.0 indicate marginal contribution.

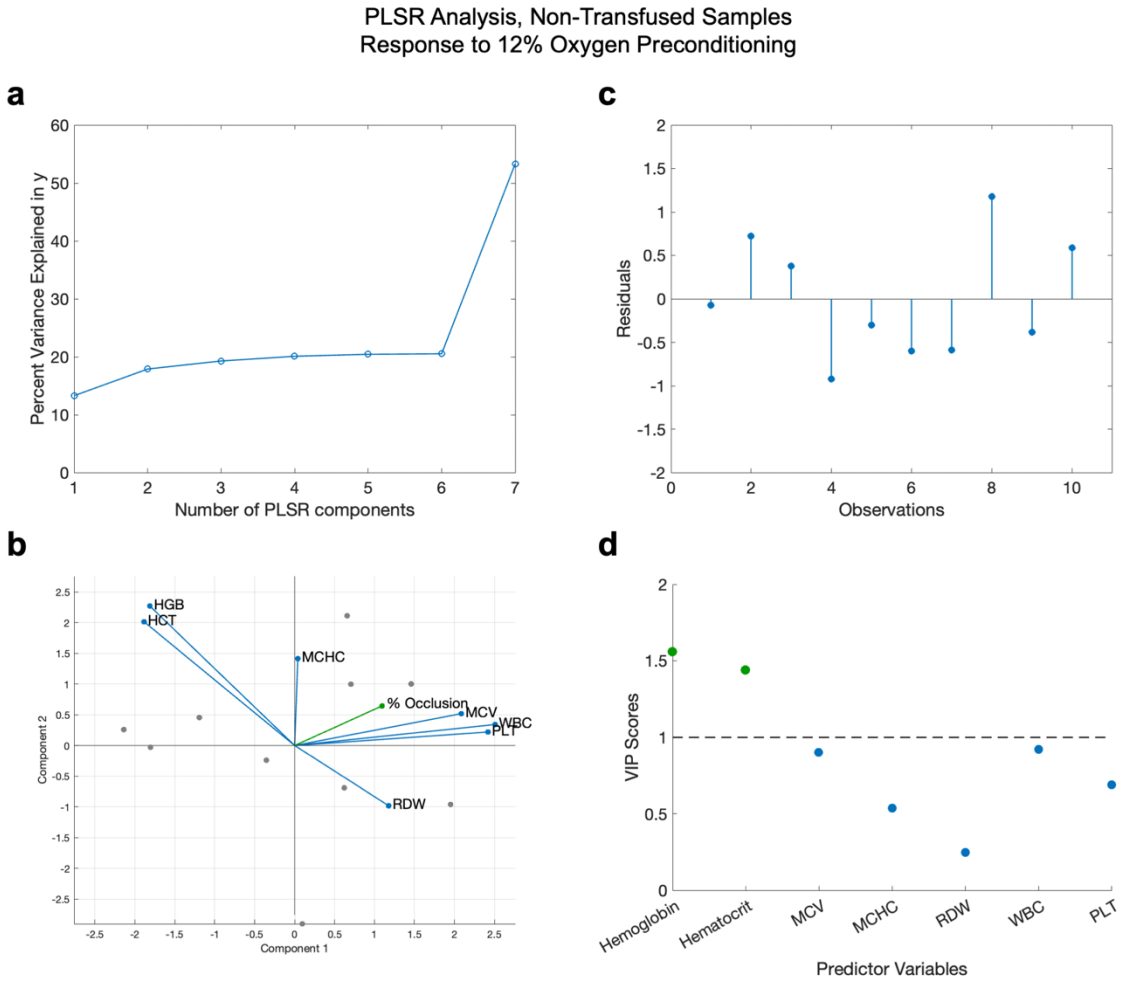


Figure 4.S5: PLSR analysis of occlusion results among endothelium pretreated with physiologic control (non-transfused samples only). PLSR analysis was performed using only the cohort patients who had not recently undergone transfusion therapy and the device set that had been preconditioned with 12% O_2. (a) Percent of variance explained in the y-value (occlusion result) increases with increasing number of PLSR model components. (b) Loading biplot demonstrates clustering of variables along first two components of the model. (c) Random distribution of residual plot confirms PLSR model goodness of fit. (d) Variable importance in projection (VIP) scores of the clinical variables hemoglobin and hematocrit show significant predictive contribution to the model. VIP scores greater than 1 indicate significant contribution to the model. VIP scores between 0.8 and 1.0 indicate marginal contribution.

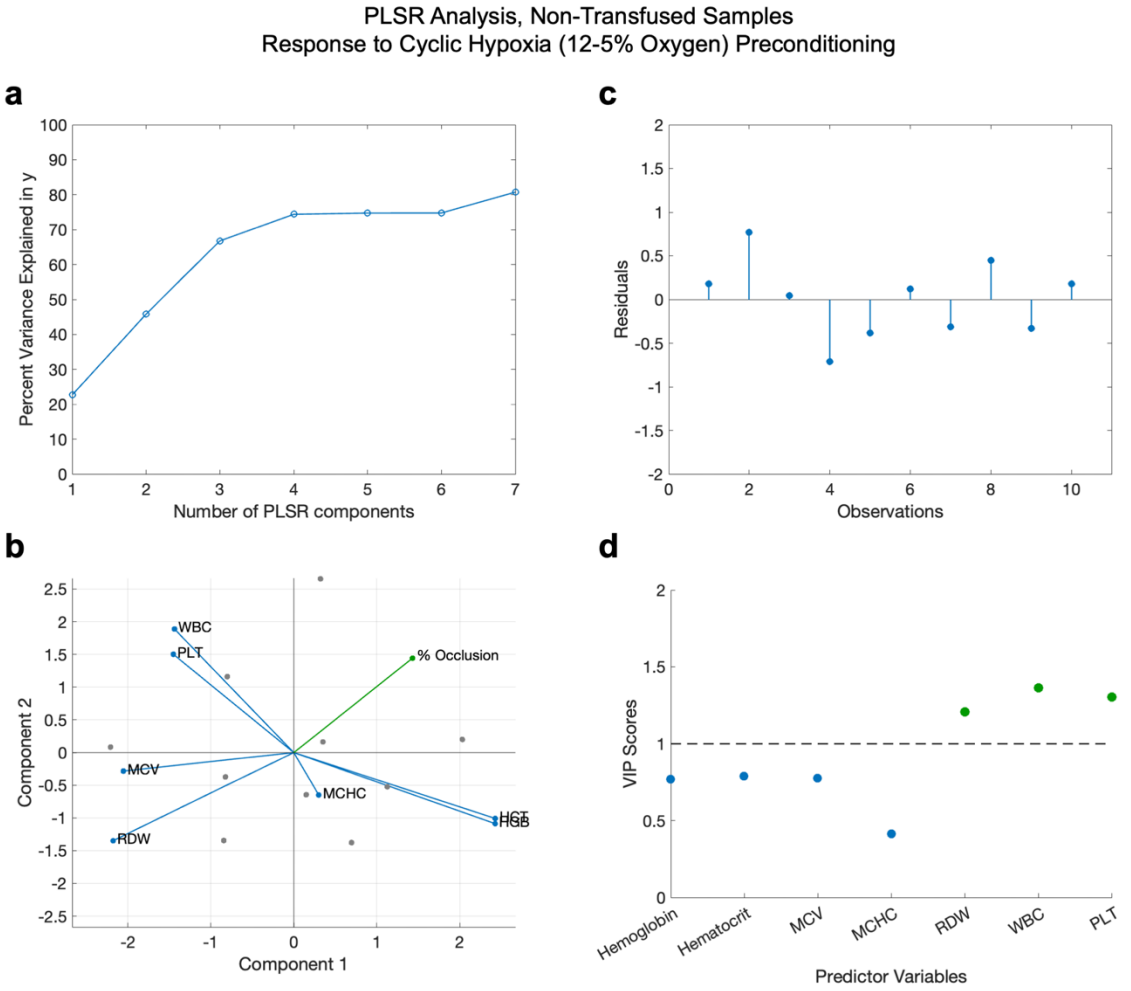


Figure 4.S6: PLSR analysis of occlusion results among endothelium pretreated with cyclic hypoxia (non-transfused samples only). PLSR analysis was performed using only the cohort patients who had not recently undergone transfusion therapy and the device set that had been preconditioned with cycling of 12% and 5% O_2. (a) Percent of variance explained in the y-value (occlusion result) increases with increasing number of PLSR model components. (b) Loading biplot demonstrates clustering of variables along first two components of the model. (c) Random distribution of residual plot confirms PLSR model goodness of fit. (d) Variable importance in projection (VIP) scores of the clinical variables RDW, WBC, and PLT show significant predictive contribution to the model. VIP scores greater than 1 indicate significant contribution to the model. VIP scores between 0.8 and 1.0 indicate marginal contribution.

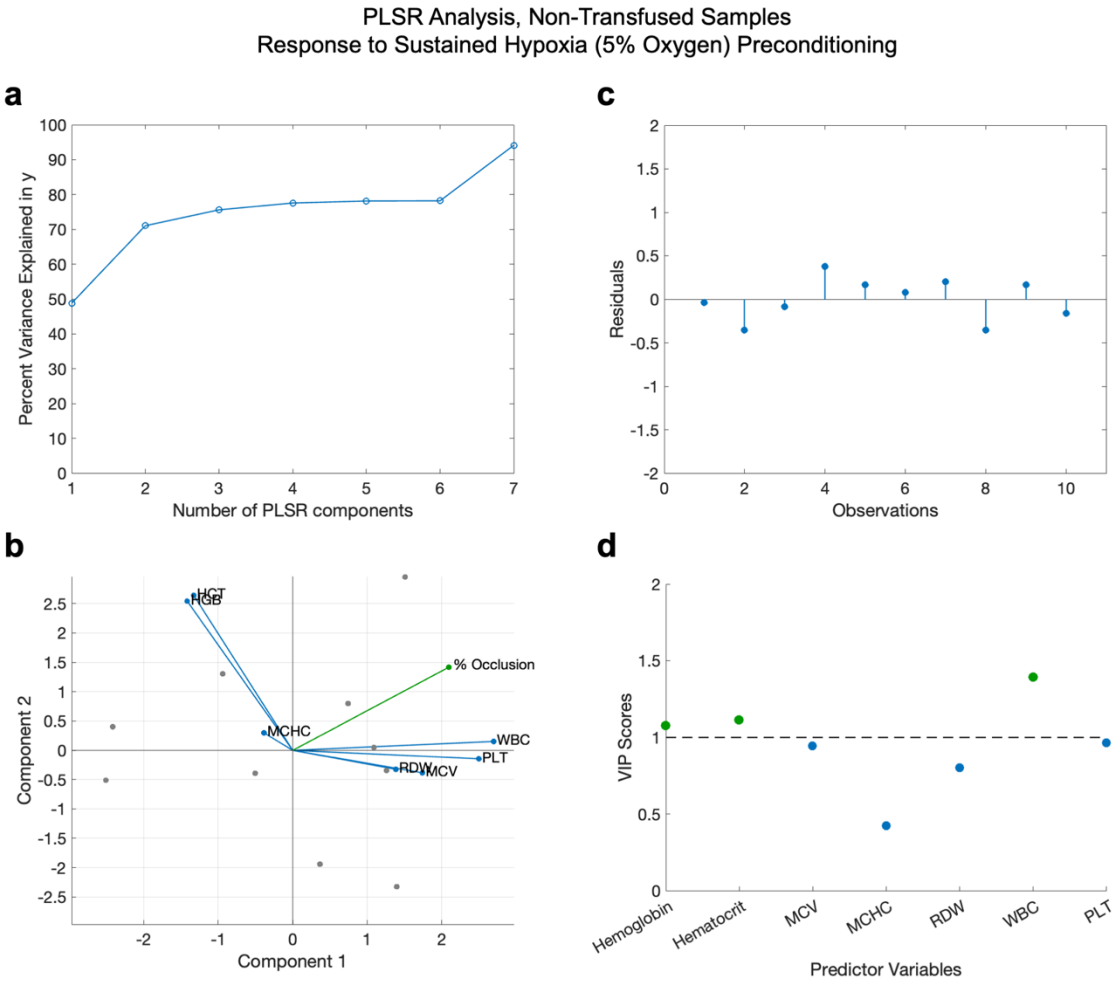


Figure 4.S7: PLSR analysis of occlusion results among endothelium pretreated with sustained hypoxia control (non-transfused samples only). PLSR analysis was performed using only the cohort patients who had not recently undergone transfusion therapy and the device set that had been preconditioned with 5% O_2. (a) Percent of variance explained in the y-value (occlusion result) increases with increasing number of PLSR model components. (b) Loading biplot demonstrates clustering of variables along first two components of the model. (c) Random distribution of residual plot confirms PLSR model goodness of fit. (d) Variable importance in projection (VIP) scores of the clinical variables hemoglobin, hematocrit, and WBC show significant predictive contribution to the model. VIP scores greater than 1 indicate significant contribution to the model. VIP scores between 0.8 and 1.0 indicate marginal contribution.

ID	Age	Sex	HU	Genotype	Hemoglobin Variant Analysis				
					HbS	HbF	HbA	HbA2	HbC
1	31	M	Y	HbSS	78.4%	18.8%	0%	2.8%	0%
2	39	M	Y	HbSS	64.5%	19.9%	13.4%	2.2%	0%
3	28	F	Y	HbSS	56.5%	26.5%	13.3%	3.7%	0%
4	21	F	Y	HbSS	78.3%	18.9%	0%	2.8%	0%
5	27	M	Y	HbSC	48.4%	6.4%	0%	3.8%	41.4%
6	21	F	Y	HbSS	78.6%	18.4%	0%	3.0%	0%
7	23	F	Y	HbSS	84.9%	11.8%	0%	3.3%	0%
8	29	F	Y	HbSC	49.6%	9.3%	0%	3.2%	38.0%
9	13	M	Y	HbSS	89.2%	7.4%	0%	3.4%	0%
10	31	M	Y	HbSS	81.6%	14.9%	0%	3.5%	0%
11	14	M	Y	HbSS	84.7%	12.7%	0%	2.6%	0%
12	29	M	Y	HbSS	61.9%	17.0%	18.7%	2.4%	0%
13	7	M	Y	HbSS	77.1%	19.9%	0%	3.0%	0%

Table 4.S1: Patient blood sample datasheet II. Table includes patient identifying number, age, sex, hydroxyurea usage (HU: Yes (Y) or No (N)), SCD genotype, and metrics from hemoglobin variant testing (HbS: sickle hemoglobin, HbF: fetal hemoglobin, HbA: normal adult hemoglobin, HbA2: hemoglobin A2, HbC: hemoglobin C). Additional description of blood samples from these studies can be found in Table 4.S2. Normal reference ranges can be found in the appendix (Table A.1).

ID	History of Recent Transfusion?	Complete Blood Count Analysis						
		HGB	HCT	MCV	MCHC	RDW	WBC	PLT
1	No	6.5	18.2	115.9	35.7	18.5	8.54	446
2	Yes	7.2	21.6	107.5	33.3	18.9	8.35	335
3	Yes	10.0	27.7	102.2	36.1	15.6	4.00	122
4	No	8.4	23.1	84.6	36.4	20.5	9.75	539
5	No	9.3	24.5	84.5	38.0	17.2	4.52	61
6	No	8.9	24.2	86.1	36.8	17.4	6.53	500
7	No	6.8	20.6	84.4	33.0	18.9	9.28	381
8	No	9.7	27.3	80.8	35.5	14.5	4.96	196
9	No	9.8	27.8	96.0	35.3	17.8	11.10	460
10	No	9.5	27.5	93.0	34.5	16.9	5.30	277
11	No	8.9	24.0	102.0	37.7	19.9	8.10	365
12	Yes	9.1	24.3	103.0	37.4	21.6	8.10	331
13	No	8.4	22.8	92.7	36.8	14.7	12.02	676

Table 4.S2: Patient blood sample datasheet III. Table includes patient identifying number, transfusion history, and clinical variables from complete blood count testing (HGB: hemoglobin (g/dL), HCT: hematocrit (%), MCV: mean corpuscular volume (fL), MCHC: mean corpuscular hemoglobin concentration (g/dL), RDW: red cell distribution width (%), WBC: white blood cell count (k/μL), PLT: platelet count (k/μL). Additional description of blood samples from these studies can be found in Table 4.S1. Normal reference ranges can be found in the appendix (Table A.1).

Preconditioning Treatment	Percent of Variance Explained in Occlusion Result PLSR (all samples)						
	1C	2C	3C	4C	5C	6C	7C
21%	33.66	36.19	37.22	38.01	38.03	38.032	38.252
12%	15.36	19.32	20.11	20.74	20.84	20.85	22.67
Cyclic	14.06	46.67	58.72	60.17	60.21	60.24	65.3
5%	32.39	43.66	46.13	47.52	47.71	47.73	56.22
Preconditioning Treatment	**Percent of Variance Explained in Occlusion Result** PLSR (non-transfused samples only)						
	1C	2C	3C	4C	5C	6C	7C
21%	26.44	29.21	30.36	31.16	31.48	31.54	69.34
12%	13.3	17.91	19.28	20.1	20.44	20.53	53.34
Cyclic	22.72	45.83	66.77	74.41	74.76	74.78	80.75
5%	48.81	71.09	75.63	77.6	78.17	78.23	94.15

Table 4.S3: Percent of variance explained in occlusion result by PLSR modeling. PLSR analysis was performed using both the entire cohort of samples (top) and only the cohort of samples from patients that had not recently undergone transfusion therapy (bottom). This table presents a summary of percent of variance explained in occlusion result by each PLSR model component (1C = 1 component, 2C = 2 components, etc.) for each treatment set.

Preconditioning Treatment	**VIP Scores** (all samples)						
	HGB	HCT	MCV	MCHC	RDW	WBC	PLT
21%	0.967	0.787	**1.283**	0.926	0.651	0.825	**1.356**
12%	0.842	0.831	0.400	0.469	0.793	**1.556**	**1.474**
Cyclic	0.786	0.747	0.405	0.366	0.883	**1.531**	**1.550**
5%	0.994	**1.028**	0.373	0.434	0.390	**1.663**	**1.308**
Preconditioning Treatment	**VIP Scores** (non-transfused samples only)						
	HGB	HCT	MCV	MCHC	RDW	WBC	PLT
21%	**1.655**	**1.465**	0.430	0.845	0.323	0.582	0.878
12%	**1.559**	**1.441**	0.903	0.537	0.247	0.923	0.690
Cyclic	0.768	0.788	0.774	0.414	**1.206**	**1.363**	**1.305**
5%	**1.080**	**1.115**	0.945	0.425	0.804	**1.393**	0.964

Table 4.S4: Variable Importance in projection scores of PLSR analysis. PLSR analysis was performed using both the entire cohort of samples (top) and only the cohort of samples from patients that had not recently undergone transfusion therapy (bottom). The clinical variables hemoglobin (HGB), hematocrit (HCT), mean corpuscular volume (MCV), mean corpuscular hemoglobin concentration (MCHC), red blood cell distribution width (RDW, %), white blood cell count (WBC), and platelet count (PLT) were loaded as predictor variables and percent microchannel occlusion was loaded as the response variable. Variable importance in projection scores (VIP) greater than 1 are bolded and indicate significant variable contribution to the model. VIP scores between 0.8 and 1.0 indicate marginal variable contribution.

Chapter 5: Leveraging Next-Generation Sequencing to Investigate Effects of Hypoxia Preconditioning

5.1 Introduction

Sickle cell disease (SCD) is chronic multisystem disorder affecting millions of people worldwide.[1,3] Treatment options for SCD are limited and fail to adequately address disease pathology.[20,98] A more comprehensive understanding of underlying biological mechanisms will better inform future study and the development of more effective therapies. SCD pathophysiology is highly complex; hemoglobin polymerization initiates a cascade of downstream effects resulting in painful vaso-occlusive crisis (VOC). Notably, the endothelium plays a significant role in the development of VOC in SCD.[20,98] While increased attention has been directed to hypoxia reperfusion injury as a driving mechanism of SCD in recent years, much about it is still poorly understood.[62,86–88] In particular, we set out to investigate the relationship between hypoxia reperfusion, the endothelium, and VOC in SCD.

In the previous chapter, we demonstrated that mild and cyclic hypoxia preconditioning reduce incidence of occlusion on-chip. We hypothesized that changes in genetic expression of the endothelium due to hypoxic preconditioning may better explain this protective effect. In this chapter, we leveraged next-generation sequencing (NGS) technology to explore the transcriptional changes

responsible for this functional result. Extraction of cells from endothelialized microfluidic devices for RNA sequencing (RNA-seq) is a unique application of microfluidics. At the time of writing this, one other lab has recently published such a methodology.[182] However, NGS has been widely used in the last several decades in other biological applications, enabling exploration of biological pathways and identification of therapeutic targets.

We developed a unique device extraction method to obtain RNA from cells cultured in microfluidic devices and thoroughly validated the quality control and efficacy of this method. RNA-seq was then performed to identify transcriptional changes associated with hypoxia and VOC. We observed significant modulation in gene regulation across preconditioning treatments, especially among gene ontology pathways of interest such as blood coagulation, cell adhesion, and endothelial cell functional behavior. We hypothesized that modulation of specific genes within these pathways may contribute to variance in occlusion. Ultimately, we identified a number of key genes that were differentially regulated in response to hypoxia treatments (*CYBB, SERPINA1, SERPINF2, SERPING1, and RELN*) that are thought to affect incidence of occlusion in SCD. Together, these conclusions better inform our understanding of the factors and processes affecting VOC in SCD.

5.2 Materials and Methods

The experiments in this chapter utilize the microfluidic platform that was originally introduced in Chapter 3 of this document. An abbreviated summary of key device methodologies is included here. Refer to Chapter 3.2 Materials and Methods for a more thorough representation of microfluidic device design, fabrication, and endothelialization. Briefly, the methods of this chapter include endothelialized device preparation, hypoxia preconditioning, and RNA sequencing. The schematic below provides an overview of the methods and experimental timeline, highlighting hypoxia preconditioning and RNA sequencing in particular (Figure 5.1).

5.2.1 Microfluidic device design, fabrication, and endothelialization

The microfluidic platform comprises three layers: (1) a gas layer to modulate oxygen tension in the device to initiate hypoxia, (2) a hydration layer to provide humidity and avoid cell dehydration, and (3) a cell layer that is fully coated with endothelial cells to mimic a vascular network. The cell layer geometry features a bifurcating network of 32 individual channels, with each channel measuring 60 μm wide by 50 μm tall. The gas and hydration layers contain wide channels that are directly above the bifurcating network of the cell layer. Due to the gas permeable quality of PDMS, oxygen tension in the gas layer is diffusively coupled to the cell layer to allow for hypoxic treatment of endothelial cells cultured in the device's

vascular network. The designs for each layer were constructed in AutoCAD (Autodesk) and printed on mylar photomasks (Fineline Imaging) for fabrication via photolithography, soft lithography, compression molding, and oxygen-plasma bonding techniques.

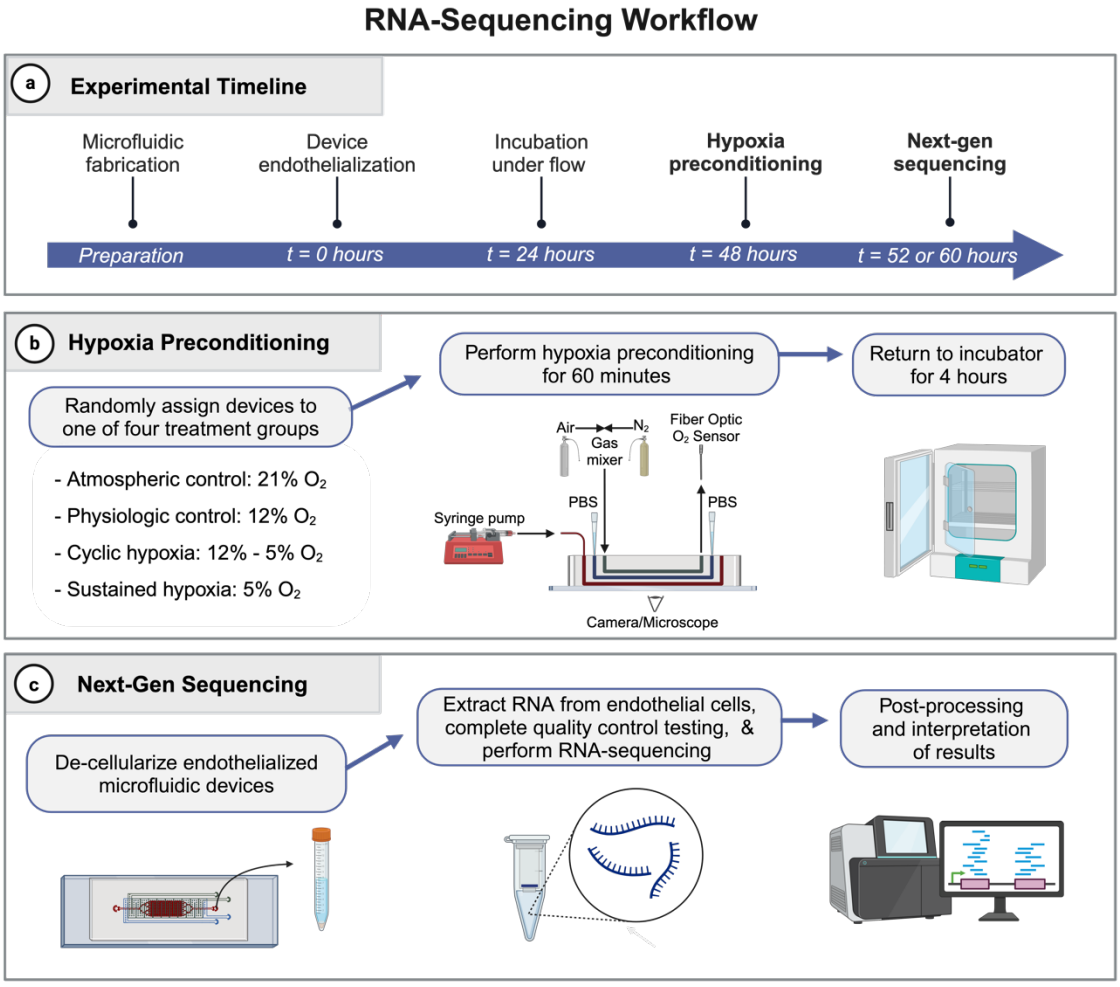


Figure 5.1: Visual summary of chapter 5 experimental timeline and workflow. Schematic featuring (a) experimental timeline of key steps in Chapter 5, with panels highlighting the workflow of (b) hypoxia preconditioning and (c) next-generation sequencing. Created using BioRender.

The cell layer was vascularized using human umbilical vein endothelial cells (HUVECs) sourced from ATCC. The endothelial cells were cultured aseptically according to manufacturer's recommended specifications using endothelial cell growth medium-2 (EGM-2, Lonza). Devices were endothelialized as previously described in Chapter 3.2.4 of this document. Briefly, microfluidic devices were functionalized with 50 µg/mL fibronectin from human plasma in phosphate-buffered saline (PBS) before injecting a cell suspension of 15 x 10^6 cells/mL in 8% dextran-EGM-2 media. Cells were allowed to adhere under static conditions for approximately 90 minutes, then syringe pumps were used to perfuse EGM-2 media through the endothelialized cell layer at flow rate of 60 µL/hr. Endothelialized devices were cultured under flow conditions for 48 hours, which established a confluent, aligned monolayer.

5.2.2 Hypoxia preconditioning

Endothelialized microfluidic devices were preconditioned using a solenoid valve gas mixing system adapted from one used in previous works.[162,165] Further reference can be made to Chapters 3.2.7 and 4.2.2 of this document, which present in-depth description of the hypoxia preconditioning setup and methodology. Briefly, a custom Python code was used to specify precise oxygen concentrations between 0% and 21%. Compressed air (21% O_2, 5% CO_2, balance N_2) was combined with compressed nitrogen (0% O_2, 5% CO_2, balance N_2) in a solenoid valve-controlled mixing chamber. Oxygen percentage was monitored

using a calibrated fiber optic oxygen sensor (NeoFox-GT, Ocean Optics). Hypoxia preconditioning of the devices occurred in a 37°C temperature-controlled chamber.

Devices were randomly divided into four preconditioning treatment groups, including: (1) atmospheric control: 21% O_2, (2) physiologic control: 12% O_2, (3) cyclic hypoxia: alternating 12% O_2 and 5% O_2 at 10-minute intervals, or (4) sustained hypoxia: 5% O_2. For all conditions, devices were treated for 60 minutes then returned to the incubator and maintained for an additional 4 (standard incubation) or 12 hours (extended incubation) at 37°C, 5% CO_2 under media flow. This additional incubation period allowed the endothelial cells to respond to the treatment stimulus. The time interval was chosen based on previous studies regarding delay of genomic response to hypoxia in endothelial cells.[92,193]

5.2.3 Microfluidic device de-cellularization and RNA extraction

A custom protocol was established to de-cellularize microfluidic devices for RNA extraction. Initial attempts to extract RNA directly on-chip resulted in low yield and poor RNA sample quality. However, an alternate method was developed involving de-cellularization of the microfluidic device to isolate endothelial cells, followed by RNA extraction of the isolated cell pellet. An extensive optimization process allowed us to achieve high viability of isolated cells (>80% viability) as well as sufficient yield, quality, and integrity of extracted RNA. Requirements for downstream processes necessitated at least 100 ng total RNA yield, a 260/280

purity ratio between 1.8 and 2.2, and an RNA integrity number (RIN) greater than 6 for each sample.

Briefly, the cell isolation protocol includes the following steps. First, endothelialized microfluidic devices were removed from the incubator at the appropriate time point (4 or 12 hours after hypoxia preconditioning). The cell layer was first rinsed with 100 µL of Hanks' balanced salt solution (HBSS) to remove media serum. Then, a quick trypsin rinse was performed before incubating with trypsin for approximately 3 minutes. Trypsinized cell suspension was then flushed from the device into the collection reservoir containing neutralization media (EGM-2 with additional 3% fetal bovine serum (FBS)). Neutralizing with a higher serum concentration and collecting on ice minimized cellular stress and damage associated with the isolation process, improving viability. Isolated cell suspension was centrifuged at 200g for 5 minutes to pellet the cells and allow for removal of trypsin. Each cell pellet was resuspended in 100 µL PBS and rinsed via centrifugation at 200g for another 5 minutes. Finally, PBS supernatant was removed, and the isolated cell pellet was ready for RNA extraction.

After determining the optimal the cell isolation method, several RNA extraction methods were performed and compared (Figure 5.2). These included the Qiagen RNeasy micro kit for RNA purification, the Norgen single cell RNA purification kit with optional on-column DNA removal via RNase-free DNase I kit, and the Norgen single cell RNA purification kit without optional on-column DNA removal. Preliminary quality control testing was performed at the University of

Minnesota Genomics Core (UMGC) via RiboGreen fluorometric quantitation, Nanodrop, and Agilent Tape Station analyses.

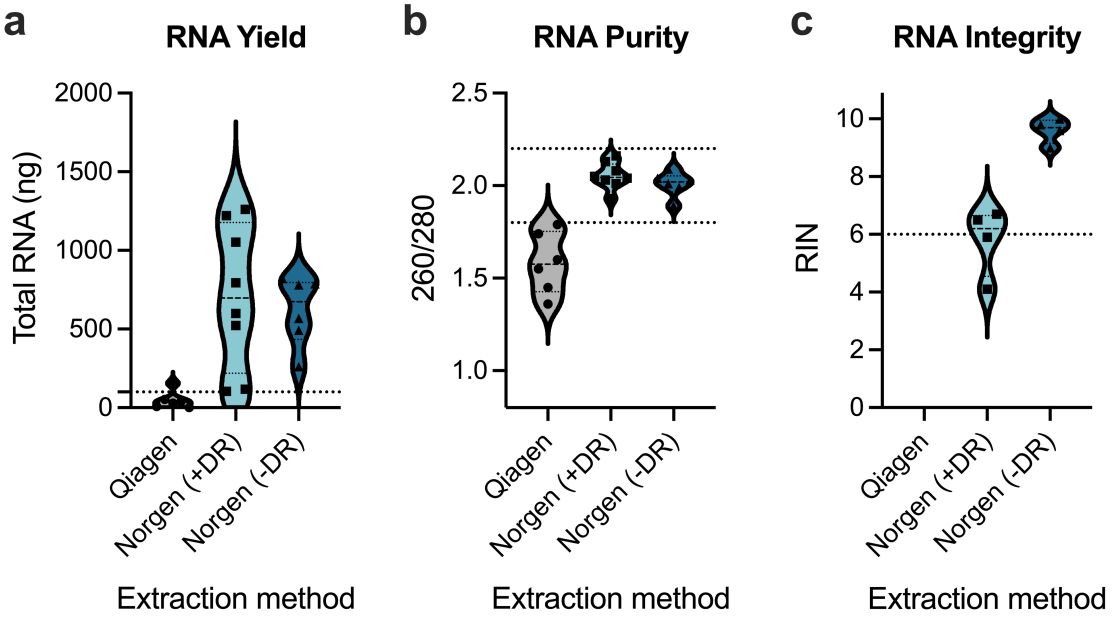


Figure 5.2: Comparison of RNA extraction methods. Several RNA extraction methods were compared, including the Qiagen RNeasy micro kit for RNA purification, the Norgen single cell RNA purification kit with optional DNA removal (+DR) via RNase-free DNase I kit, and the Norgen single cell RNA purification kit without optional DNA removal (-DR). Quality control testing was performed to examine the RNA sample (a) yield, (b) purity, and (c) integrity obtained via each method. Qiagen kit did not yield sufficient RNA quantity for integrity testing. Note that downstream analyses required at least 100 ng total RNA yield, a 260/280 purity ratio between 1.8 and 2.2, and an RNA integrity number (RIN) greater than 6, each of which are indicated on the graphs via dotted lines. All subsequent experiences were pursued using the Norgen method without DNA removal.

The Norgen Biotek single cell RNA purification kit without optional on-column DNA removal yielded sufficient RNA yield, quality, and integrity results for downstream analyses. Additionally, these results were consistent and repeatable across several experimental trials. The Norgen Biotek Single Cell RNA Purification Kit was used to extract RNA from each sample according to the manufacturer's

instructions. RNA was stored at -80°C and used for downstream application within 3 months.

5.2.4 RNA quality testing, sequencing, and post-processing

Frozen samples were shipped to Genewiz (Azenta) for quality testing and RNA sequencing. Quality control testing via NanoDrop 2000, Qubit fluorometer, and Agilent TapeStation technologies confirmed sufficient sample concentration, RIN, and distribution value 200 (DV200) for downstream processing (Table 5.S1). RIN is a value used to assess quality and integrity of an RNA sample, indicating amount of sample degradation. RIN scores range from 1 (highly degraded) to 10 (no degradation). For RNA sequencing, a RIN above 6 is acceptable but a RIN above 8 is preferred. DV200 is an RNA quality assessment that measures the percentage of RNA fragments that are greater than 200 nucleotides in length. A DV200 of above 30% is considered acceptable, while a DV200 above 70% is preferred.

RNA sequencing workflow included polyA selection-based mRNA enrichment, mRNA fragmentation, random priming, first- and second- strand cDNA synthesis, end repair, 5' phosphorylation, dA-tailing, adaptor ligation, PCR enrichment, and sequencing. Illumina sequencing configuration HiSeq with 2x150 base pair (bp) read length was used. Sequence reads were trimmed using Trimmomatic v.0.36 to remove possible adapter sequences or nucleotides with

poor quality. Trimmed reads were aligned to *homo sapiens* GRCh38 reference genome. FeatureCounts from the Subread package v.1.5.2 was used to calculate unique gene hit counts. Comparison of gene expression between sample groups was performed to generate p-values and log2 fold changes. Genes with an absolute log2 fold change greater than 1 and an adjusted p-value less than 0.05 were considered differentially expressed genes (DEGs) for each comparison. Gene ontology (GO) analysis was performed using GeneSCF v.1.1-p2 software, which used the Gene Ontology Annotation (GOA) human database to cluster genes based on their biological processes, while noting statistical significances.

5.3 Results and Discussion

5.3.1 Endothelial cells cultured on-chip can be extracted for NGS.

After much optimization, a unique protocol was refined that involved de-cellularization of the microfluidic device to isolate an endothelial cell pellet followed by RNA extraction to purify RNA from the cell culture. The protocol development can be referenced in the Materials and Methods section 5.2.3 above. In a similar manner to Chapter 4, endothelialized devices were preconditioned to one of four treatments: atmospheric control, physiologic control, cyclic hypoxia, or sustained hypoxia, then RNA was isolated via the above method. Despite the complexity of decellularizing the microfluidic devices, this method reliably produced RNA

samples of sufficient yield, quality, and integrity for downstream processing (Figure 5.3; Table 5.S1).

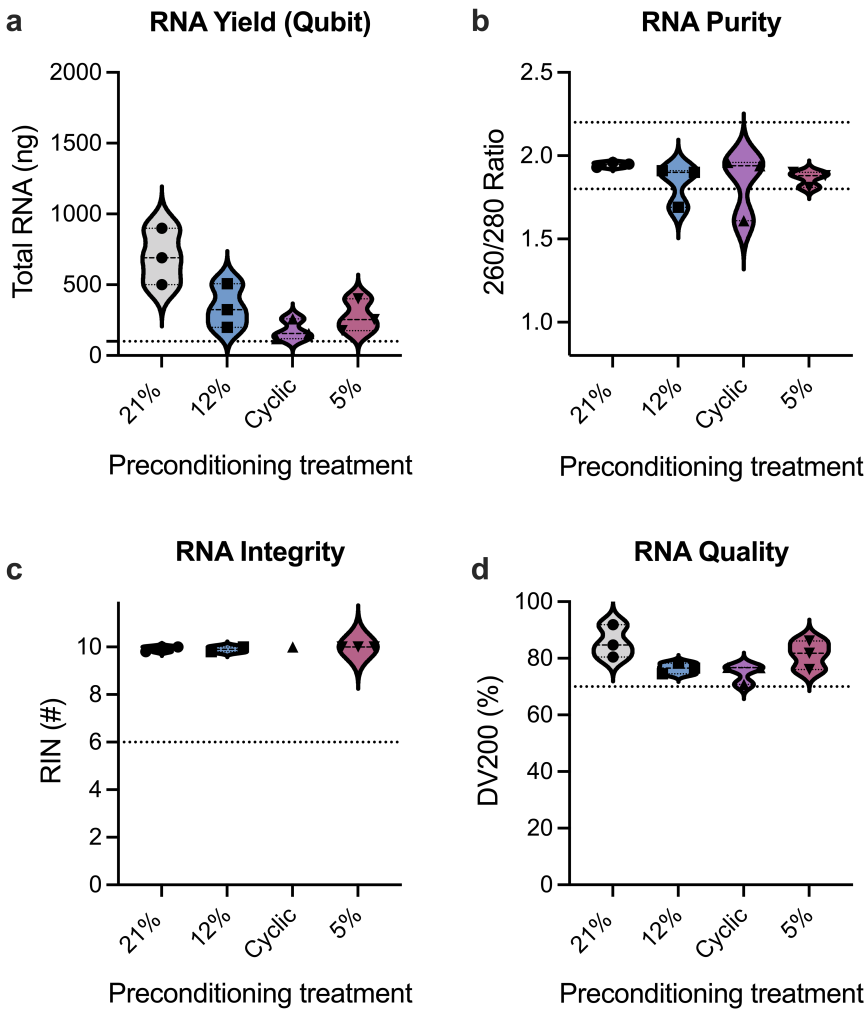


Figure 5.3: Comparison of extracted RNA across treatment groups. Quality control testing was performed to ensure RNA samples met prerequisites for RNA sequencing. Results are presented for each treatment condition, and include (a) total RNA yield, (b) RNA purity ratio, (c) RNA integrity number (RIN), and (d) distribution value 200 (DV200) (n=3 samples per condition, note three samples failed to produce RINs due to low RNA concentrations but gel analysis showed distinct bands which were indicative of non-degraded material). Recommendations for RNA sequencing included at least 100 ng total RNA yield, a 260/280 purity ratio between 1.8 and 2.2, a RIN greater than 6, and a DV200 above 70%, each of which are indicated on the graphs via dotted lines.

RNA quality/integrity from this extraction method was deemed excellent (RIN: 9.96 ± 0.09; DV200: 79.55 ± 5.78%) and the total RNA quantity generated was above the necessary threshold for processing. It was noted that RNA extraction from the devices treated with physiologic oxygen levels and more so from those treated with cyclic or sustained hypoxia resulted in lower RNA yield. Others have shown similar changes in HUVEC due to hypoxia.[209] They demonstrated that hypoxic exposure led to decreased transcription rates, increased RNA degradation rates, and decreased total RNA content per cell. Silencing *ARNT*, *HIF1A* or *EPAS1* prevented the decrease in RNA content per cell, indicating that the hypoxia-mediated changes to the EGLN/HIF1A-EPAS1 axis likely contributed to this effect. The hypoxia-treated endothelium in our microfluidic system likely underwent similar pathway modulation, which reduced RNA content per cell and therefore lowered total RNA yield.

The high quality and adequate yield of RNA generated by this microfluidic extraction method permitted downstream analysis via RNA sequencing, while further validating the efficacy of the procedure. The success of this method provides a foundation for genomic investigation into other cell types cultured on-chip, including and beyond vascular research.

5.3.2 Cyclic hypoxia preconditioning results in more abundant differential gene regulation than sustained hypoxia preconditioning.

RNA sequencing of preconditioned endothelial cells was performed to better understand the effect of hypoxia reperfusion on sickle cell endothelial biology. We hypothesized that changes in genetic expression of the endothelium due to hypoxia reperfusion injury in SCD may ameliorate subsequent endothelial injury or vaso-occlusion. The RNA sequencing study clearly demonstrated that hypoxia preconditioning results in a significant number of differentially expressed genes (DEGs) compared to either control condition (Figure 5.4). Compared to atmospheric control, cyclic hypoxia resulted in significant differential gene regulation of 503 genes (477 up-regulated, 26 down-regulated) whereas sustained hypoxia resulted in significant modulation of 37 genes (36 up-regulated, 1 down-regulated). Compared to physiologic control, cyclic hypoxia resulted in significant differential gene regulation of 219 genes (210 up-regulated, 9 down-regulated), whereas sustained hypoxia resulted in significant modulation of 39 genes (35 up-regulated, 4 down-regulated). Broadly, hypoxia preconditioning was linked to frequent up-regulation of genes (89.7 - 97.3% of total DEGs across previously mentioned comparisons), with less frequent down-regulation of genes (corresponding 10.3 - 2.7%). This suggests that hypoxia preconditioning may initiate endothelial protective mechanisms by means of up-regulation of a number of principal genes of interest.

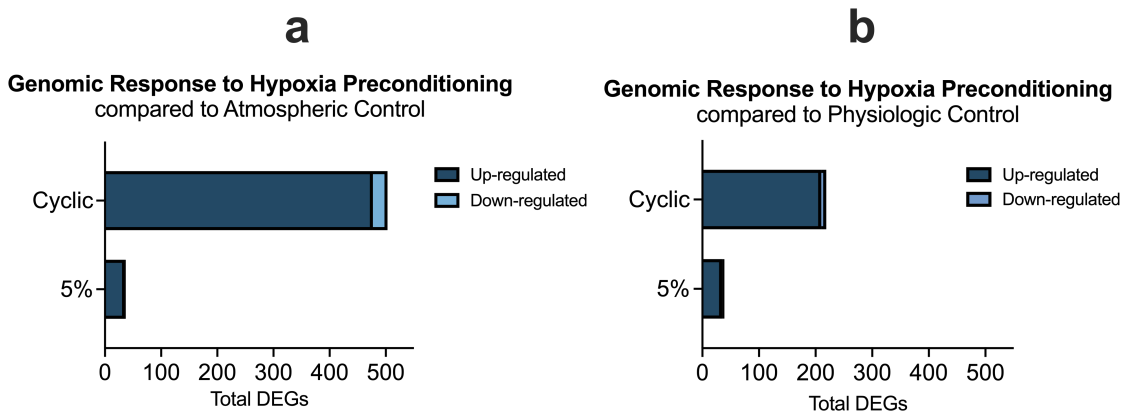


Figure 5.4: Global gene expression profile due to hypoxia preconditioning. Genomic response to hypoxia preconditioning is reported for both cyclic hypoxia and sustained hypoxia treatments in comparison to (a) atmospheric control, and (b) physiologic control. Data is reported as total number of differentially expressed genes (DEGs). Type of regulation (either up- or down-regulated) is indicated by the legend.

5.3.3 Hypoxia preconditioning modulates a number of pathways in SCD.

Gene ontology clustering was performed to identify enriched gene pathways modulated by hypoxia preconditioning that may contribute to vaso-occlusive risk in SCD (Figure 5.5). There was notable modulation of pathways involving hypoxia sensitivity, blood vessel modification, coagulation, inflammation, and adhesion, among others. This section will delve into several key results from the gene ontology pathway analysis.

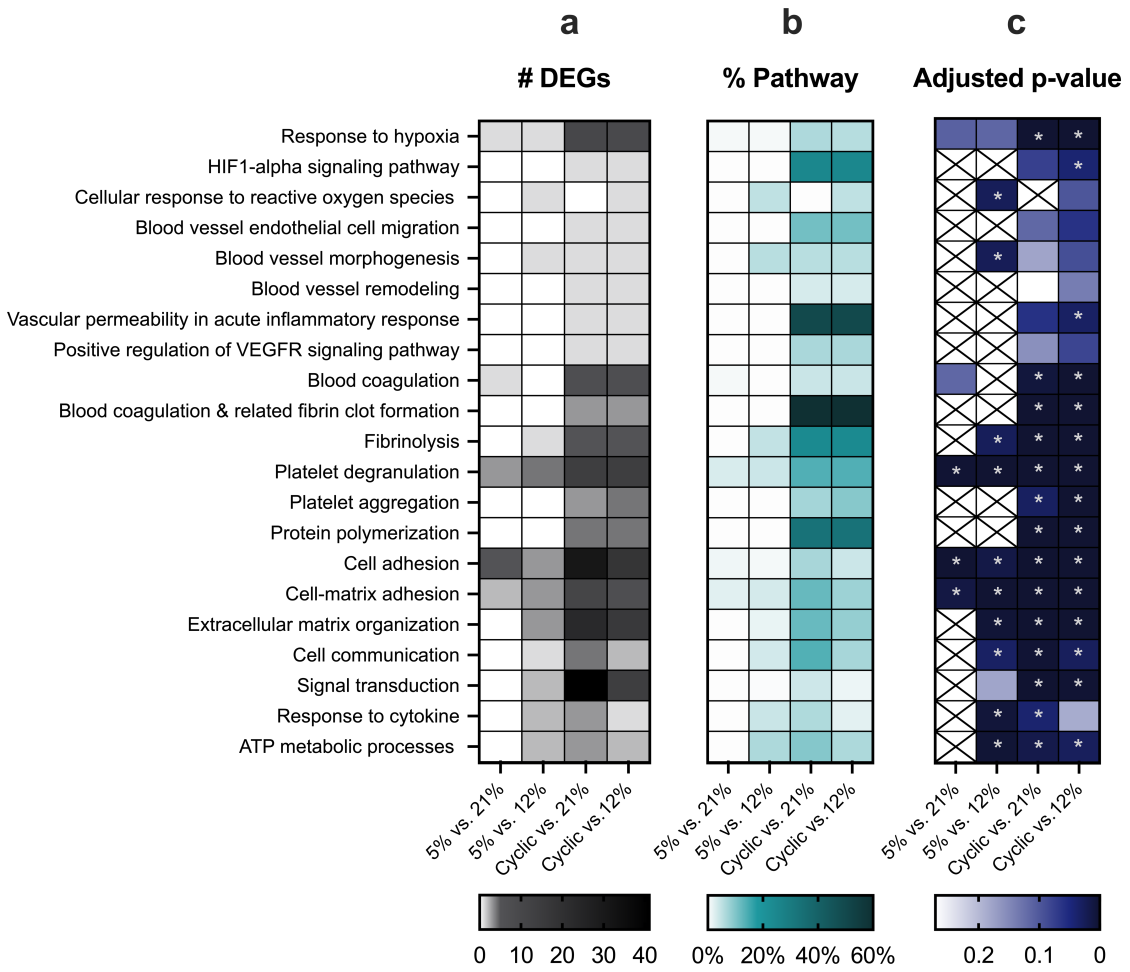


Figure 5.5: Pathway analysis of RNA sequencing results. RNA sequencing was performed on preconditioned endothelial cells after a 4-hour incubation window. For each comparison, differentially expressed genes were clustered by gene ontology using the Gene Ontology Annotation (GOA) human database for gene enrichment. (a) Number of differentially expressed genes in gene ontology pathways of interest are indicated by the gradient legend below the chart. (b) Percentage of differentially regulated genes in each pathway of interest are indicated by center legend. (c) Adjusted p-value indicates confidence of each comparison. Data is significant when adjusted p-value < 0.05 via Fisher exact test, indicated by rightmost legend and denoted by asterisks. X's indicate lack of any DEGs in corresponding comparison.

All gene ontology comparisons showed evidence that the cells respond to hypoxia with cyclic hypoxia having the most significant effect (differential regulation of 9-10 hypoxia-responsive genes) compared to sustained hypoxia (differential regulation of just 1 hypoxia-responsive gene). The hypoxia-inducible factor 1-alpha

(HIF1-alpha) signaling pathway was also significantly modulated by cyclic hypoxia (25% of pathway), though not by sustained hypoxia treatment in our tests. Meanwhile, differential regulation of the cellular response to reactive oxygen species was observed only in comparison to the physiologic control.

A number of gene ontology pathways involving blood vessel regulation were also modulated in this study. Among them, blood vessel endothelial cell migration, morphogenesis, and remodeling were all correlated with hypoxia preconditioning in addition to vascular permeability in acute inflammatory response and positive regulation of vascular endothelial growth factor receptor (VEGFR) signaling.

Coagulation and inflammation play a significant role in SCD and, notably, are differentially regulated in response to hypoxia preconditioning in this in vitro study.[210] In response to cyclic hypoxia, blood coagulation gene ontology was significantly regulated (differential regulation of 7 blood coagulation-related genes (4.1%)). Related, platelet aggregation and degranulation gene ontologies were also affected by hypoxia preconditioning. The platelet degranulation pathway saw differential regulation of 3-4 genes (3.0-4.0% of pathway) due to sustained hypoxia preconditioning, and regulation of 14 genes (13.9% of pathway) due to cyclic hypoxia preconditioning when compared to controls. Platelet degranulation involves protein release from activated platelets into the plasma, further potentiating the coagulation cascade and affecting VOC in SCD. Moreover, the platelet aggregation pathway saw differential regulation of 3-4 genes (7.1-9.5% of

pathway) in cyclic hypoxia preconditioning compared to controls but no modulation in the sustained hypoxia preconditioning case.

Across all conditions, significant modulation of cell adhesion-related genes was observed in response to hypoxia preconditioning. In line with other findings, cyclic hypoxia showed a more dynamic response within cell adhesion pathways than sustained hypoxia (differential regulation of 18 or 31 cell-adhesion related genes due to cyclic hypoxia, compared to 3 and 5 due to sustained hypoxia in relation to controls). Significant differential gene regulation within cell adhesion pathways indicates that hypoxia preconditioning likely ameliorates some vaso-occlusive incidence by reducing the adhesivity of endothelial cells.

Altogether, it was demonstrated that gene ontology clustering can be implemented to identify enriched gene pathways that further explain the effects of hypoxia preconditioning on endothelial cells. Collectively, these results can be interpreted to better inform the results in the previous chapter, which concluded that hypoxia preconditioning reduces incidence of occlusion in an endothelialized system. We note significant modulation in pathways involving hypoxia sensitivity, blood vessel modification, coagulation, inflammation, adhesion, and endothelial cell functional behavior. Taken together, these changes in pathways of interest may contribute to the protective effect garnered by hypoxia preconditioning. A particularly interesting conclusion from the gene ontology analysis is the heightened effect by cyclic hypoxia preconditioning in comparison to sustained hypoxia preconditioning. The blood occlusion results did not show a significant

difference between these two treatment conditions, but the RNA findings clearly demonstrate that additional events are occurring at the genomic level that are not entirely apparent in the occlusion assay.

5.3.4 Differential regulation of gene expression by hypoxia preconditioning may contribute to vaso-occlusive risk.

It is critical to examine which genes are being differentially regulated under hypoxia preconditioning to better understand the contributing factors to vaso-occlusion. Gene-specific modulation can be visualized using volcano plots and bi-clustering heat maps (Figure 5.6), drawing attention to genes of interest. For reference, a representation of the most highly regulated genes is also included in the supplement (Figure 5.S1).

Several hypoxia-responsive genes of interest were modulated due to preconditioning. When comparing sustained hypoxia to either control, just a single hypoxia-responsive gene was differentially regulated (*CYP1A1* in reference to atmospheric, *RYR2* in reference to physiologic preconditioning). In contrast, cyclic hypoxia preconditioning more dynamically affected a number of hypoxia-sensitive genes (*NPPA, MB, TRH, CD24, EDNRA, MYOCD, RYR2* in both control comparisons, as well as *CHRNA4, ABAT, ARNT2* compared to atmospheric and *CXCL12, POSTN* compared to physiologic control).

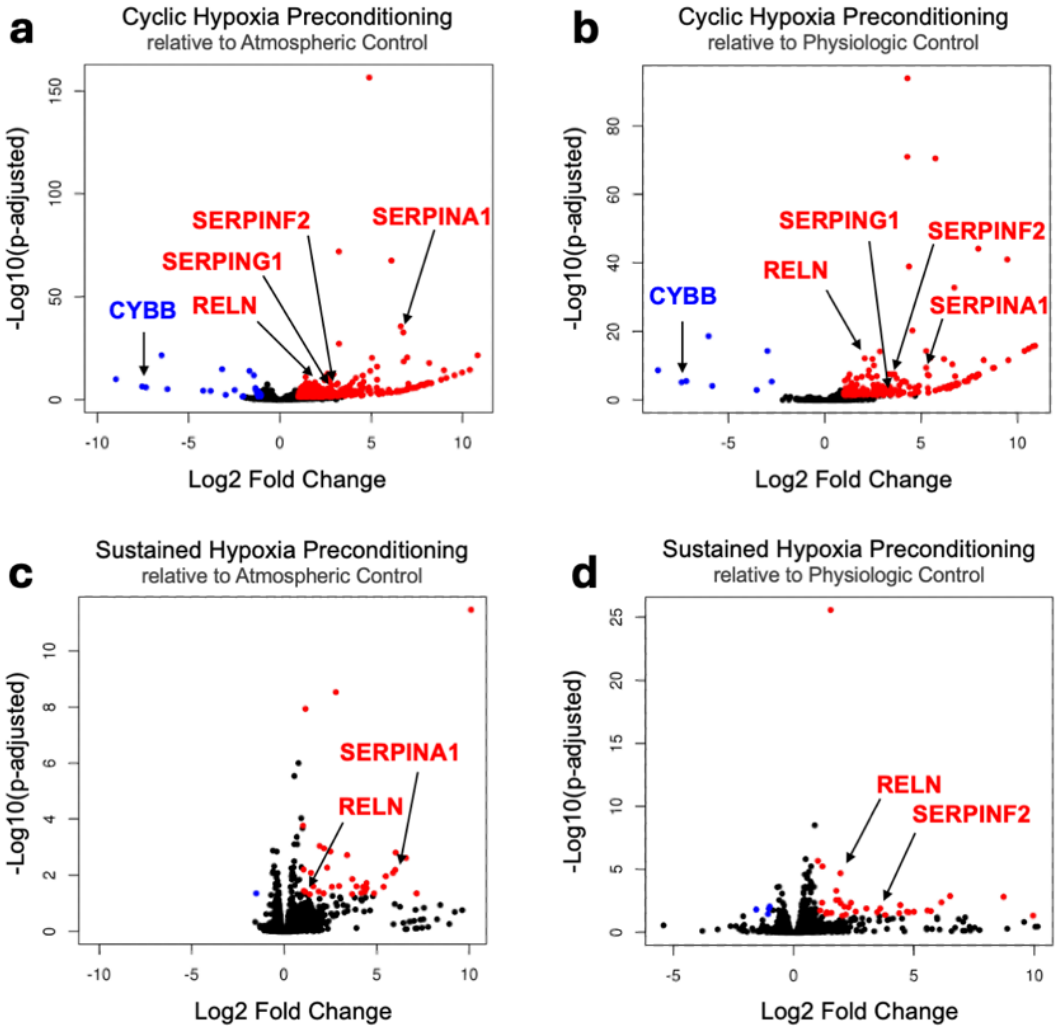


Figure 5.6: Visualization of global transcriptional changes due to hypoxia preconditioning. RNA sequencing results are represented via volcano plots for each treatment comparison including (a) cyclic hypoxia preconditioning relative to atmospheric control, (b) cyclic hypoxia preconditioning relative to physiologic control, (c) sustained hypoxia preconditioning relative to atmospheric control, and (d) sustained hypoxia preconditioning relative to physiologic control. The log2fold changes in gene expression are indicated by the x-axes and the significances (adjusted p-value) are indicated by the y-axes. Upregulated genes (adjusted p-value < 0.05, log2 fold change > 1) are indicated by red dots. Down-regulated genes (adjusted p-value < 0.05, log2 fold change < -1) are indicated by blue dots. Genes of interest are marked with arrows.

Regarding the HIF1-alpha signaling pathway, cyclic hypoxia preconditioning resulted in a significant differential expression change in the *CYBB* gene, compared to either control. The effect of cyclic hypoxia nearly silenced *CYBB* gene

expression, resulting in -7.55 and -7.19 log2fold change compared to atmospheric and physiologic controls, respectively (p-adj < 0.001 for both). The *CYBB* gene encodes the cytochrome b-245 beta chain, a subunit of the NADPH oxidase protein (NOX2).[211] NOX2 is known to be a major reactive oxygen species-producing isoform and animal studies have demonstrated that chronic intermittent hypoxia activates NOX2, causing arterial hypertension.[211,212] Our study indicates that cyclic hypoxia likely reduces NOX2-related reactive oxygen species production via *CYBB* suppression. This result may contribute to an endothelial protective effect, reducing occlusion in cyclic hypoxia-preconditioned devices.

Hypoxia preconditioning resulted in modulation of several key coagulatory genes of interest. In particular, *SERPINA1* was significantly upregulated in 3 of 4 comparisons (on average, a 6.00-fold change in differential gene expression, p < 0.01 for all 3 comparisons). The *SERPINA1* gene encodes the alpha 1-antitrypsin (AAT) protein, which inhibits inflammatory proteases.[213] Mutation in *SERPINA1* has been correlated with venous thromboembolism and a number of pulmonary disorders.[214,215] AAT was also shown to be elevated in SCD patients and positively correlated with hemolytic and inflammatory patient indices, suggesting a relationship between AAT and disease severity.[213] This suggests that hypoxia reperfusion is responsible, at least in part, for the elevated levels of AAT and associated pro-coagulatory, occlusive phenotype of SCD patients.

Genes correlated with platelet aggregation and degranulation processes were significantly modulated in response to hypoxia preconditioning. *SERPINA1*,

previously mentioned in relationship to coagulation, is also correlated with platelet degranulation.[216] The upregulation of *SERPINA1* in this study due to hypoxia preconditioning may be correlated with significant platelet involvement in SCD pathophysiology. Related genes, *SERPINF2* and *SERPING1* were also modulated in several comparisons. The average log2fold change of *SERPINF2* was 3.67 ± 0.38 ($p < 0.05$ in all cases excluding sustained hypoxia compared to atmospheric control) while the average log2fold change of *SERPING1* was 3.16 ± 0.27 (in both cyclic comparisons, $p < 0.001$). The *SERPINF2* gene encodes the alpha 2-antiplasmin (A2AP) protein, which inhibits plasmin, preventing fibrin breakdown.[217] The *SERPING1* gene encodes the C1 inhibitor protein, which controls vascular inflammation by blocking the activity of several pro-inflammatory proteins in the blood.[218,219] Deficiency of the C1 inhibitor protein has also been correlated with increased thrombosis.[220] The upregulation of *SERPINF2* in our study in response to hypoxia preconditioning helps to explain hypoxia reperfusion's contribution to the pro-coagulatory cascade in SCD. Meanwhile, the upregulation of *SERPING1* in our study due to hypoxia preconditioning suggests that hypoxia reperfusion may ameliorate platelet-associated inflammation and clotting in the body, consequently reducing vaso-occlusion.

Additionally, a large number of cell adhesion-related genes were modulated in response to hypoxia preconditioning. Notably, a single gene, *RELN*, was up-regulated across all 4 comparisons (on average, a 1.60 ± 0.48 fold change in differential gene expression, $p < 0.05$ for all comparisons). The *RELN* gene

encodes the protein reelin, which has been shown to influence morphology, membrane permeability, and membrane resistance of vascular endothelial cells as a means of vessel wall integrity regulation.[221] More specifically, reelin was also shown to increase expression of VCAM-1, ICAM-1, and E-selectin in cultured endothelial cells, which resulted in a significant increase in activation, inflammation, and adhesion between endothelial cells and monocytes. Reelin is understood to initiate these effects via suppression endothelial nitric oxide synthase (eNOS) activity and amplification of nuclear factor KB (NF-KB) activity.[222] Moreso, reelin has been implicated with disease severity in a number of studies including one in which circulating reelin promoted inflammation and modulated disease activity in COVID cases.[223] The upregulation of reelin under hypoxia preconditioning in our system may help explain the contribution of hypoxia-reperfusion injury to overall vaso-occlusion in SCD. Inhibition or reduction of circulating reelin has been proposed a possible approach for the prevention of cardiovascular disease due to its protection against atherosclerosis,[222] and the results here suggest its inhibition may also be useful in protection against vaso-occlusion in SCD.

5.3.5 Temporal response to hypoxia differentially regulates gene expression.

Previous studies have shown that changes in gene expression in response to stimuli vary over time.[92,193,224] Some transcriptional changes occur rapidly (within 2 hours) then fade; whereas, others may be delayed in onset or persist over time.

For the bulk of our studies presented here, endothelialized devices were incubated for 4 hours after preconditioning treatments to allow for temporal delay in gene response. The experiments were then repeated at one additional time point to expand the scope of these results, shedding light on temporal gene response of endothelium to hypoxia. A 12-hour incubation window was chosen to evaluate delayed and/or persistent gene modulation to hypoxia. RNA-sequencing again showed significant gene expression of the endothelium compared to either control condition (Figure 5.7).

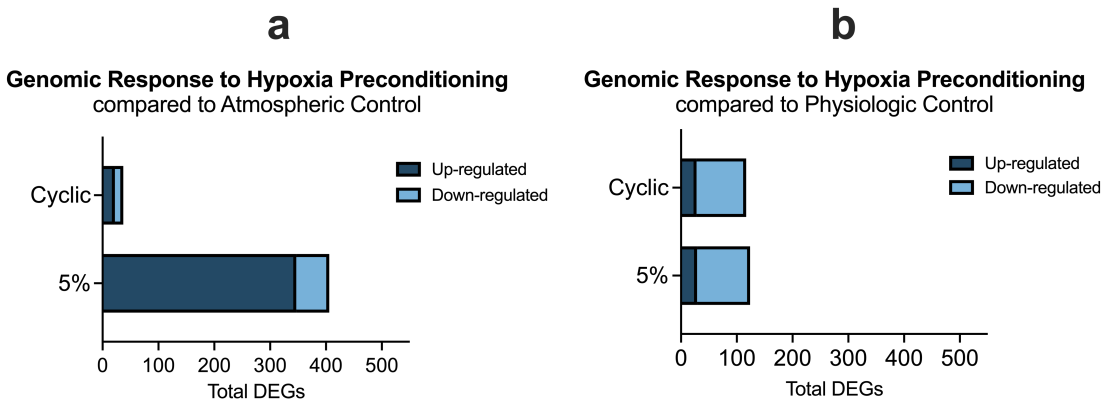


Figure 5.7: Global gene expression profile due to hypoxia preconditioning in the extended incubation group. Genomic response to hypoxia preconditioning after 12-hour incubation period is reported for both cyclic hypoxia and sustained hypoxia treatments in comparison to (a) atmospheric control, and (b) physiologic control. Data is reported as total number of differentially expressed genes (DEGs). Type of regulation (either up- or down-regulated) is indicated by the legend.

Compared to atmospheric control, cyclic hypoxia resulted in significant differential gene regulation of 37 genes (22 up-regulated, 15 down-regulated) whereas sustained hypoxia resulted in significant modulation of 406 genes (347 up-regulated, 59 down-regulated). Compared to physiologic control, cyclic hypoxia

resulted in significant differential gene regulation of 117 genes (28 up-regulated, 89 down-regulated) whereas sustained hypoxia resulted in significant modulation of 124 genes (29 up-regulated, 95 down-regulated). Notably, differential expression of genes in the extended incubation group included significantly higher frequency of down-regulation (14.5 - 76.6% of total DEGs across previously mentioned conditions) compared to the standard incubation group (2.7 - 10.3%). This suggests that many delayed or persistent effects of hypoxia reperfusion in SCD may act via down-regulation or suppression of genes associated with VOC. Additional results including associated pathway analysis, volcano plots of differential gene expression, and lists of top 30 highly regulated genes for each condition are included in the supplemental documents and can be used to support future studies (Figures 5.S2, 5.S3, and 5.S4).

5.4 Conclusion

In the previous chapter, we determined that mild and cyclic hypoxia preconditioning decrease occlusion incidence in endothelialized devices. In this chapter, we leveraged NGS to explore transcriptional changes to the endothelium in response to various hypoxia/oxygen treatments to better understand this result.

This process first necessitated the optimization and validation of a method to extract high quality RNA samples from devices that was suitable for downstream processing. We then performed RNA sequencing and detected significant

modulation of pathways related to VOC including hypoxia sensitivity, blood vessel modification, coagulation, inflammation, and adhesion. Additionally, several highly regulated genes were identified that are related to hypoxia preconditioning and may contribute to occlusion incidence.

The conclusions gathered in this study offer great opportunity for future work further validating and targeting these genes. Additionally, we showed preliminary results that draw attention to the changes in the gene expression over time. Collectively, these findings support the hypothesis that hypoxia preconditioning mitigates severe occlusion on-chip by drawing attention to several potential biological pathways and specific genes of interest that are correlated with the process.

5.5 Acknowledgments

Portions of this work were conducted in the Minnesota Nano Center (MNC). The MNC enabled access to photolithography and microfabrication equipment, which assisted in the development of this microfluidic platform and all related applications. The MNC is supported in part by the National Science Foundation (NSF) through the National Nano Coordinated Infrastructure Network (NNCI) under Award Number ECCS-1542202. A special thanks is extended to Dr. Emilio Tarcitano, for his helpful advice that guided both the RNA extraction and RNA-Seq data interpretation sections of this chapter.

Preliminary RNA quality control testing was performed with the support of the University of Minnesota Genomics Center (UMGC). Use of these services enabled optimization of the protocol to extract high-quality RNA samples from endothelial cells cultured in microfluidic devices. Additionally, RNA sequencing was performed by GeneWiz (Azenta Life Sciences). Much gratitude is expressed to the team at GeneWiz for their genomic biology expertise and their help expediting the workflow of the RNA sequencing portion of this project.

5.6 Supplemental Materials

The supplemental materials included below comprise four supplemental figures and one supplemental table to be referenced in context with Chapter 5.

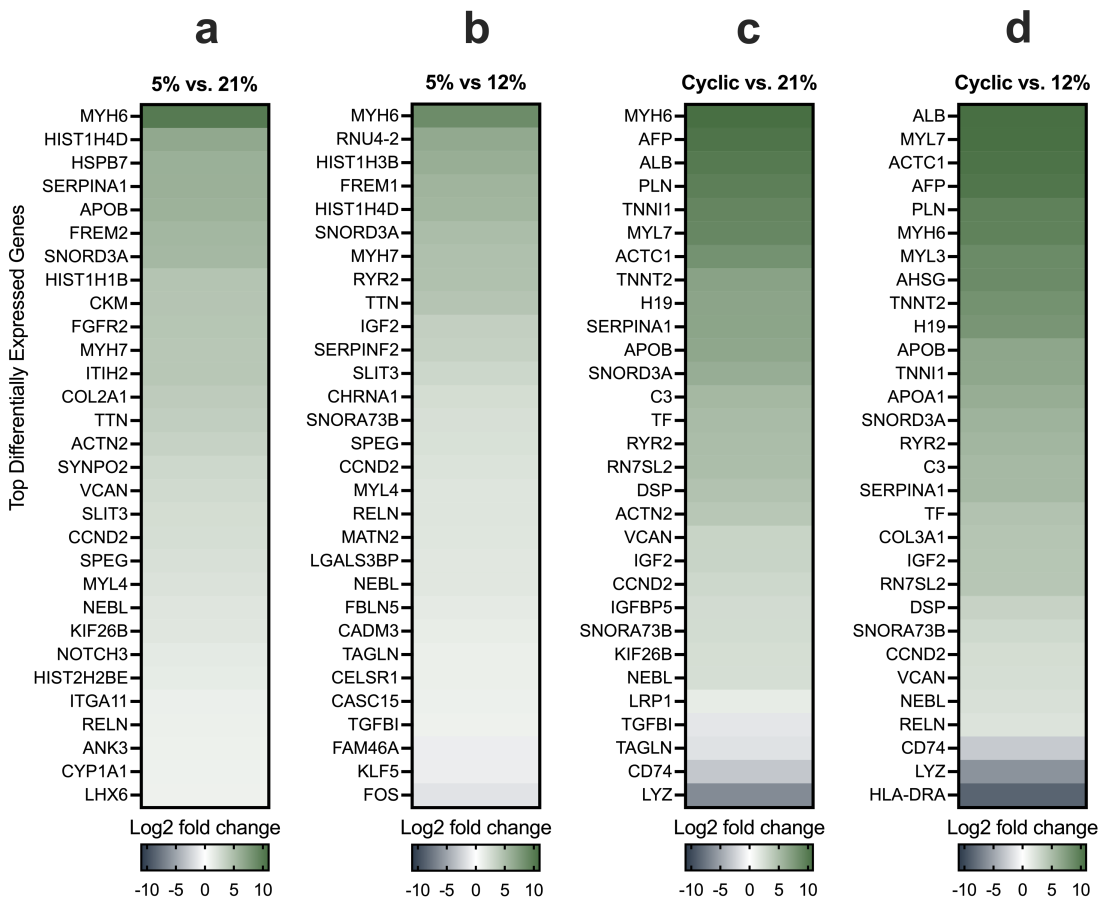


Figure 5.S1: Heatmap of highly regulated genes in the standard incubation group. RNA sequencing was completed on preconditioned endothelial cells after a 4-hour incubation period. (a-d) These heatmaps offer visualization of the expression profiles of the top 30 differentially expressed genes for each comparison. The differential gene expression data was sorted by adjusted p-value and the log2fold change of the top 30 significant genes were plotted. The legend indicates magnitude of log2fold change upregulation (+, green) or downregulation (-, grey).

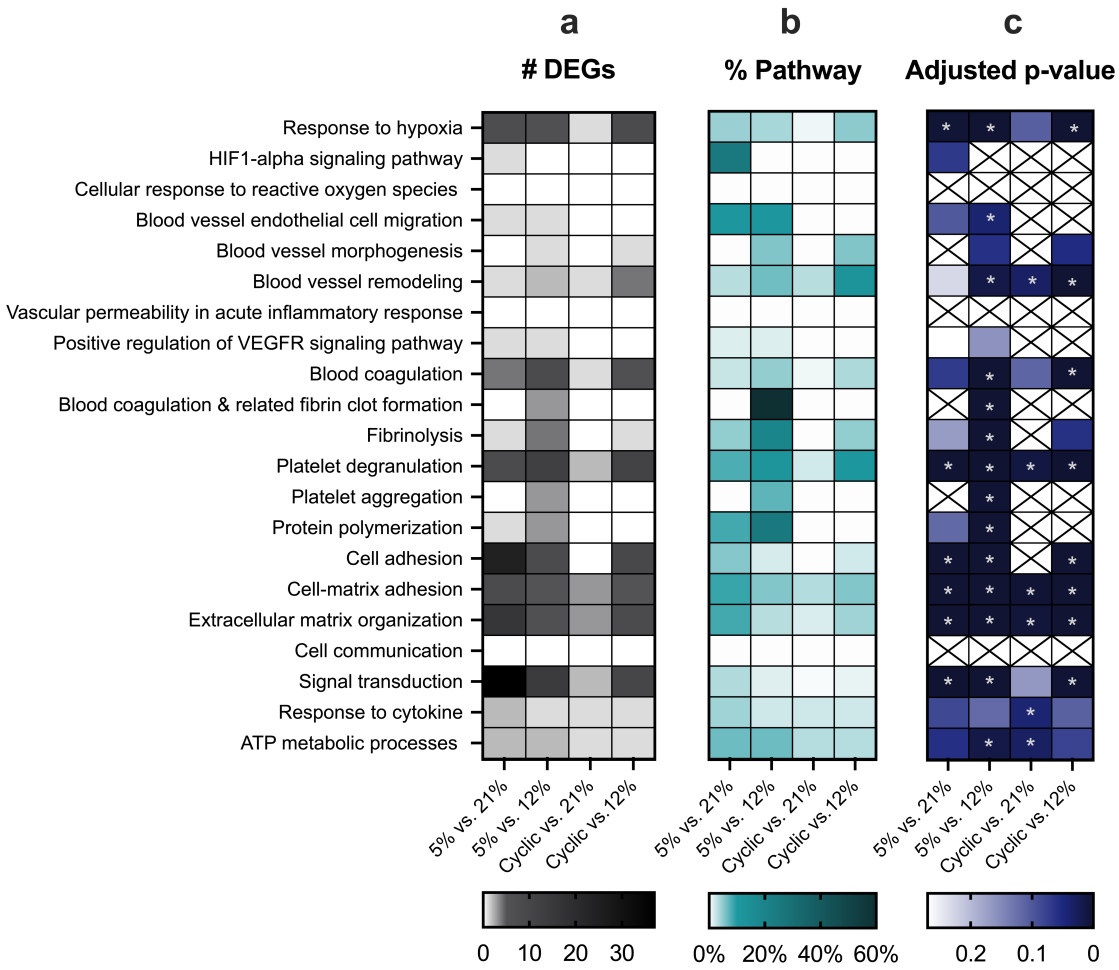


Figure 5.S2: Pathway analysis of RNA sequencing results for the extended incubation group. RNA sequencing was performed on preconditioned endothelial cells after a 12-hour incubation window. For each comparison, differentially expressed genes were clustered by gene ontology using the Gene Ontology Annotation (GOA) human database for gene enrichment. (a) Number of differentially expressed genes in gene ontology pathways of interest are indicated by the gradient legend below the chart. (b) Percentage of differentially regulated genes in each pathway of interest are indicated by center legend. (c) Adjusted p-value indicates confidence of each comparison. Data is significant when adjusted p-value < 0.05 via Fisher exact test, indicated by rightmost legend and denoted by asterisks. X's indicate lack of any DEGs in corresponding comparison.

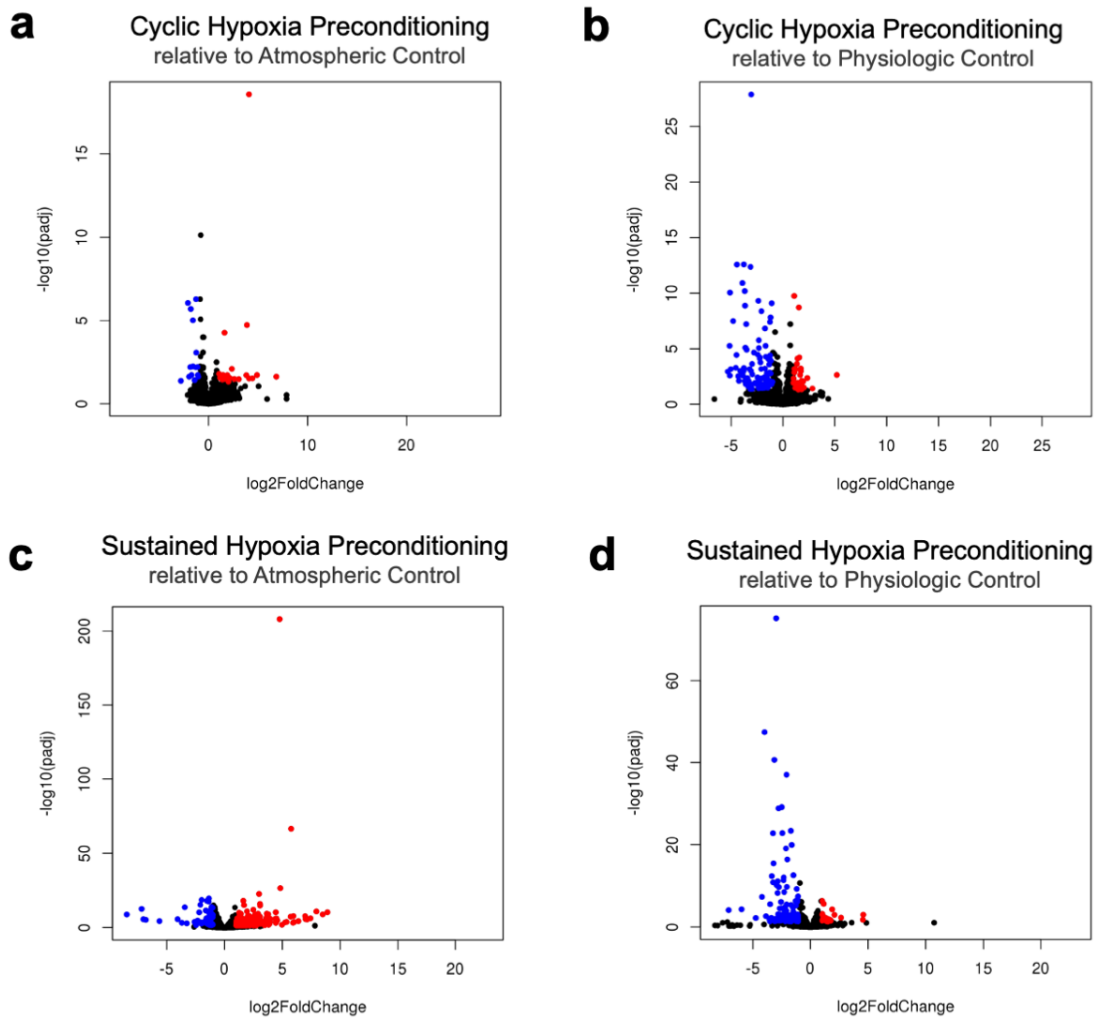


Figure 5.S3: Visualization of global transcriptional changes due to hypoxia preconditioning in the extended incubation group. RNA sequencing results are represented via volcano plots for each treatment comparison including (a) cyclic hypoxia preconditioning relative to atmospheric control, (b) cyclic hypoxia preconditioning relative to physiologic control, (c) sustained hypoxia preconditioning relative to atmospheric control, and (d) sustained hypoxia preconditioning relative to physiologic control. The log2fold changes in gene expression are indicated by the x-axes and the significances (adjusted p-value) are indicated by the y-axes. Upregulated genes (adjusted p-value < 0.05, log2 fold change > 1) are indicated by red dots. Down-regulated genes (adjusted p-value < 0.05, log2 fold change < -1) are indicated by blue dots.

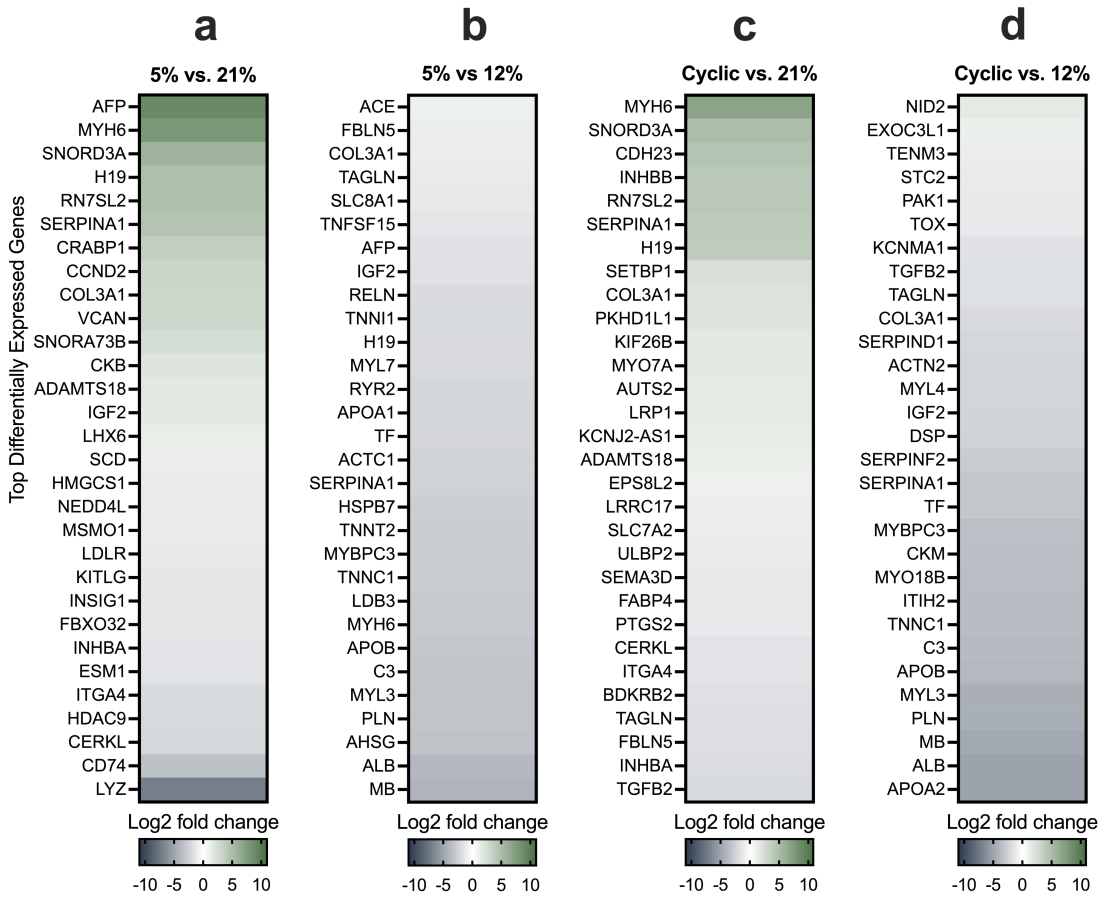


Figure 5.S4: Heatmap of highly regulated genes in the extended incubation group. RNA sequencing was completed on preconditioned endothelial cells after a 12-hour incubation period. (a-d) These heatmaps offer visualization of the expression profiles of the top 30 differentially expressed genes for each comparison. The differential gene expression data was sorted by adjusted p-value and the log2fold change of the top 30 significant genes were plotted. The legend indicates magnitude of log2fold change upregulation (+, green) or downregulation (-, grey).

ID	Pre-conditioning Treatment	Nanodrop			Qubit		Tape Station	
		Nucleic Acids (ng/μL)	**Total RNA** (ng)	**260/ 280** Ratio	**Nucleic Acids** (ng/μL)	**Total RNA** (ng)	**RIN** (#)	**DV200** (%)
A1	21%	28.9	404.6	1.93	35.8	501.2	9.8	80.46
A2	21%	38.9	544.6	1.95	49.4	691.6	10	84.73
A3	21%	98.4	1377.6	1.96	64.2	898.8	10	91.85
P1	12%	18.4	257.6	1.69	14.2	198.8	-	74.54
P2	12%	19.4	271.6	1.9	23.2	324.8	10	78.32
P3	12%	28.8	403.2	1.91	36.2	506.8	9.8	76.52
C1	Cyclic	16.2	226.8	1.96	11.1	155.4	-	76.83
C2	Cyclic	19.5	273.0	1.61	8.5	119.3	-	70.78
C3	Cyclic	26.8	375.2	1.94	18.5	259.0	10	76.68
S1	5%	30.8	431.2	1.88	18.2	254.8	10	76.01
S2	5%	38.5	269.5	1.9	25.0	175.0	10	86.09
S3	5%	40.7	569.8	1.81	28.6	400.4	10	81.80
Avg	Average	33.8	450.4	1.87	27.7	373.8	9.96	79.55
SD	Standard Deviation	22.0	312.8	0.11	16.4	238.1	0.09	5.78

Table 5.S1: RNA sequencing quality control assessment. Table includes sample ID, preconditioning treatment, and various quality control results (nucleic acid concentration, total RNA quantity, RNA integrity number (RIN), and DV200). Samples P1, C1, and C2 did not produce a RIN score due to low input sample concentration, however review of the 18S and 28S peaks indicated good quality.

Chapter 6: Concluding Remarks

6.1 Summary of Key Findings and Interpretations

This thesis discussed the complex pathophysiology of sickle cell disease (SCD) and many of the remaining questions surrounding the onset of vaso-occlusive crisis (VOC). It is evident that more research needs to be done to better comprehend the underlying biological processes that contribute to vaso-occlusion and present potential targets for therapeutic intervention. Current treatment options do not adequately manage SCD pathology and leave patients to cope with a range of acute and chronic complications.[102,152,153] Existing in vivo and in vitro models do not reliably inform clinical trials in part because they lack biological relevance. Therefore, development of more physiologically relevant model systems is necessary.

This thesis introduces a microfluidic platform that is unique in its ability to recapitulate many of the physiologic components of SCD. Its applications are two-fold: (1) its use as an occlusion assay that quantifies the occlusion incidence of patient blood samples through microvasculature, and (2) its potential to leverage next generation sequencing, with the ability to extract endothelial cells from microvascular networks on-chip to investigate genomic changes in response to treatment. Several methods were extensively developed and refined to accomplish these tasks. The microfluidic design is novel, incorporating fully endothelialized

microchannels and implementation of oxygen-control to initiate hypoxia reperfusion injury and red cell sickling.

The presence of key endothelial physiologic features in the model system were validated including adhesion marker expression, synthesis of biological factors, cytoskeletal development, and ability to tolerate fluctuations in hypoxia. The device can also be used to visualize adhesive and occlusive events as they develop on-chip in real-time. To our knowledge, this is the first microfluidic model of SCD to date that has integrated both oxygen-control and a 3D microvascular system at relevant size scales.

Our results highlight the critical importance of both endothelium and hypoxia in a SCD model system. First, we explored the relationship between hypoxia reperfusion and occlusion. The patient-to-patient variability in our model was representative of heterogeneity in SCD pathology and clinical presentation, drawing attention to the predictive capability of patient demographic and hematologic variables such as transfusion history, genotype, sex, and white blood cell count and platelet count. By analyzing occlusion incidence of many patient samples across pre-treated devices, we also concluded that endothelial hypoxia preconditioning provides a protective effect that reduces incidence of occlusion on-chip.

Moreover, we investigated endothelial gene regulation via next generation sequencing (NGS) to identify pathways of interest and specific genes that may directly contribute to this protective result. Notably, hypoxia preconditioning

resulted in significant differential gene expression among gene ontology pathways such as hypoxia sensitivity, blood vessel modification, coagulation, inflammation, and cell adhesion. A number of genes interest were identified, including some which may better explain the occlusive mechanisms of SCD generally and others which may inform the protective effect of hypoxia preconditioning. The *RELN* finding was particularly interesting, as reelin has been implicated with disease severity in a number of studies, including one in which an anti-reelin antibody (CR-50) was used in mice models to emphasize the potential therapeutic effect of anti-reelin therapy.[223] A future study examining the effectiveness of an anti-reelin antibody against VOC in SCD could be performed in our preclinical microfluidic model, to assess whether targeting reelin may provide significant therapeutic benefit. Overall, the modulation of many genes in the RNA-seq study present potential therapeutic targets to reduce endothelial cell adhesion, oxidative stress, inflammation, or coagulation in SCD, thereby reducing incidence of VOC.

Ultimately, we were able to use this microfluidic platform to investigate the occlusive incidence of patient blood samples and explore hypoxia-induced endothelial gene modulation. These results offer a better understanding of the mechanistic changes affecting the endothelium during hypoxia reperfusion injury, while supporting the theory that hypoxia reperfusion may offer a protective effect against vaso-occlusion in SCD.

6.2 Limitations

Although the microfluidic platform presented in this thesis offers a significant contribution to the field, it is not without limitations. There are some drawbacks to microfluidic platforms in general, including oversimplification and poor scalability. This microfluidic platform is inherently a reductionist model that isolates several fundamental physical processes (hypoxia, cell sickling, shear stress, adhesion, occlusion) and core cell types (red blood cells, endothelial cells), while intentionally excluding others (white blood cells, platelets, etc.). This approach allows for precise investigation into the relationship of several variables while minimizing complexity, though it can exclude relevant information. Additionally, multi-layer device fabrication can be extremely time consuming and labor intensive, limiting rapid reproducibility. While the inclusion of endothelium added significant biological value to the research, it also increased experimental complexity. Throughput and scalability can certainly be limited by these factors, as well as the advanced training and expertise required to fabricate multi-layer endothelialized microfluidic devices.

The experimental design of this microfluidic platform also had some biological limitations. The current device design does not accommodate other vessel features such as pulsatile flow or vasoconstriction/vasodilation. Additionally, the microvascular system in our model was composed entirely of endothelial cells and did not include supportive cells. It was not feasible to include vascular supportive cells such as smooth muscle cells, fibroblasts, or pericytes within this

study, which could have offered additional physiologic relevance in some vascular contexts. However, co-culture with these cell types presents an interesting possibility for future work. Since we were specifically interested in modeling the post-capillary venules to study SCD, these limitations were not particularly concerning; however, they would make it more challenging to apply this model to arterial or venous flow studies.

6.3 Future Directions

The development of this model system presents a wide array of possibilities for future research and exploration. The conclusions presented in Chapters 4 and 5 represent only a portion of the full potential of this model system, whereas this chapter draws attention to the potential versatility of the platform.

In particular, substantial progress could be made by expanding upon the RNA sequencing results from Chapter 5. In that section, we identified a number of key genes of interest that were differentially regulated in response to hypoxia preconditioning. A potentially ground-breaking future study would involve the inhibition of those genes or associated functional proteins to validate our outcomes. These studies could valuably inform drug development for the disease.

The noticeable patient heterogeneity in occlusion result inspired many ideas for future study. If we were able to identify additional factors causing some patient samples to occlude more often than others, this may better explain clinical

heterogeneity of patient phenotype and present an opportunity for therapeutic intervention. First, our study demonstrated a weak correlation between sex and occlusive incidence, indicating that male patients may be more likely to occlude on-chip. Increasing cohort size while controlling for other variables would help to expand upon this conclusion. Additionally, some analyses were not possible in this study due to limitations of the patient dataset. It would be especially valuable to repeat this study and stratify occlusion result by active medication usage and patient outcomes (reported number of complications such as VOC, acute chest syndrome (ACS), emergency hospital visits, etc.) in addition to genotype and occlusion history. This may help to examine the efficacy of new therapies on-chip. Moreover, further investigation into the occlusive profile of samples from patients with hemoglobin SC disease would be of particular interest. Hemoglobin SC disease is poorly researched, and investigation into patient 8's complete lack of occlusive response may shed light on the clinical severity of the SC genotype in comparison to the SS genotype. Identifying mechanisms of occlusion-evasion in HbSC could again provide valuable insight in the development of therapies for SCD.

Lastly, results from both the Spearman correlation and the partial least squares regression analysis (PLSR) demonstrated that high white blood cell count, and platelet count are correlated with endothelial cell-mediated red blood cell occlusion on-chip. Performing whole blood experiments with fluorescent labeling

of white blood cells and platelets could help to elucidate each cell type's contributions to the occlusive process.

Overall, much has been gained by the development of a more physiologic microfluidic model of SCD. The optimization of many methodologies including endothelialization of small microfluidic channels, quantification of sample occlusion on-chip, and extraction of endothelial cells from devices for NGS offers wide-ranging potential for studies in SCD as well as the overall vascular research field.

Chapter 7: References

1. Weatherall, David. J. The inherited diseases of hemoglobin are an emerging global health burden. *Blood* **115**, 4331–4336 (2010).
2. Modell, B. & Darlison, M. Global epidemiology of haemoglobin disorders and derived service indicators. *Bull World Health Organ* **86**, 480–487 (2008).
3. Hassell, K. L. Population Estimates of Sickle Cell Disease in the U.S. *American Journal of Preventive Medicine* **38**, (2010).
4. Piel, F. B., Hay, S. I., Gupta, S., Weatherall, D. J. & Williams, T. N. Global Burden of Sickle Cell Anaemia in Children under Five, 2010–2050: Modelling Based on Demographics, Excess Mortality, and Interventions. *PLoS Medicine* **10**, e1001484–e1001484 (2013).
5. Piel, F. B. *et al.* Global epidemiology of sickle haemoglobin in neonates: a contemporary geostatistical model-based map and population estimates. *The Lancet* **381**, 142–151 (2013).
6. Piel, F. B., Steinberg, M. H. & Rees, D. C. Sickle Cell Disease. 1561–1573 (2017) doi:10.1056/NEJMra1510865.
7. Piel, F. B. *et al.* Global distribution of the sickle cell gene and geographical confirmation of the malaria hypothesis. *Nat Commun* **1**, 104 (2010).
8. Motulsky, A. G. Frequency of Sickling Disorders in U.S. Blacks. *New England Journal of Medicine* **288**, 31–33 (1973).
9. Uddin, D. E., Dickson, L. G. & Brodine, C. E. Screening of Military Recruits for Hemoglobin Variants. *JAMA: The Journal of the American Medical Association* **227**, 1405–1407 (1974).
10. CDC. Data and Statistics on Sickle Cell Disease. *Sickle Cell Disease (SCD)* https://www.cdc.gov/sickle-cell/data/index.html (2024).
11. Lanzkron, S., Carroll, C. P. & Haywood, C. The burden of emergency department use for sickle-cell disease: an analysis of the national emergency department sample database. *Am J Hematol* **85**, 797–799 (2010).

12. Kamath, D., Hayes, A., Vissa, M., Agrawal, A. & Long, L. Benefit of Inpatient Pain Plan Utilization on Hospital Length of Stay in Adolescents and Young Adults with Sickle Cell Disease. *Blood* **142**, 2324 (2023).
13. Ingram, V. M. A specific chemical difference between the globins of normal human and sickle-cell anaemia haemoglobin. *Nature* **178**, 792–794 (1956).
14. Ingram, V. M. Gene mutations in human haemoglobin: the chemical difference between normal and sickle cell haemoglobin. *Nature* **180**, 326–328 (1957).
15. Pauling, L., Itano, H. A., Singer, S. J. & Wells, I. C. Sickle cell anemia, a molecular disease. *Science* **110**, 543–548 (1949).
16. Steinberg, M. H. & Rodgers, G. P. HbA2 : biology, clinical relevance and a possible target for ameliorating sickle cell disease. *Br J Haematol* **170**, 781–787 (2015).
17. Ghunney, W. K. *et al.* Most adults with severe HbSC disease are not treated with hydroxyurea. *Blood Advances* **7**, 3312–3319 (2023).
18. Pecker, L. H., Schaefer, B. A. & Luchtman-Jones, L. Knowledge insufficient: the management of haemoglobin SC disease. *Br J Haematol* **176**, 515–526 (2017).
19. Habara, A. & Steinberg, M. H. Minireview: Genetic basis of heterogeneity and severity in sickle cell disease. *Experimental Biology and Medicine* **241**, 689–696 (2016).
20. Kato, G. J. *et al.* Sickle cell disease. *Nature Reviews Disease Primers* **4**, (2018).
21. Herrick, J. B. Peculiar Elongated and Sickle-Shaped Red Blood Corpuscles in a Case of Severe Anemia. *JAMA* **312**, 1063 (2014).
22. Brittenham, G. M., Schechter, A. N. & Tom Noguchi, C. Hemoglobin S polymerization: Primary determinant of the hemolytic and clinical severity of the sickling syndromes. *Blood* **65**, 183–189 (1985).
23. Noguchi, C. T. & Schechter, A. N. Sickle hemoglobin polymerization in solution and in cells. *Annu Rev Biophys Biophys Chem* **14**, 239–263 (1985).

24. Rees, D. C., Williams, T. N. & Gladwin, M. T. Sickle-cell disease. in vol. 376 2018–2031 (Elsevier, 2010).
25. Aygun, B. & Odame, I. REVIEW A Global Perspective on Sickle Cell Disease. *Pediatr Blood Cancer* **59**, 386–390 (2012).
26. Lubeck, D. *et al.* Estimated Life Expectancy and Income of Patients With Sickle Cell Disease Compared With Those Without Sickle Cell Disease. *JAMA network open* **2**, e1915374–e1915374 (2019).
27. Mulumba, L. L. & Wilson, L. Sickle cell disease among children in Africa: An integrative literature review and global recommendations. *International Journal of Africa Nursing Sciences* **3**, 56–64 (2015).
28. Ballas, S. K. & Lusardi, M. Hospital readmission for adult acute sickle cell painful episodes: Frequency, etiology, and prognostic significance. *American Journal of Hematology* **79**, 17–25 (2005).
29. Darbari, D. S., Sheehan, V. A. & Ballas, S. K. The vaso-occlusive pain crisis in sickle cell disease: Definition, pathophysiology, and management. *European Journal of Haematology* **105**, 237–246 (2020).
30. Vichinsky, E. P. *et al.* Causes and Outcomes of the Acute Chest Syndrome in Sickle Cell Disease. *New England Journal of Medicine* **342**, 1855–1865 (2000).
31. Thomas, A. N., Pattison, C. & Serjeant, G. R. Causes of death in sickle-cell disease in Jamaica. *British Medical Journal* **285**, 633–635 (1982).
32. Sant'Ana, P. G. dos S. *et al.* Clinical and laboratory profile of patients with sickle cell anemia. *Revista Brasileira de Hematologia e Hemoterapia* **39**, 40–45 (2017).
33. Jain, S., Bakshi, N. & Krishnamurti, L. Acute Chest Syndrome in Children with Sickle Cell Disease. *Pediatric, Allergy, Immunology, and Pulmonology* **30**, 191–201 (2017).
34. Powars, D. *et al.* Sickle cell chronic lung disease: Prior morbidity and the risk of pulmonary failure. *Medicine (United States)* **67**, 66–76 (1988).

35. Chou, S. T. & Fasano, R. M. Management of Patients with Sickle Cell Disease Using Transfusion Therapy: Guidelines and Complications. *Hematology/Oncology Clinics of North America* **30**, 591–608 (2016).
36. Platt, O. S. *et al.* Mortality In Sickle Cell Disease -- Life Expectancy and Risk Factors for Early Death. *New England Journal of Medicine* **330**, 1639–1644 (1994).
37. Ohene-Frempong, K. *et al.* Cerebrovascular accidents in sickle cell disease: Rates and risk factors. *Blood* **91**, 288–294 (1998).
38. Balkaran, B. *et al.* Stroke in a cohort of patients with homozygous sickle cell disease. *The Journal of Pediatrics* **120**, 360–366 (1992).
39. Hoppe, C. Defining stroke risk in children with sickle cell anaemia. *British Journal of Haematology* **128**, 751–766 (2005).
40. Martin, S. *et al.* Neurocognitive functioning in symptomatic adults with sickle cell disease: A description and comparison with unaffected siblings. *Neuropsychological Rehabilitation* **30**, 1666–1681 (2020).
41. Prussien, K. V., Jordan, L. C., Debaun, M. R. & Compas, B. E. Cognitive Function in Sickle Cell Disease across Domains, Cerebral Infarct Status, and the Lifespan: A Meta-Analysis. *Journal of Pediatric Psychology* **44**, 948–958 (2019).
42. Brousse, V. *et al.* Acute splenic sequestration crisis in sickle cell disease: cohort study of 190 paediatric patients. *Br J Haematol* **156**, 643–648 (2012).
43. Powell, R. W., Levine, G. L., Yang, Y. M. & Mankad, V. N. Acute splenic sequestration crisis in sickle cell disease: Early detection and treatment. *Journal of Pediatric Surgery* **27**, 215–219 (1992).
44. Topley, J. M., Rogers, D. W., Stevens, M. C. & Serjeant, G. R. Acute splenic sequestration and hypersplenism in the first five years in homozygous sickle cell disease. *Archives of Disease in Childhood* **56**, 765–769 (1981).
45. Emond, A. M. *et al.* Acute splenic sequestration in homozygous sickle cell disease: Natural history and management. *The Journal of Pediatrics* **107**, 201–206 (1985).

46. Ellory, J. C. *et al.* Abnormal permeability pathways in human red blood cells. *Blood Cells, Molecules, and Diseases* **39**, 1–6 (2007).
47. Kuypers, F. A. Hemoglobin S polymerization and red cell membrane changes. *Hematology/Oncology Clinics of North America* **28**, 155–179 (2014).
48. Piccin, A. *et al.* Insight into the complex pathophysiology of sickle cell anaemia and possible treatment. *European Journal of Haematology* **102**, 319–330 (2019).
49. Noguchi, C. T., Rodgers, G. P., Serjeant, G. & Schechter, A. N. Levels of fetal hemoglobin necessary for treatment of sickle cell disease. *N Engl J Med* **318**, 96–99 (1988).
50. Ballas, S. K. & Smith, E. D. Red blood cell changes during the evolution of the sickle cell painful crisis. *Blood* **79**, 2154–2163 (1992).
51. Connes, P. *et al.* The role of blood rheology in sickle cell disease. *Blood Reviews* **30**, 111–118 (2016).
52. Lubin, B., Chiu, D., Bastacky, J., Roelofsen, B. & Van Deenen, L. L. Abnormalities in membrane phospholipid organization in sickled erythrocytes. *J Clin Invest* **67**, 1643–1649 (1981).
53. Liu, S. C. *et al.* Red cell membrane remodeling in sickle cell anemia. Sequestration of membrane lipids and proteins in Heinz bodies. *J Clin Invest* **97**, 29–36 (1996).
54. Rice-Evans, C., Omorphos, S. C. & Baysal, E. Sickle cell membranes and oxidative damage. *Biochem J* **237**, 265–269 (1986).
55. Goodman, S. R. The irreversibly sickled cell: a perspective. *Cell Mol Biol (Noisy-le-grand)* **50**, 53–58 (2004).
56. Rodgers, G. P., Noguchi, C. T. & Schechter, A. N. Irreversibly sickled erythrocytes in sickle cell anemia: a quantitative reappraisal. *Am J Hematol* **20**, 17–23 (1985).
57. Alayash, A. I. Oxidative pathways in the sickle cell and beyond. *Blood Cells Mol Dis* **70**, 78–86 (2018).

58. Quinn, C. T. *et al.* Biochemical surrogate markers of hemolysis do not correlate with directly measured erythrocyte survival in sickle cell anemia. *Am J Hematol* **91**, 1195–1201 (2016).
59. Schaer, D. J., Buehler, P. W., Alayash, A. I., Belcher, J. D. & Vercellotti, G. M. Hemolysis and free hemoglobin revisited: Exploring hemoglobin and hemin scavengers as a novel class of therapeutic proteins. *Blood* **121**, 1276–1284 (2013).
60. Wood, K. C., Hebbel, R. P. & Granger, D. N. Endothelial cell NADPH oxidase mediates the cerebral microvascular dysfunction in sickle cell transgenic mice. *The FASEB Journal* **19**, 989–991 (2005).
61. George, A. *et al.* Erythrocyte NADPH oxidase activity modulated by Rac GTPases, PKC, and plasma cytokines contributes to oxidative stress in sickle cell disease. *Blood* **121**, 2099–2107 (2013).
62. Belcher, J. D. *et al.* Critical role of endothelial cell activation in hypoxia-induced vasoocclusion in transgenic sickle mice. *Am J Physiol Heart Circ Physiol* **288**, H2715-2725 (2005).
63. Francis, R. B. & Haywood, L. J. Elevated immunoreactive tumor necrosis factor and interleukin-1 in sickle cell disease. *Journal of the National Medical Association* **84**, 611–615 (1992).
64. Croizat, H. Circulating cytokines in sickle cell patients during steady state. *British Journal of Haematology* **87**, 592–597 (1994).
65. Graido-Gonzalez, E. *et al.* Plasma endothelin-1, cytokine, and prostaglandin E2 levels in sickle cell disease and acute vaso-occlusive sickle crisis. *Blood* **92**, 2551–2555 (1998).
66. Proença-Ferreira, R. *et al.* Endothelial activation by platelets from sickle cell anemia patients. *PLoS ONE* **9**, 89012–89012 (2014).
67. Solovey, A. *et al.* Circulating activated endothelial cells in sickle cell anemia. *N Engl J Med* **337**, 1584–1590 (1997).
68. Matsui, N. M. *et al.* P-selectin mediates the adhesion of sickle erythrocytes to the endothelium. *Blood* **98**, 1955–1962 (2001).

69. Polanowska-Grabowska, R. *et al.* P-selectin-mediated platelet-neutrophil aggregate formation activates neutrophils in mouse and human sickle cell disease. *Arteriosclerosis, Thrombosis, and Vascular Biology* **30**, 2392–2399 (2010).

70. Zhang, D., Xu, C., Manwani, D. & Frenette, P. S. Neutrophils, platelets, and inflammatory pathways at the nexus of sickle cell disease pathophysiology. *Blood* **127**, 801–809 (2016).

71. Kansas, G. S. Selectins and their ligands: Current concepts and controversies. *Blood* **88**, 3259–3287 (1996).

72. Hattori, R., Hamilton, K. K., Fugate, R. D., McEver, R. P. & Sims, P. J. Stimulated secretion of endothelial von Willebrand factor is accompanied by rapid redistribution to the cell surface of the intracellular granule membrane protein GMP-140. *Journal of Biological Chemistry* **264**, 7768–7771 (1989).

73. Ley, K. The role of selectins in inflammation and disease. *Trends in Molecular Medicine* **9**, 263–268 (2003).

74. Goncharov, N. V., Nadeev, A. D., Jenkins, R. O. & Avdonin, P. V. Markers and Biomarkers of Endothelium: When Something Is Rotten in the State. *Oxidative Medicine and Cellular Longevity* **2017**, (2017).

75. Lorant, D. E. *et al.* Coexpression of GMP-140 and PAF by endothelium stimulated by histamine or thrombin: A juxtacrine system for adhesion and activation of neutrophils. *Journal of Cell Biology* **115**, 223–234 (1991).

76. Stenberg, P. E., McEver, R. P., Shuman, M. A., Jacques, Y. V. & Bainton, D. F. A platelet alpha-granule membrane protein (GMP-140) is expressed on the plasma membrane after activation. *Journal of Cell Biology* **101**, 880–886 (1985).

77. Closse, C. *et al.* Influence Of Hypoxia And Hypoxia-Reoxygenation On Endothelial P-Selectin Expression. *Pathophysiology of Haemostasis and Thrombosis* **26**, 177–181 (1996).

78. Matsui, N. M., Varki, A. & Embury, S. H. Heparin inhibits the flow adhesion of sickle red blood cells to P-selectin. *Blood* **100**, 3790–3796 (2002).

79. Belcher, J. D. *et al.* Heme triggers TLR4 signaling leading to endothelial cell activation and vaso-occlusion in murine sickle cell disease. *Blood* **123**, 377–390 (2014).
80. Belcher, J. D., Marker, P. H., Weber, J. P., Hebbel, R. P. & Vercellotti, G. M. Activated monocytes in sickle cell disease: Potential role in the activation of vascular endothelium and vaso-occlusion. *Blood* **96**, 2451–2459 (2000).
81. Chen, G. *et al.* Heme-induced neutrophil extracellular traps contribute to the pathogenesis of sickle cell disease. *Blood* **123**, 3818–3827 (2014).
82. Solovey, A. A., Solovey, A. N., Harkness, J. & Hebbel, R. P. Modulation of endothelial cell activation in sickle cell disease: a pilot study. *Blood* **97**, 1937–1941 (2001).
83. Nader, E., Romana, M. & Connes, P. The Red Blood Cell-Inflammation Vicious Circle in Sickle Cell Disease. *Front Immunol* **11**, 454 (2020).
84. Kalogeris, T., Baines, C. P., Krenz, M. & Korthuis, R. J. Cell Biology of Ischemia/Reperfusion Injury. in *International Review of Cell and Molecular Biology* vol. 298 229–317 (Elsevier Inc., 2012).
85. Eltzschig, H. K. & Eckle, T. Ischemia and reperfusion--from mechanism to translation. *Nat Med* **17**, 1391–1401 (2011).
86. Ansari, J. & Gavins, F. N. E. Ischemia-Reperfusion Injury in Sickle Cell Disease: From Basics to Therapeutics. *American Journal of Pathology* **189**, 706–718 (2019).
87. Hebbel, R. P., Belcher, J. D. & Vercellotti, G. M. The multifaceted role of ischemia/reperfusion in sickle cell anemia. *J Clin Invest* **130**, 1062–1072 (2020).
88. Hebbel, R. P. Ischemia-reperfusion injury in sickle cell anemia: Relationship to acute chest syndrome, endothelial dysfunction, arterial vasculopathy, and inflammatory pain. *Hematology/Oncology Clinics of North America* **28**, 181–198 (2014).
89. Stray-Gundersen, S., Massoudian, S. D., Wojan, F., Tanaka, H. & Lalande, S. Hypoxic preconditioning reduces endothelial ischemia-reperfusion injury in

older adults. *Am J Physiol Regul Integr Comp Physiol* **323**, R832–R838 (2022).

90. Halder, S. K., Kant, R. & Milner, R. Hypoxic pre-conditioning suppresses experimental autoimmune encephalomyelitis by modifying multiple properties of blood vessels. *Acta Neuropathologica Communications* **6**, 86 (2018).
91. Kalogeris, T., Baines, C. P., Krenz, M. & Korthuis, R. J. Ischemia/Reperfusion. *Compr Physiol* **7**, 113–170 (2016).
92. Baldea, I. *et al.* Effects of different hypoxia degrees on endothelial cell cultures-Time course study. *Mech Ageing Dev* **172**, 45–50 (2018).
93. Chatel, B. *et al.* Exacerbated metabolic changes in skeletal muscle of sickle cell mice submitted to an acute ischemia-reperfusion paradigm. *Clin Sci (Lond)* **132**, 2103–2115 (2018).
94. Siciliano, A. *et al.* Abnormal modulation of cell protective systems in response to ischemic/reperfusion injury is important in the development of mouse sickle cell hepatopathy. *Haematologica* **96**, 24–32 (2011).
95. Kaul, D. K., Finnegan, E. & Barabino, G. A. Sickle red cell-endothelium interactions. *Microcirculation* **16**, 97–111 (2009).
96. Telen, M. J., Malik, P. & Vercellotti, G. M. Therapeutic strategies for sickle cell disease: towards a multi-agent approach. *Nature Reviews Drug Discovery* **18**, 139–158 (2019).
97. Kato, G. J., Steinberg, M. H. & Gladwin, M. T. Intravascular hemolysis and the pathophysiology of sickle cell disease. *J Clin Invest* **127**, 750–760 (2017).
98. Sundd, P., Gladwin, M. T. & Novelli, E. M. Pathophysiology of Sickle Cell Disease.
99. Gladwin, M. T. & Ofori-Acquah, S. F. Erythroid DAMPs drive inflammation in SCD. *Blood* **123**, 3689–3690 (2014).
100. Murphy, M. M. *et al.* Role of Rap1 in promoting sickle red blood cell adhesion to laminin via BCAM/LU. *Blood* **105**, 3322–3329 (2005).

101. Canalli, A. A. *et al.* Participation of Mac-1, LFA-1 and VLA-4 integrins in the in vitro adhesion of sickle cell disease neutrophils to endothelial layers, and reversal of adhesion by simvastatin. *Haematologica* **96**, 526–533 (2011).
102. Costa, E. *et al.* Successes and pitfalls in orphan drug development for sickle cell disease. *Blood Adv* **8**, 2455–2465 (2024).
103. Research, C. for D. E. and. FDA approves hydroxyurea for treatment of pediatric patients with sickle cell anemia. *FDA* (2024).
104. Silva, M., Coelho, A., Vargas, S. & Faustino, P. VCAM1, HMOX1 and NOS3 differential endothelial expression may impact sickle cell anemia vasculopathy. *Blood Cells Mol Dis* **93**, 102639 (2022).
105. Kinney, T. R. *et al.* Safety of hydroxyurea in children with sickle cell anemia: Results of the HUG-KIDS study, a phase I/II trial. *Blood* **94**, 1550–1554 (1999).
106. Brandow, A. M. & Panepinto, J. A. Hydroxyurea use in sickle cell disease: The battle with low prescription rates, poor patient compliance and fears of toxicities. *Expert Review of Hematology* **3**, 255–260 (2010).
107. FDA approved L-glutamine powder for the treatment of sickle cell disease | FDA.
108. Niihara, Y. *et al.* A phase 3 trial of l-glutamine in sickle cell disease. *New England Journal of Medicine* **379**, 226–235 (2018).
109. Ali, M. A. *et al.* Efficacy and safety of recently approved drugs for sickle cell disease: a review of clinical trials. *Experimental Hematology* **92**, 11-18.e1 (2020).
110. FDA approves crizanlizumab-tmca for sickle cell disease. *FDA* (2019).
111. Blair, H. A. Crizanlizumab: First Approval. *Drugs* **80**, 79–84 (2020).
112. Kutlar, A. *et al.* Effect of crizanlizumab on pain crises in subgroups of patients with sickle cell disease: A SUSTAIN study analysis. *American Journal of Hematology* **94**, 55–61 (2019).
113. Ataga, K. I. *et al.* Crizanlizumab for the Prevention of Pain Crises in Sickle Cell Disease. *N Engl J Med* **376**, 429–439 (2017).

114. Gardner, R. V. Crizanlizumab in vaso-occlusive crisis caused by sickle cell disease. *Drugs Today (Barc)* **56**, 705–714 (2020).
115. Class 2 Medicines Recall: Novartis Pharmaceuticals UK Limited, Adakveo 10 mg/ml concentrate for solution for infusion, EL(24)A/06. *GOV.UK* https://www.gov.uk/drug-device-alerts/class-2-medicines-recall-novartis-pharmaceuticals-uk-limited-adakveo-10-mg-slash-ml-concentrate-for-solution-for-infusion-el-24-a-slash-06.
116. Migotsky, M., Beestrum, M. & Badawy, S. M. Recent Advances in Sickle-Cell Disease Therapies: A Review of Voxelotor, Crizanlizumab, and L-glutamine. *Pharmacy* **10**, 123 (2022).
117. Brandow, A. M. & Liem, R. I. Advances in the diagnosis and treatment of sickle cell disease. *Journal of Hematology & Oncology* **15**, 20 (2022).
118. Hutchaleelaha, A. *et al.* Pharmacokinetics and pharmacodynamics of voxelotor (GBT440) in healthy adults and patients with sickle cell disease. *British Journal of Clinical Pharmacology* **85**, 1290–1302 (2019).
119. Pfizer Voluntarily Withdraws All Lots of Sickle Cell Disease Treatment OXBRYTA® (voxelotor) From Worldwide Markets | Pfizer. https://www.pfizer.com/news/press-release/press-release-detail/pfizer-voluntarily-withdraws-all-lots-sickle-cell-disease.
120. Haimed, A., Weiss, R., Kwon, S., Bhat, R. & Badawy, S. M. Intravenous fluid therapy and hospital outcomes for vaso-occlusive episodes in children, adolescents, and young adults with sickle cell disease. *Pediatric Blood & Cancer* **71**, e30781 (2024).
121. Ojo, A. S., Ojukwu, S., Asmare, W., Odipe, O. & Larbi, D. Intravenous Fluid Administration and the Risk of Adverse Outcomes in Sickle Cell Disease Patients Hospitalized for Vaso-Occlusive Crisis. *J Hematol* **11**, 159–166 (2022).
122. Carden, M. A. *et al.* Extracellular fluid tonicity impacts sickle red blood cell deformability and adhesion. *Blood* **130**, 2654–2663 (2017).

123. Carden, M. A. *et al.* Normal saline is associated with increased sickle red cell stiffness and prolonged transit times in a microfluidic model of the capillary system. *Microcirculation* **24**, (2017).
124. Carden, M. A. *et al.* Normal saline bolus use in pediatric emergency departments is associated with poorer pain control in children with sickle cell anemia and vaso-occlusive pain. *Am J Hematol* **94**, 689–696 (2019).
125. Bartolucci, P. *et al.* A randomized, controlled clinical trial of ketoprofen for sickle-cell disease vaso-occlusive crises in adults. *Blood* **114**, 3742–3747 (2009).
126. Howard, J. Sickle cell disease: when and how to transfuse. *Hematology* **2016**, 625–631 (2016).
127. Turner, J. M., Kaplan, J. B., Cohen, H. W. & Billett, H. H. Exchange versus simple transfusion for acute chest syndrome in sickle cell anemia adults. *Transfusion* **49**, 863–868 (2009).
128. Koehl, B. *et al.* Continuous manual exchange transfusion for patients with sickle cell disease: An efficient method to avoid iron overload. *Journal of Visualized Experiments* **2017**, (2017).
129. Chou, S. T. *et al.* American Society of Hematology 2020 guidelines for sickle cell disease: transfusion support. *Blood Adv* **4**, 327–355 (2020).
130. J, H. *et al.* The Transfusion Alternatives Preoperatively in Sickle Cell Disease (TAPS) study: a randomised, controlled, multicentre clinical trial. *Lancet (London, England)* **381**, (2013).
131. Miller, S. T. *et al.* Impact of chronic transfusion on incidence of pain and acute chest syndrome during the Stroke Prevention Trial (STOP) in sickle-cell anemia. *Journal of Pediatrics* **139**, 785–789 (2001).
132. DeBaun, M. R. *et al.* Controlled Trial of Transfusions for Silent Cerebral Infarcts in Sickle Cell Anemia. *New England Journal of Medicine* **371**, 699–710 (2014).

133. Hankins, J. *et al.* Chronic transfusion therapy for children with sickle cell disease and recurrent acute chest syndrome. *Journal of Pediatric Hematology/Oncology* **27**, 158–161 (2005).
134. Powars, D., Wilson, B., Imbus, C., Pegelow, C. & Allen, J. The natural history of stroke in sickle cell disease. *The American Journal of Medicine* **65**, 461–471 (1978).
135. Hulbert, M. L. *et al.* Silent cerebral infarcts occur despite regular blood transfusion therapy after first strokes in children with sickle cell disease. *Blood* **117**, 772–779 (2011).
136. Dzik, S. Risk of recurrent stroke in children with sickle cell disease receiving blood transfusion therapy for at least five years after initial strokeD.J. Scothorn, C Price, D. Schwartz, et al. J Peds 140:348–54, 2002. *Transfusion Medicine Reviews* **16**, 332–332 (2002).
137. Adams, R. J. *et al.* Prevention of a First Stroke by Transfusions in Children with Sickle Cell Anemia and Abnormal Results on Transcranial Doppler Ultrasonography. *New England Journal of Medicine* **339**, 5–11 (1998).
138. Josephson, C. D., Su, L. L., Hillyer, K. L. & Hillyer, C. D. Transfusion in the Patient With Sickle Cell Disease: A Critical Review of the Literature and Transfusion Guidelines. *Transfusion Medicine Reviews* (2007) doi:10.1016/j.tmrv.2006.11.003.
139. Hudson, K. E., Fasano, R. M., Karafin, M. S., Hendrickson, J. E. & Francis, R. O. Mechanisms of alloimmunization in sickle cell disease. *Current Opinion in Hematology* **26**, 434–441 (2019).
140. Pandey, H., Das, S. S. & Chaudhary, R. Red cell alloimmunization in transfused patients: A silent epidemic revisited. *Asian Journal of Transfusion Science* **8**, 75–77 (2014).
141. Fasano, R. M. *et al.* Impact of Red Blood Cell Antigen Matching on Alloimmunization and Transfusion Complications in Patients with Sickle Cell Disease: A Systematic Review. *Transfusion Medicine Reviews* **33**, 12–23 (2019).

142. Redman, M., Regan, F. & Contreras, M. A prospective study of the incidence of red cell allo-immunisation following transfusion. *Vox Sang* **71**, 216–220 (1996).
143. Vichinsky, E. P. *et al.* Alloimmunization in Sickle Cell Anemia and Transfusion of Racially Unmatched Blood. *New England Journal of Medicine* **322**, 1617–1621 (1990).
144. Fong, I. W. & Fong, I. W. Blood Transfusion-Associated Infections in the Twenty-First Century: New Challenges. in *Current Trends and Concerns in Infectious Diseases* 191–215 (Springer International Publishing, 2020). doi:10.1007/978-3-030-36966-8_8.
145. Allali, S., de Montalembert, M., Brousse, V., Chalumeau, M. & Karim, Z. Management of iron overload in hemoglobinopathies. *Transfusion Clinique et Biologique* **24**, 223–226 (2017).
146. Ballas, S. K. Iron overload is a determinant of morbidity and mortality in adult patients with sickle cell disease. in vol. 38 30–36 (W.B. Saunders, 2001).
147. Walter, P. B. *et al.* Oxidative stress and inflammation in iron-overloaded patients with β-thalassaemia or sickle cell disease. *British Journal of Haematology* **135**, 254–263 (2006).
148. Porter, J. & Garbowski, M. Consequences and management of iron overload in sickle cell disease. *Hematology / the Education Program of the American Society of Hematology. American Society of Hematology. Education Program* **2013**, 447–456 (2013).
149. Commissioner, O. of the. FDA Approves First Gene Therapies to Treat Patients with Sickle Cell Disease. *FDA* https://www.fda.gov/news-events/press-announcements/fda-approves-first-gene-therapies-treat-patients-sickle-cell-disease (2024).
150. Jagadeeswaran, R. & Rivers, A. Evolving treatment paradigms in sickle cell disease. *Hematology* **2017**, 440–446 (2017).

151. Hoppe, C. & Neumayr, L. Sickle Cell Disease: Monitoring, Current Treatment, and Therapeutics Under Development. *Hematology/Oncology Clinics of North America* **33**, 355–371 (2019).
152. van der Worp, H. B. *et al.* Can Animal Models of Disease Reliably Inform Human Studies? *PLoS Med* **7**, e1000245 (2010).
153. Hackam, D. G. & Redelmeier, D. A. Translation of Research Evidence From Animals to Humans. *JAMA* **296**, 1727–1732 (2006).
154. Higgins, J. M., Eddington, D. T., Bhatia, S. N. & Mahadevan, L. Sickle cell vasoocclusion and rescue in a microfluidic device. *Proceedings of the National Academy of Sciences* **104**, 20496–20500 (2007).
155. Horton, R. E. Microfluidics for investigating vaso-occlusions in sickle cell disease. *Microcirculation* **24**, (2017).
156. Aich, A. *et al.* Microfluidics in Sickle Cell Disease Research: State of the Art and a Perspective Beyond the Flow Problem. *Front Mol Biosci* **7**, 558982 (2020).
157. Kim, M., Alapan, Y., Adhikari, A., Little, J. A. & Gurkan, U. A. Hypoxia-enhanced adhesion of red blood cells in microscale flow. *Microcirculation* **24**, e12374 (2017).
158. Papageorgiou, D. P. *et al.* Simultaneous polymerization and adhesion under hypoxia in sickle cell disease. *Proceedings of the National Academy of Sciences of the United States of America* **115**, 9473–9478 (2018).
159. Higgins, J. M., Eddington, D. T., Bhatia, S. N. & Mahadevan, L. Review of an in vitro microfluidic model of sickle cell vaso-occlusion. *Transfus Clin Biol* **15**, 12–13 (2008).
160. Wood, D. K., Soriano, A., Mahadevan, L., Higgins, J. M. & Bhatia, S. N. A biophysical indicator of vaso-occlusive risk in sickle cell disease. *Sci Transl Med* **4**, 123ra26 (2012).
161. Qiang, Y., Dieujuste, D., Liu, J., Alvarez, O. & Du, E. Rapid electrical impedance detection of sickle cell vaso-occlusion in microfluidic device. *Biomed Microdevices* **25**, 23 (2023).

162. Lu, X., Wood, D. K. & Higgins, J. M. Deoxygenation Reduces Sickle Cell Blood Flow at Arterial Oxygen Tension. *Biophys J* **110**, 2751–2758 (2016).
163. Lu, X., Galarneau, M. M., Higgins, J. M. & Wood, D. K. A microfluidic platform to study the effects of vascular architecture and oxygen gradients on sickle blood flow. *Microcirculation* **24**, (2017).
164. Lu, X., Chaudhury, A., Higgins, J. M. & Wood, D. K. Oxygen-dependent flow of sickle trait blood as an in vitro therapeutic benchmark for sickle cell disease treatments. *Am J Hematol* **93**, 1227–1235 (2018).
165. Valdez, J. M., Datta, Y. H., Higgins, J. M. & Wood, D. K. A microfluidic platform for simultaneous quantification of oxygen-dependent viscosity and shear thinning in sickle cell blood. *APL Bioeng* **3**, 046102 (2019).
166. Hansen, S., Wood, D. K. & Higgins, J. M. 5-(Hydroxymethyl)furfural restores low-oxygen rheology of sickle trait blood in vitro. *Br J Haematol* **188**, 985–993 (2020).
167. Hansen, S. & Wood, D. K. Simultaneous quantification of blood rheology and oxygen saturation to evaluate affinity-modifying therapies in sickle cell disease. *Lab Chip* **22**, 4141–4150 (2022).
168. Geisness, A. C. *et al.* Ionophore-mediated swelling of erythrocytes as a therapeutic mechanism in sickle cell disease. *Haematologica* **107**, 1438–1447 (2022).
169. Szafraniec, H. M. *et al.* Feature tracking microfluidic analysis reveals differential roles of viscosity and friction in sickle cell blood. *Lab Chip* **22**, 1565–1575 (2022).
170. Man, Y. *et al.* Microfluidic assessment of red blood cell mediated microvascular occlusion. *Lab Chip* **20**, 2086–2099 (2020).
171. Man, Y. *et al.* OcclusionChip: A functional microcapillary occlusion assay complementary to ektacytometry for detection of small-fraction red blood cells with abnormal deformability. *Front Physiol* **13**, 954106 (2022).

172. Tsai, M. *et al.* In vitro modeling of the microvascular occlusion and thrombosis that occur in hematologic diseases using microfluidic technology. *J Clin Invest* **122**, 408–418 (2012).
173. Fay, M. E. *et al.* iCLOTS: open-source, artificial intelligence-enabled software for analyses of blood cells in microfluidic and microscopy-based assays. *Nat Commun* **14**, 5022 (2023).
174. Myers, D. R. *et al.* Endothelialized Microfluidics for Studying Microvascular Interactions in Hematologic Diseases. *J Vis Exp* 3958 (2012) doi:10.3791/3958.
175. Kucukal, E., Ilich, A., Key, N. S., Little, J. A. & Gurkan, U. A. Red Blood Cell Adhesion to Heme-Activated Endothelial Cells Reflects Clinical Phenotype in Sickle Cell Disease. *Am J Hematol* 10.1002/ajh.25159 (2018) doi:10.1002/ajh.25159.
176. Beckman, J. D. *et al.* JAK-STAT inhibition reduces endothelial prothrombotic activation and leukocyte-endothelial proadhesive interactions. *J Thromb Haemost* **21**, 1366–1380 (2023).
177. Sakurai, Y. *et al.* A microengineered vascularized bleeding model that integrates the principal components of hemostasis. *Nat Commun* **9**, 509 (2018).
178. Gee, B. E. *et al.* Whole Blood Transcriptome Analysis in Children with Sickle Cell Anemia. *Front. Genet.* **12**, (2022).
179. Creary, S. *et al.* Baseline and Disease-Induced Transcriptional Profiles in Children with Sickle Cell Disease. *Sci Rep* **10**, 9013 (2020).
180. Mathur, T., Flanagan, J. M. & Jain, A. Tripartite collaboration of blood-derived endothelial cells, next generation RNA sequencing and bioengineered vessel-chip may distinguish vasculopathy and thrombosis among sickle cell disease patients. *Bioengineering & Translational Medicine* **6**, e10211 (2021).
181. Topper, J. N. & Jr, M. A. G. Blood flow and vascular gene expression: fluid shear stress as a modulator of endothelial phenotype. *Molecular Medicine Today* **5**, 40–46 (1999).

182. Caruso, C. *et al.* Less-deformable erythrocyte subpopulations biomechanically induce endothelial inflammation in sickle cell disease. *Blood* **144**, 2050–2062 (2024).
183. Mannino, R. G., Qiu, Y. & Lam, W. A. Endothelial cell culture in microfluidic devices for investigating microvascular processes. *Biomicrofluidics* **12**, 042203 (2018).
184. Hesh, C. A., Qiu, Y. & Lam, W. A. Vascularized microfluidics and the blood-endothelium interface. *Micromachines* **11**, (2020).
185. Mannino, R. G., Pandian, N. K., Jain, A. & Lam, W. A. Engineering 'Endothelialized' Microfluidics for Investigating Vascular and Hematologic Processes Using Non-Traditional Fabrication Techniques. *Current opinion in biomedical engineering* **5**, 13–20 (2018).
186. Qiu, Y. *et al.* Microvasculature-on-a-chip for the long-term study of endothelial barrier dysfunction and microvascular obstruction in disease. *Nat Biomed Eng* **2**, 453–463 (2018).
187. Kim, S., Kim, W., Lim, S. & Jeon, J. S. Vasculature-on-a-chip for in vitro disease models. *Bioengineering* **4**, (2017).
188. Caruso, C. *et al.* Stiff Erythrocyte Subpopulations Biomechanically Induce Endothelial Inflammation in Sickle Cell Disease. *Blood* **134**, 3560–3560 (2019).
189. Naik, N., Hanjaya-Putra, D., Haller, C. A., Allen, M. G. & Chaikof, E. L. Rapid homogeneous endothelialization of high aspect ratio microvascular networks. *Biomedical microdevices* **17**, 83–83 (2015).
190. Li, X., Xu, S., He, P. & Liu, Y. In vitro recapitulation of functional microvessels for the study of endothelial shear response, nitric oxide and [Ca2+]i. *PloS one* **10**, e0126797–e0126797 (2015).
191. Zhang, X. *et al.* A microfluidic-informatics assay for quantitative physical occlusion measurement in sickle cell disease. *Lab Chip* **22**, 1126–1136 (2022).
192. Kim, L., Toh, Y.-C., Voldman, J. & Yu, H. A practical guide to microfluidic perfusion culture of adherent mammalian cells. *Lab Chip* **7**, 681–694 (2007).

193. Tellier, C. *et al.* Cycling hypoxia induces a specific amplified inflammatory phenotype in endothelial cells and enhances tumor-promoting inflammation in vivo. *Neoplasia* **17**, 66–78 (2015).

194. Healey, G., Veale, M. F. & Sparrow, R. L. A fluorometric quantitative erythrophagocytosis assay using human THP-1 monocytic cells and PKH26-labelled red blood cells. *J Immunol Methods* **322**, 50–56 (2007).

195. Steward, R., Tambe, D., Hardin, C. C., Krishnan, R. & Fredberg, J. J. Fluid shear, intercellular stress, and endothelial cell alignment. *Am J Physiol Cell Physiol* **308**, C657–C664 (2015).

196. Cerutti, C. & Ridley, A. J. Endothelial cell-cell adhesion and signaling. *Exp Cell Res* **358**, 31–38 (2017).

197. Prasain, N. & Stevens, T. The actin cytoskeleton in endothelial cell phenotypes. *Microvasc Res* **77**, 53–63 (2009).

198. Tousoulis, D., Kampoli, A.-M., Tentolouris, C., Papageorgiou, N. & Stefanadis, C. The role of nitric oxide on endothelial function. *Curr Vasc Pharmacol* **10**, 4–18 (2012).

199. Zhao, M. *et al.* HIF-1α/JMJD1A signaling regulates inflammation and oxidative stress following hyperglycemia and hypoxia-induced vascular cell injury. *Cellular & Molecular Biology Letters* **26**, 40 (2021).

200. Liao, Y., Zou, Y. & Zhang, H. MicroRNA-126-5p Facilitates Hypoxia-Induced Vascular Endothelial Cell Injury via HIPK2. *Ann Clin Lab Sci* **52**, 918–926 (2022).

201. Vercellotti, G. M. *et al.* Critical role of C5a in sickle cell disease. *Am J Hematol* **94**, 327–337 (2019).

202. Akahori, D. *et al.* Effect of Hypoxia on Pulmonary Endothelial Cells from Bleomycin-Induced Pulmonary Fibrosis Model Mice. *Int J Mol Sci* **23**, 8996 (2022).

203. Osei, S. Y., Ahima, R. S., Fabry, M. E., Nagel, R. L. & Bank, N. Immunohistochemical localization of hepatic nitric oxide synthase in normal

and transgenic sickle cell mice: the effect of hypoxia. *Blood* **88**, 3583–3588 (1996).

204. Thompson, J. W., Dave, K. R., Young, J. I. & Perez-Pinzon, M. A. Ischemic preconditioning alters the epigenetic profile of the brain from ischemic intolerance to ischemic tolerance. *Neurotherapeutics* **10**, 789–797 (2013).

205. Malatesha, G., Singh, N. K., Bharija, A., Rehani, B. & Goel, A. Comparison of arterial and venous pH, bicarbonate, PCO2 and PO2 in initial emergency department assessment. *Emerg Med J* **24**, 569–571 (2007).

206. Ortiz-Prado, E., Dunn, J. F., Vasconez, J., Castillo, D. & Viscor, G. Partial pressure of oxygen in the human body: a general review. *Am J Blood Res* **9**, 1–14 (2019).

207. Stimpson, S.-J., Rebele, E. C. & DeBaun, M. R. Common gynecological challenges in adolescents with sickle cell disease. *Expert Review of Hematology* **9**, 187–196 (2016).

208. Ceglie, G. *et al.* Gender-Related Differences in Sickle Cell Disease in a Pediatric Cohort: A Single-Center Retrospective Study. *Front Mol Biosci* **6**, 140 (2019).

209. Tiana, M. *et al.* Metabolic labeling of RNA uncovers the contribution of transcription and decay rates on hypoxia-induced changes in RNA levels. *RNA* **26**, 1006–1022 (2020).

210. Sparkenbaugh, E. & Pawlinski, R. Interplay between coagulation and vascular inflammation in sickle cell disease. *Br J Haematol* **162**, 3–14 (2013).

211. Liu, C., Li, Z. & Xi, H. Bioinformatics analysis and in vivo validation of ferroptosis-related genes in ischemic stroke. *Front. Pharmacol.* **13**, (2022).

212. Schulz, R. *et al.* Arterial hypertension in a murine model of sleep apnea: role of NADPH oxidase 2. *J Hypertens* **32**, 300–305 (2014).

213. Carvalho, M. O. S. *et al.* Evaluation of Alpha-1 Antitrypsin Levels and SERPINA1 Gene Polymorphisms in Sickle Cell Disease. *Front Immunol* **8**, 1491 (2017).

214. Riis, J., Nordestgaard, B. G. & Afzal, S. α1-Antitrypsin Z allele and risk of venous thromboembolism in the general population. *Journal of Thrombosis and Haemostasis* **20**, 115–125 (2022).
215. DeLuca, D. S. *et al.* SERPINA1 gene polymorphisms in a population-based ALSPAC cohort. *Pediatric Pulmonology* **54**, 1474–1478 (2019).
216. Misra, S. *et al.* Blood-based protein biomarkers for the diagnosis of acute stroke: A discovery-based SWATH-MS proteomic approach. *Front Neurol* **13**, 989856 (2022).
217. PubChem. SERPINF2 - serpin family F member 2 (human). https://pubchem.ncbi.nlm.nih.gov/gene/SERPINF2/human.
218. Drouet, C. *et al.* SERPING1 Variants and C1-INH Biological Function: A Close Relationship With C1-INH-HAE. *Front. Allergy* **3**, (2022).
219. Hausburg, M. A. *et al.* C1 esterase inhibitor-mediated immunosuppression in COVID-19: Friend or foe? *Clinical Immunology Communications* **2**, 83–90 (2022).
220. Grover, S. P. *et al.* C1 inhibitor deficiency enhances contact pathway-mediated activation of coagulation and venous thrombosis. *Blood* **141**, 2390–2401 (2023).
221. Scott, E., Dougherty, T. J., Gorski, G. & Hatcher, C. J. Reelin Signaling in Vascular Endothelial Cell Biology. *The FASEB Journal* **33**, 83.4-83.4 (2019).
222. Ding, Y. *et al.* Loss of Reelin protects against atherosclerosis by reducing leukocyte-endothelial cell adhesion and lesion macrophage accumulation. *Sci Signal* **9**, ra29 (2016).
223. Calvier, L. *et al.* Circulating Reelin promotes inflammation and modulates disease activity in acute and long COVID-19 cases. *Front. Immunol.* **14**, (2023).
224. Bendjilali, N. *et al.* Time-Course Analysis of Gene Expression During the Saccharomyces cerevisiae Hypoxic Response. *G3 Genes|Genomes|Genetics* **7**, 221–231 (2017).

Appendix

Metric	Normal Reference Ranges					
	Adult Male	Adult Female	12 to 18 yr Male	12 to 18 yr Female	6 to 12 yr Male	6 to 12 yr Female
HGB (g/dL)	13.5 – 17.5	12.0 – 16.0	13.0 – 16.0	12.0 – 16.0	11.5 – 15.5	11.5 – 15.5
HCT (%)	37 – 53	33 – 51	36 – 51	33 – 51	35 – 45	35 – 45
MCV (fL)	80 – 100	80 – 100	79 – 98	78 – 102	77 – 95	77 – 95
MCHC (g/dL)	32 – 36	32 – 36	32 – 36	32 – 36	32 – 36	32 – 36
RDW (%)	11.5 – 13.1	11.5 – 13.1	11.5 – 14.0	11.5 – 14.0	11.5 – 15.0	11.5 – 15.0
	Adult		13 to 18 yr		9 to 12 yr	5 to 8 yr
WBC (k/µL)	4.5 – 11.0		4.5 – 13.0		4.5 – 13.5	5.0 – 14.5
PLT (k/µL)	140 – 450		140 – 450		140 – 450	140 – 450

Table A.1: Normal reference ranges for clinical metrics. Normal reference ranges for hemoglobin (HGB), hematocrit (HCT), mean corpuscular volume (MCV), mean corpuscular hemoglobin concentration (MCHC), red blood cell distribution width (RDW), white blood cell count (WBC), and platelet count (PLT). Reference metrics sourced from Children's Hospitals and Clinics of Minnesota hematology/CBC reference tables.